

Installation Method Analysis for a Large Diameter Cold Water Pipe for Land - Based OTEC Plants

Maichel van Nauta Lemke

MSc Thesis Report

This page is intentionally left blank

MSc THESIS REPORT

**INSTALLATION METHOD ANALYSIS
FOR A LARGE DIAMETER
COLD WATER PIPE FOR
LAND - BASED OTEC PLANTS**

30th June 2017

Author

Maichel van Nauta Lemke

Student ID: 4049772

Thesis committee

Prof. Dr. A. Metrikine

Ir. J.S. Hoving

Ir.B.J. Kleute

Ir. J. Brugmans

An electronic version of this thesis is available at <http://repository.tudelft.nl/>

Offshore and Dredging Engineering
Delft University of Technology



This page is intentionally left blank

Acknowledgements

I started with this thesis, by hearing about OTEC which sparked great interest in me. I am very thankful for the opportunity which Bluerise has given to me by letting me graduate there. They have been very supportive, and have enabled to gain great new experiences such as going to the OTEC symposium. Eventually the experience of doing tests at MARIN came by, from which I have learnt so much. Not only where the tests useful, it was a very fun environment to work with. I should mention that the tests could not have been done without the great help of Fabian Koppes, Ikbal Kelkitli and Bram Harmsen, as building the setup and measurement system took a tremendous amount of time.

Within Bluerise, I would like to thank Berend Jan Kleute, for the interesting open hearted conversations, and for giving the freedom to fill in my thesis as I wished, for example by doing the tests at MARIN. Furthermore I would like to thank all of the other graduates and interns at Bluerise, for the fun conversations and exciting ping pong matches.

Besides working at Bluerise, I have spent a large part of my time at INTECSEA. I would like to say thanks to Joost Brugmans, who has accepted to coach me throughout my graduation. It was an incredible experience to spend time at INTECSEA, where I have learnt a lot on pipe laying in general, as well as having had a taste of what it is like to work at an engineering company.

I also must thank Jeroen Hoving, who especially in the last few months has helped me tremendously. You have always been willing to make time for me, and to check my work. Besides giving me advice and steering me in the right direction, I have enjoyed our lengthy discussions, also on a personal level.

Professor Metrikine, as you have very busy the last year we have had only several brief meetings. During these meetings however, you have always taken the time to give me advice.

Finally, I would like to say thanks to my family and girlfriend. My family has continuously supported me throughout my graduation, and has motivated me to keep on going. Especially my parents have helped me throughout the last weeks of my graduation. I could not have done this without them.

Maichel van Nauta Lemke

Delft, June 2017

This page is intentionally left blank

Abstract

Ocean thermal energy conversion (OTEC) is a technology which uses the temperature difference between cold deep water and warmer surface water in the ocean to generate electricity. This technology is most applicable in remote tropical locations, as it can produce a continuous year-round base load that supplies the remote region with reliable and sustainable energy.

One of the main challenges of large scale OTEC plants is the installation of the cold water pipe (CWP), which is used to pump the cold water from the depths of the ocean to the plant. Bluerise is currently developing 10 MW land-based OTEC plants. For these plants, the CWP has an internal diameter of 2.5 meters and is installed over the seabed up to a water depth of 1000 meters. A CWP of these dimensions has never been installed yet and thus the optimal installation method is unknown. The main aim of this graduation was to find the optimal installation method and the preferred material for these large cold water pipes.

First, research was conducted to evaluate several materials, assessing similarities and experience in other industries and the specific requirements for OTEC. Furthermore, several existing and new installation methods were investigated and discussed. In order to compare these materials and methods, a base case project was used that Bluerise is currently developing in Curacao for which parameters such as seabed slope and water density are known. The different options for materials and installation methods were evaluated using a multi-criteria analysis taking into account non-technical aspects such as risks and costs.

Based on this analysis, HDPE was identified as the preferred material. Regarding the installation, it was found that the “modified Float and Sink” and the “Hold and Sink”-methods were optimal, both being similarly ranked. As the details of these installation methods are not yet known in practice, it is not yet clear if the CWP can be successfully installed using either of these methods - thus an installation model was developed for the CWP based on Euler–Bernoulli beam theory. This model simulates the pipe installation and describes the pipe in the vertical direction. In the model, forcing or loading (such as buoys and ballast) can be variably applied to the CWP thereby allowing for the simulation of any possible installation method.

In addition to this model, scale model tests were done at MARIN in Wageningen to investigate the practical aspects of the CWP installation, as well as to collect data for the validation of the Matlab model. As the computer model was validated, it was found that 3-dimensional effects, observed during the scale model tests, had a large influence on the drag and displacement of the pipe. The numerical model consistently overestimates the velocities seen during the tests at MARIN, however trend-wise the numerical model gives similar results when simulating different installation methods for the pipe.

As the main issue for the pipe is the bending, the key challenge is to minimize bending during the installation. Taking this into account, it was found that the best installation method was a combination of the “Float and Sink” and the “Hold and Sink”-method, as the shape and position of the pipe can meticulously be controlled by a combination of buoys (attached to the pipe) and vessels (manipulating the pipe end). It was found that with this combined installation method, the total Von Mises stress is kept well under the limit for HDPE. Nevertheless, it is recommended that these results are further verified using a more detailed model that takes 3-dimensional effects into account so that the response of the cold water pipe can be calculated more accurately.

This page is intentionally left blank

Table of Contents

Acknowledgements	v
Abstract	vii
List of Figures	xii
List of Tables	xiv
List of Abbreviations	xv
1. Introduction to OTEC and Thesis Objective	1
1.1. Ocean Thermal Energy Conversion	1
1.2. History of OTEC	3
1.3. Research Objective	5
1.4. Thesis Structure	6
1.5. Broader OTEC Considerations	7
2. CWP Installation Base Case Parameters	8
2.1. Curacao Eco Park	9
2.2. Metocean Conditions	10
2.2.1. Weather Conditions	10
2.2.2. Water Depth	10
2.2.3. Water density	11
2.2.4. CWP Location Bathymetry	12
2.3. Cold Water Pipe Parameters	12
3. Cold Water Pipe Material Selection	13
3.1. HDPE	14
3.2. Steel	16
3.3. FRP	17
3.4. Concrete	18
3.5. Materials Multi Criteria Analysis & Evaluation	19
3.5.1. Multi Criteria Analysis	20
3.6. Conclusion	20
4. Cold Water Pipe Installation Method Selection	21
4.1. Pipe specifications	21
4.2. Single segment installation methods	22
4.2.1. Modified Float and Sink Method	23
4.2.2. Modified Float and Sink with Buoyancy and/or Smart Ballasting	24
Float and Sink Installation Limits	24
4.2.3. Brewers Method	25
4.2.4. F&S hybrid with brewers method	28
4.2.5. Hold and Sink installation method	29
4.3. Bottom Tow installation methods	31

4.3.1. Off-bottom tow	31
4.3.2. Bottom tow	32
4.4. Alternative installation methods	34
4.4.1. Installation by sections	34
4.4.2. Directional Drilling	36
4.5. MCA	37
4.6. Conclusion	37
5. Numerical Modelling of the CWP	39
5.1. Model Theory	39
5.2. Equation of Motion	40
5.3. Boundary conditions	41
5.4. Finite Difference Discretisation	42
5.5. Pulling force from tug	43
5.6. Displacement in the horizontal plane	43
5.6.1. Due to rotation	43
Re-initialisation	44
5.6.2. Due to tension	44
5.7. CWP Stresses	44
5.7.1. Axial stress	45
5.7.2. Hoop Stress & Radial Stress	45
5.8. Model verification	46
Local bending	49
5.9. Conclusions	50
6. Marin Tests	51
6.1. Test Setup Overview	51
6.2. Tests	52
6.2.1. Free Fall Tests	52
6.2.2. Hold & Sink tests	52
Constant tension	53
6.2.3. Test Results	53
6.3. Matlab Model validation	54
Free Fall test comparisons	54
Instability/ vortex shedding	55
Constant tension tests	57
T.2.50.50 & T.2.50.100	57
T.7.50.100 & T.7.100.100	60
6.4. Discussion	61
7. Final Installation Method Analysis	63
7.1. Modified Float and Sink Method	63

7.2.	Hold and Sink Installation Method	63
7.3.	Hold and Sink with additional ballast	65
7.4.	Hold and Sink with additional ballast and buoys	66
7.5.	Hold and Sink method for 4 meter diameter CWP	69
7.6.	Final installation method	71
8.	Conclusion and Recommendations	73
8.1.	Conclusion	73
8.2.	Recommendations	74
Appendix A:		76
Test Setup Parameters		76
Appendix B:		77
Minimum CWP Mass and Air Fill Ratio		77
Appendix C: Material Properties & MCA's		80
	Materials MCA.....	82
	Installation Method MCA	83
	The full installation method MCA is given below.	83
Appendix D: Discretisation of Equation of Motion		84
	L.H.S.	85
	R.H.S.	86

List of Figures

Figure 1: Orange regions identified as suitable for the application of OTEC	1
Figure 2: World map highlighting temperature ranges in the ocean	2
Figure 3: Illustration of shore based and offshore OTEC plants	3
Figure 4:Deployment of Claude's Cold Water Pipe	3
Figure 5: Illustration of the 'Mini-OTEC' plant.....	4
Figure 6: Thesis Methodology and Structure	6
Figure 7: Illustration of the Eco Park complex, Curacao	9
Figure 8: Temperature profile of the ocean[6]	11
Figure 9: General water density profile of the ocean[6].....	11
Figure 10: Installation of a ballasted HDPE Pipe.....	14
Figure 11: Transport of HDPE Pipe Segments.....	14
Figure 12: Mirror Welding Technique	14
Figure 13: Allseas Solitaire pipelay vessel.....	16
Figure 14: Preparing FRP pipes for installation	17
Figure 15: Connecting Concrete Pipe Segments	18
Figure 16:Spigot Joint	19
Figure 17: Depiction of the float and sink installation procedure	23
Figure 18: F&S with Lazy Wave / Smart Ballasting.....	24
Figure 19: Dependence of the Maximum Stress on the Pull Tension	25
Figure 20: Brewers Method - Illustration of Replacement of Vessels with Buoys	25
Figure 21: Buoyant FRP Pipe Installation (Deep Oil Technology Inc).....	26
Figure 22: Illustration of Upward Pipe Displacement.....	27
Figure 23: Comparison of Segment Length and Stress for a 2.5m CWP	28
Figure 24: F&S Hybrid with Brewers	29
Figure 25: Hold and Sink Method.....	29
Figure 26: Illustration of Downward Pipe Displacement.....	30
Figure 27: Comparison of Segment Length and Bending Moment.....	30
Figure 28: Illustration of Off-bottom Tow	31
Figure 29: Illustration of Bottom Tow	32
Figure 30: Pipeline Length versus Total Stress (2.5m HDPE).....	33
Figure 31: Pipeline Length versus Total Pulling Force (2.5m HDPE).....	34
Figure 32: Installation by Sections	34
Figure 33: Calculation to Determine the Maximum Length	35
Figure 34: Directional Drilling.....	36
Figure 35: Illustration of the basic pipe configuration	40
Figure 36: Euler-Bernoulli beam theory.....	40
Figure 37: Illustration of vico-elastic foundation.....	41
Figure 38: Illustration of Axial Stress	45
Figure 39: Illustration of hoop and radial stress	46
Figure 40: Velocity of the pipe at L=75% with 60 nodes	47
Figure 41: Maximum displacement of pipe with 390mT tension	48
Figure 42: Displacement comparison for 40 and 60 nodes	48
Figure 43: Velocity comparison for 40 and 60 nodes	49
Figure 44: Displacement comparison for 40 and 100 nodes	49
Figure 45: Displacement comparison for an increasing amount of nodes.....	50
Figure 46: Artists impression of the tank test setup	51
Figure 47: Photograph of the lifting points	52
Figure 48: Installation with constant velocity of the pipe	53
Figure 49: Installation with minimized pipe bending.....	53
Figure 50: Illustration of investigated pipe location.....	54
Figure 51: Simulation of the FF experiment in Matlab	55

Figure 52: Displacement of the pipe over time	55
Figure 53: Displacement comparison between the numerical and physical model.....	56
Figure 54: Velocity comparison between the numerical and physical model.....	57
Figure 55: Displacement of the pipe with constant tension.....	58
Figure 56: Comparison of numerical model with physical model	58
Figure 57: Displacement comparison between the numerical and physical model for CT tests	59
Figure 58: Velocity comparison between the numerical and physical model for CT tests	59
Figure 59: Displacement comparison between the numerical and physical model.....	60
Figure 60: Velocity comparison between the numerical and physical model.....	61
Figure 61: Displacement of 2.5m CWP with the Hold and Sink test.....	64
Figure 62: Von Mises stress in the CWP during H&S installation	64
Figure 63: Von Mises stress without hydrostatic pressure	65
Figure 64: Hold and Sink installation with increased ballast	65
Figure 65: Velocity of the CWP during installation.....	66
Figure 66: H&S installation with buoys	67
Figure 67: Velocity of the pipe with buoys attached.....	68
Figure 68: Von Mises stress	68
Figure 69: Von Mises stress without hydrostatic pressure	69
Figure 70: 4m CWP installation	70
Figure 71: 4m CWP velocity	70
Figure 72: Von Mises stress 4m CWP	71
Figure 73: Drag and lift coefficient vs Reynolds number.....	78

List of Tables

Table 1: OTEC Plant Types and CWP Implementation.....	2
Table 2: Curacao Eco Park Project – Parameters and Assumptions	10
Table 3: CWP Parameters	12
Table 4: HDPE properties	15
Table 5: Properties of steel.....	16
Table 6: FRP properties.....	18
Table 7: Concrete properties	19
Table 8: Shortened MCA of materials.....	20
Table 9: HDPE CWP properties.....	22
Table 10: Maximum pipe segment length for Brewers method	28
Table 11: Maximum segment length for H&S	31
Table 12: Axial stress and pull force for bottom tow installation methods.....	33
Table 13: Segment length limit for installation by segments	36
Table 14: Summarized installation method MCA.....	37
Table 15: Free Fall velocity verification	47
Table 16: Displacement and bending verification.....	48
Table 17: Local bending verification	50
Table 18: FF test validation.....	55
Table 19: Installation test description.....	57
Table 20: Constant tension validation	60
Table 21: Test description	60
Table 22: Constant tension test data.....	61
Table 23: Hold and sink installation parameters	63
Table 24: Von Mises stress in CWP.....	66
Table 25: H&S with additional ballast installation parameters.....	67
Table 26: Von Mises stress comparison between H&S installation scenarios.....	69
Table 27: 4m CWP installation parameters.....	70
Table 28: Relevant MARIN test setup parameters.....	76
Table 29: Minimum pipe ballast parameters	77
Table 30: List of material properties	81
Table 31: Materials MCA.....	82
Table 32: Installation method MCA.....	83

List of Abbreviations

OTEC	Ocean thermal energy conversion
SWAC	Seawater air conditioning
CWP	Cold water pipe
H&S	Hold and sink
F&S	Float and sink
HDPE	High density Poly-ethylene
FRP	Fibreglass reinforced plastic
ID	Internal Diameter
OD	External Diameter
DNV	Das Norske Veritas
MCA	Multi Criteria Analysis

This page is intentionally left blank

1. Introduction to OTEC and Thesis Objective

1

Two of the most discussed topics are currently climate change and CO₂ emissions. The current general belief is that we are in a phase of global warming, which is either caused or strengthened by greenhouse gas emissions such as carbon dioxide.

Furthermore, pollution and smog in many large cities results in health problems for the local population. These factors, in combination with volatile oil and gas prices result in an increasing demand for renewable clean energy.

Large investments are being made in renewable energy sources. These are increasingly driven by recent political initiatives such as the Paris Agreement, which has been ratified by 151 parties[1]. China alone has announced plans to invest over 360 billion USD in sustainable energy by 2020[2].

In addition to generating less pollution, renewable energy has the potential to provide energy in the form of relatively small standalone systems which do not require large scale energy grids. This can result in accessible and affordable energy in remote regions with a low population density.

The most known types of renewable energy are wind and solar energy. These forms of sustainable energy are already widely used, yet they have one major downside. As they are dependent on favourable weather conditions, they cannot generate a base load. They can be added to the energy mix of a region or country to lower the total CO₂ emissions, yet without major energy storage it is nearly impossible to use these forms of sustainable energy as standalone systems.

1.1. Ocean Thermal Energy Conversion

One alternative method to generate sustainable energy is Ocean Thermal Energy Conversion (OTEC).

OTEC is a technology which uses the temperature difference between cold water at great depths and warmer surface water in the ocean to generate electricity. By pumping the cold and warm water into the power plant, electricity can be generated by using a thermodynamic cycle. In this cycle, the warm water is used to evaporate a working fluid such as ammonia. This then drives a turbine which generates electricity. After going through the turbine, the ammonia is condensed using the cool water. After exchanging heat, the seawater is discharged back into the ocean.

Besides generating electricity, ocean thermal energy can be used for seawater air conditioning (SWAC). With SWAC, the cold seawater which is pumped up is used directly for cooling air. SWAC can greatly reduce the energy required compared to conventional air conditioning systems, it can also be done in conjunction with electricity generation.

OTEC is especially suitable for tropical regions where the ocean surface temperature is around 24 to 27°C and where the cold deep-seawater is around 5°C, as the temperature difference must be approximately 20° to be feasible.

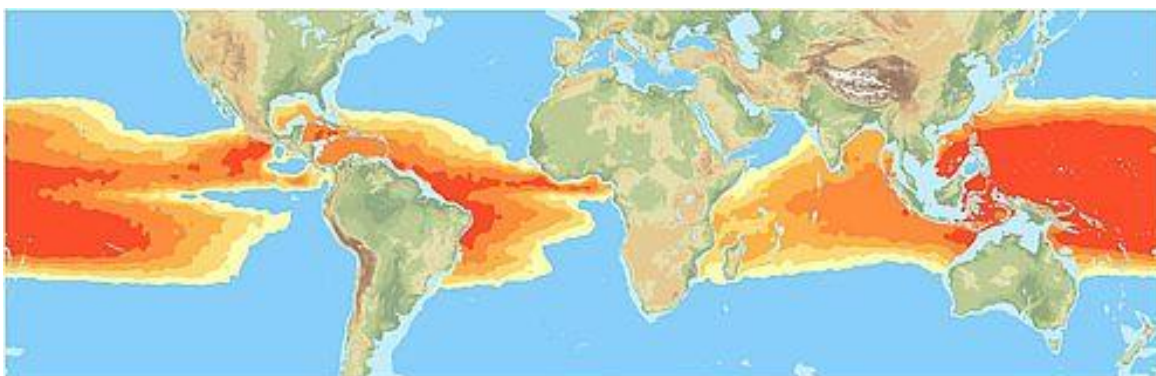


Figure 1: Orange regions identified as suitable for the application of OTEC

One of the large benefits of OTEC is that it is a very constant power source, with only small and predictable changes in power output as the water temperature slightly fluctuates throughout the

seasons. For this reason OTEC can be used as a base load energy source in locations where sustainable and reliable energy is desired. The potential of OTEC is vast as the ocean continuously absorbs great amounts of solar energy which can be utilized and tapped from.

Not only does OTEC provide clean reliable energy, it can also be financially attractive. Many remote regions and small islands do not have a large enough energy demand for large efficient power plants. Therefore it is quite common to use old diesel powered ship engines for providing base load electricity. These are often unreliable, as well as expensive due to the costs of diesel and high maintenance costs. OTEC has the potential to provide these places with reliable and less expensive energy[3].

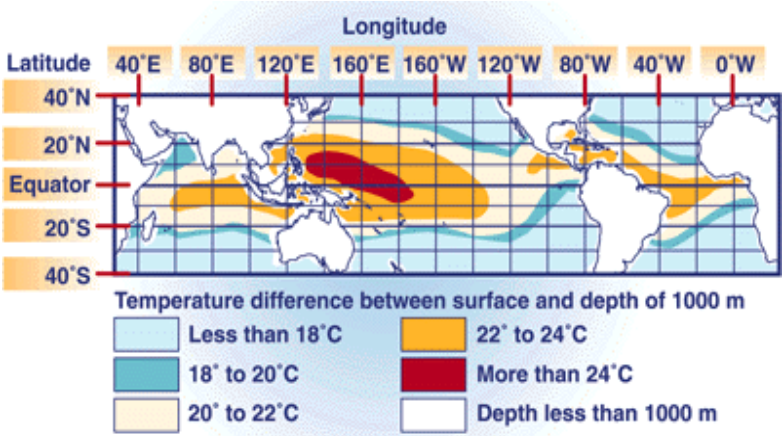


Figure 2: World map highlighting temperature ranges in the ocean

OTEC Plant Structures

There are three different types of OTEC plants with differing implications for cold water pipe (CWP) installation.

OTEC plant type	Overview
Shore based plants	The OTEC plant is built onshore, near the ocean. From this plant the cold water pipe is installed over or above the seabed up to the required water depth
Shelf mounted plants	If the water depth remains small for a large distance from shore, the plant can be built on the seabed shelf at the location where the water depth starts to increase. This results in a shorter cold water pipe length
Offshore-floating plants	OTEC plants can also be built offshore, on a floating platform. This requires a relatively short cold water pipe and results in only a power cable going to shore.

Table 1: OTEC Plant Types and CWP Implementation

For the shore based plants, the OTEC plant is built on shore, near the ocean. From here the warm and cold water intake pipes as well as the discharge pipe run into the ocean. The cold water pipe is installed on or slightly above the seabed, up to the required water depth. The offshore plants are built on floating platforms, which are moored offshore. The required pipelines are suspended vertically from the platform. Shelf mounted plants are installed at sea on the seabed shelf, in locations where the shallow seabed shelf is long, as this then decreases the required pipeline lengths. Shore based plants are generally less efficient; internal friction losses are higher due to the fact that a much longer CWP is required. Although shore based OTEC plants are less efficient, they can be an attractive option as the cold water which is pumped to shore can serve more purposes. The cold water is nutrient rich, and can be used both for aqua- and agriculture, even after using it for generating electricity. Furthermore the cold water can be used for seawater air-conditioning (SWAC), which can save costs over traditional forms of air conditioning.

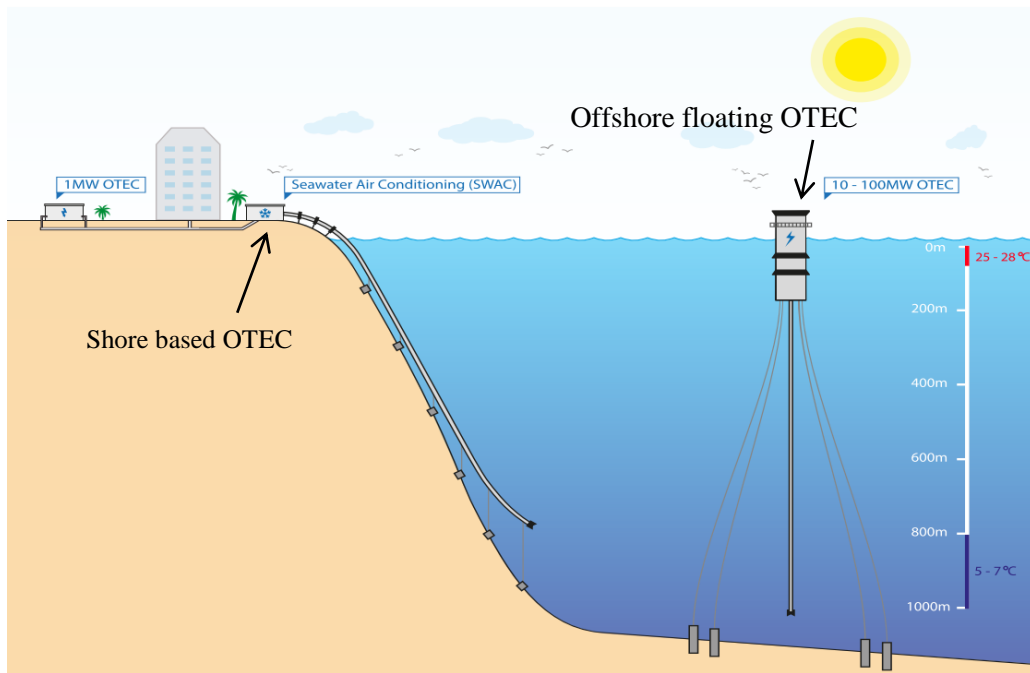


Figure 3: Illustration of shore based and offshore OTEC plants

1.2. History of OTEC

Although OTEC is not yet widely commercially available, the idea is not new. Jules Verne was the first to come up with the concept of OTEC in 1870, which he described in his book ‘Twenty Thousand Leagues Under the Sea’. In this book, Captain Nemo tells one of his shipmates how this principle would work: “By establishing a circuit between two wires plunged to different depths, [it should be possible] to obtain electricity by the difference of temperature to which they would have been exposed.”

Some 11 years later, French physicist Jacques-Arsène d’Arsonval came up with the first practical design for an OTEC plants, with pipes instead of wires, as it is still done today.

In 1930 the first OTEC plant was built by Georges Claude in Cuba. This plant was shore based and produced 22 kilowatts of electricity. Unfortunately this plant was later destroyed by a storm. Claude continued with his research and built an offshore OTEC plant in 1935 aboard a cargo vessel, called the *Tunisie*. With a 650 meter long 2,5 meter diameter inlet pipe it was a large plant, though it was unfortunately destroyed by weather conditions before being operational[4].



Figure 4:Deployment of Claude's Cold Water Pipe

Research continued throughout the 1940's and 1950's although low prices of traditional methods of power generation prevented new projects from starting. In the 1970's, when fossil fuel prices started going up again OTEC regained interest. In 1970 a shore based plant was built in Japan. The plant produced 120 kilowatts, although the net produced power was a limited 30 kilowatts. The US also showed interest by developing OTEC plants in Hawaii. In 1979 the offshore 'Mini-OTEC' was built. 'Mini-OTEC' was built on a converted navy barge. A 660 meter long, 60 centimetre diameter polyethylene cold water pipe was used. This resulted in 50KW of power, although the net power output was still only 10KW.

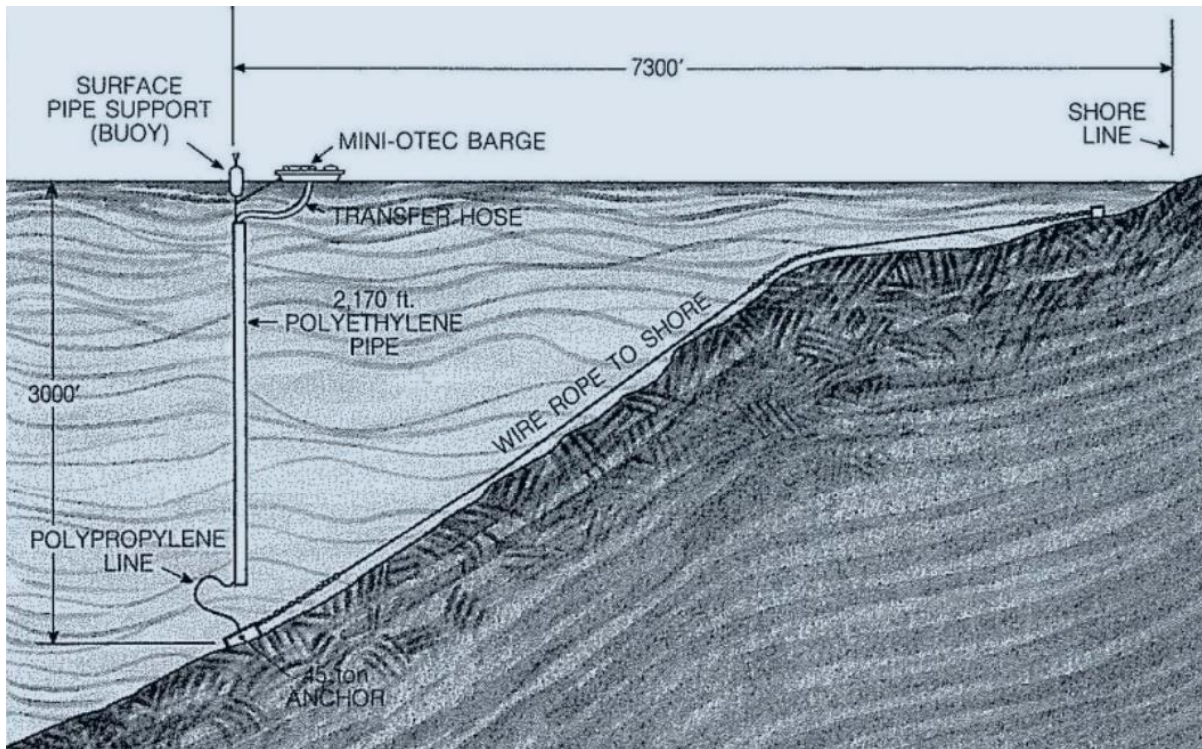


Figure 5: Illustration of the 'Mini-OTEC' plant

Besides the 'Mini-OTEC' plant, the much larger 'OTEC-1' plant was also built in the same period in Hawaii. 'OTEC-1' was built using a converting oil tanker, with 3 cold water pipes with a diameter of 1.2 metres each, reaching a depth of approximately 700 metres. 'OTEC-1' was built only for research, not power production.

After these projects, it took until 2002 for the next OTEC project to be executed. In India a 1MW floating plant was built, yet unfortunately was not successful as the CWP failed during testing proving the critical importance of the CWP.

In 2013 OTEC was put back on the map, as Saga University in Japan successfully developed a 50KW OTEC plant in Okinawa. This plant was built for research purposes, and is also used to study other uses of the nutrient rich cold water which is pumped up, such as aquaculture.

In 2015 OTEC research in Hawaii was continued, as Makai Ocean Engineering developed a 105KW shore based plant, currently providing power to approximately 120 households.

Currently, there are several companies and countries showing large interest in developing OTEC, and trying to scale up the plant designs. DCNS group for example is working on project NEMO, where they are developing a 10MW net output offshore plant near Martinique.

1.3. Research Objective

One of the main goals of Bluerise is to build 10MW OTEC plants in the future - this is viewed as an ideal size for remote locations where OTEC would be implemented. Due to the long CWP's used for shore based OTEC plants, efficiency losses due to internal pipe friction are large. To minimize these efficiency losses, Bluerise has found that for a 10MW plant the CWP must have an internal diameter of 2.5 meters. In the future, Bluerise wishes to scale up the capacity and develop significantly larger plants with correspondingly higher water exchange, requiring CWP's with diameters of up to 4 meters.

Past experiences (e.g. the failed project in India outlined previously) has reinforced that one of the greatest challenges of a successful OTEC plant is the design and installation of the CWP. The CWP is an essential component which needs to conform to a number of criteria such as:

- High flow
- Low friction
- High integrity and resilience
- Stability
- Ease of pipe laying
- Low cost

Using such large pipes results in design and construction challenges, logistical problems, and installation difficulties. Additionally, in order for OTEC to be competitive with other alternative energy sources, the project costs for an OTEC plant must remain low.

Some research has previously been done into the installation of large diameter CWP's using the float and sink (F&S) method, further explained in chapter 4. In this research, it was found that the maximum diameter CWP that can be installed in a water depth of 1000 meters using the F&S method is 2.3 meters, without taking a safety factor into account [5].

As this result is not satisfactory for larger OTEC plants, pipe design and material selection must be studied in detail, and new installation methods must be investigated.

This thesis aims to address this challenge by selecting the most suitable materials for such large diameter CWP's, and by finding an installation method, which is universally applicable in the sense that with minor modifications it can be used in most locations where shore based OTEC plants will be built. The main focus is on a 2,5 meter diameter CWP, but also taking into account the desire to scale up to 4 meter diameter.

Research question for this thesis:

Looking at all relevant aspects, what is the preferred material and installation process for a pipeline with a 2,5 meter diameter which is laid over the seabed up to a depth of 1000 meters, and is this feasible?

This question is answered by investigating and evaluating different materials and installation methods. The most preferred installation methods is then the subject of a further, more in-depth analysis, where a numerical model is used to evaluate the performance of the installation method and material.

This leads to the following sub questions:

- How do the different installation methods and pipe materials compare to each other based on the Multi Criteria Analysis?
- Is it possible to install a 2.5 meter diameter pipe in a water depth of 1000 meters with the chosen method? Can this method also be used if the diameter of the pipe is increased to 4 meters?
- How can the final installation method be improved?
- Are the model tests representative and do they validate the model?

1.4. Thesis Structure

The structure and methodology of this thesis is outlined in figure 6.

Initially, certain parameters are identified which correspond to the Curacao project base case. These include parameters such as the required water depth, the seabed slope and the required CWP diameter, as well as assumptions regarding seabed smoothness, weather conditions, etc.

After literature research, several installation methods and several different materials are investigated. Some of these installation methods have been used in other industries, and some of them resulted from brainstorm sessions, where the requirements for the installation method have been taken into account. For the materials analysis a similar approach is used, where research was done into industries with similar requirements.

To evaluate the installation methods and materials, certain parameters have been derived from the Curacao Eco park example which is used as a base case (as explained in chapter 2). Several quick calculations are done, and the materials are evaluated using a Multi Criteria Analysis. The various installation methods are also evaluated using a similar approach. This is partially done in parallel, as the performance of an installation method can depend on the used material. After determining the most suitable and the optimal installation method, a numerical Matlab model is made to further analyse the chosen installation method and material.

Parallel to the Matlab model, scale model tests have been done at MARIN which are used to validate the Matlab model, and to investigate real life aspect of a CWP installation.

After the final installation method is modelled and the forces acting on the pipe were evaluated, the thesis is finalized with conclusions and recommendations.

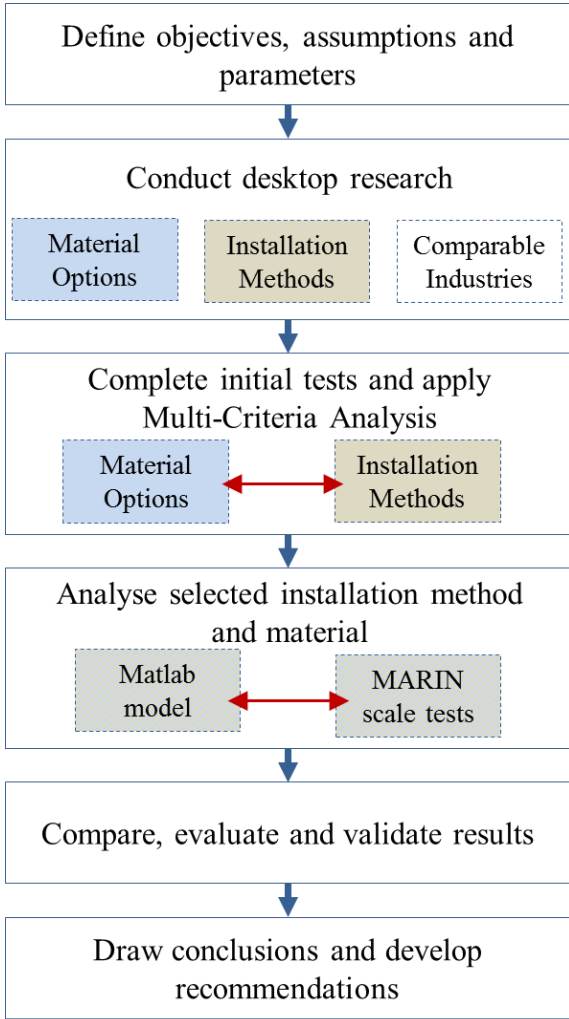


Figure 6: Thesis Methodology and Structure

1.5. Broader OTEC Considerations

This thesis gives insight in the different installation methods for large diameter pipes. As a large number of installation methods are investigated in this thesis, a broader understanding of different pipe laying methods is developed. Finally, the numerical model which is developed can be used for quick analysis of installation methods in varying locations with different properties and parameters. The knowledge which is gained can be used for future OTEC projects, as well as having relevance for other applications where large diameter pipes must be installed in large water depths.

This page is intentionally left blank

2. CWP Installation Base Case Parameters

2

In order to assess installation methods and pipe materials, it must first be determined in what type of conditions the pipe will be installed, and what type of conditions the pipe will face during its operational life. Bluerise is currently working on developing a shore based OTEC plant for the Eco Park in Curacao. It has been found that the general metocean conditions at this location are quite similar to many other potential OTEC locations. As the final installation method and material combination must be universally applicable for multiple locations, the conditions and parameters from the Eco Park location are generalized and used for this thesis, together with several assumptions which are done to simplify and generalize the problem.

2.1. Curacao Eco Park

The Eco Park is a holistic project near the airport of Curacao, providing sustainable energy, food, and water solutions based on OTEC. The OTEC plant will provide electricity, as well as cool water which will be used for district cooling of the Curacao airport. The nutrient rich water will further be used for aqua and agriculture, providing fresh sustainable food locally.



Figure 7: Illustration of the Eco Park complex, Curacao

2.2. Metocean Conditions

The metocean conditions have a large influence on the installation and the operation of the CWP. For this reason, some data is used from the Curacao Eco Park location, in conjunction with some assumptions which are made. The most important parameters are:

- Weather conditions
- Water depth
- Water density (at the surface and at 1000 meters deep)
- Seabed Bathymetry

Parameters	Bathymetry & Metocean Conditions & Assumptions
Seabed slope steepness	1/7
Water depth at end of CWP	1000 m
Average water density during CWP installation	1026.6 kg/m ³
Density of water at 1000 meters depth	1027.6 kg/m ³
Current velocity during installation	0 m/s
Wave height during installation	0 m
Wind speed during installation	0 m/s
Current at seabed during operation	0.25 m/s
Design life of OTEC plants	25 years

Table 2: Curacao Eco Park Project – Parameters and Assumptions

2.2.1. Weather Conditions

As the CWP installation is a complex process, it will be done with calm weather. For this reason, in the calculations and modelling done in this research weather conditions during installation are neglected. The effect of waves, wind and currents during installation is thus not taken into account. The CWP will only be installed if it is foreseen that the favourable weather window is large enough. After installation it is assumed that there is a current at the seabed which exerts a force on the installed pipe. This influences the choice of material and is also used to find the amount of ballast which might have to be attached to the CWP, explained further on in chapter 4.

2.2.2. Water Depth

As explained in chapter 1, OTEC requires a temperature difference of approximately 20°C to function efficiently. For the Curacao Eco Park, it has been found that to reach this the cold water from a depth of 1000 meters must be used.

Figure 8 gives an approximate ocean water temperature- depth profile, for low to middle latitudes, which are the suitable locations for OTEC applications. It can be seen that the thermocline which separates the warm surface water from the cold deep sea water reaches down to approximately 1000 meters, after which the temperature decrease slows down. This means that economically it makes

sense to go up to this limit of approximately 1000 meters. For this reason, a water depth of 1000 metres is used for this study.

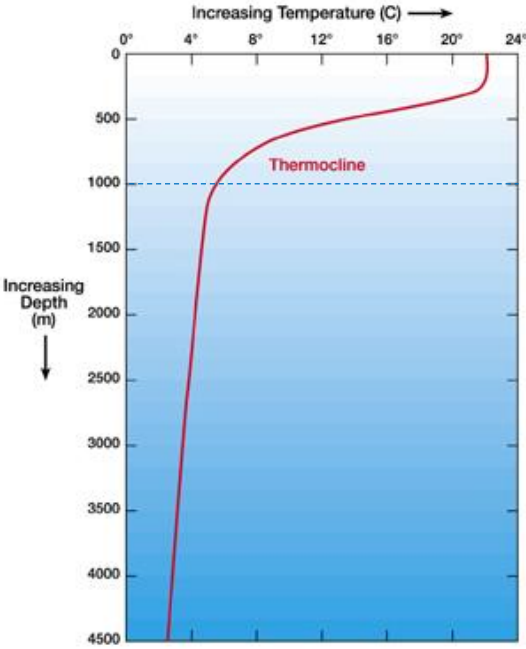


Figure 8: Temperature profile of the ocean[6]

2.2.3. Water density

The density of the seawater is important as it has an influence on the buoyancy forces acting on the pipe. The seawater density is mainly dependent on salinity and water temperature. Higher salinity results in higher water density, and lower water temperature results in higher density. Due to this, the density of the seawater at 1000 meters depth is slightly higher than at the surface. For this research, the water densities at the Curacao project location is used, although as can be seen in figure 9, the values which are used are found to be quite common for tropical regions.

There are 2 values for the density which are used, the average density during installation and the seawater density at the seabed at 1000 meters water depth. This value is used in chapter 4 to find the amount of ballast which must be added to the CWP for it to remain on the seabed without being displaced due to currents.

Average water density during CWP installation	1026.6 [kg / m ³]
Density of water at 1000 meters depth	1027.6 [kg / m ³]

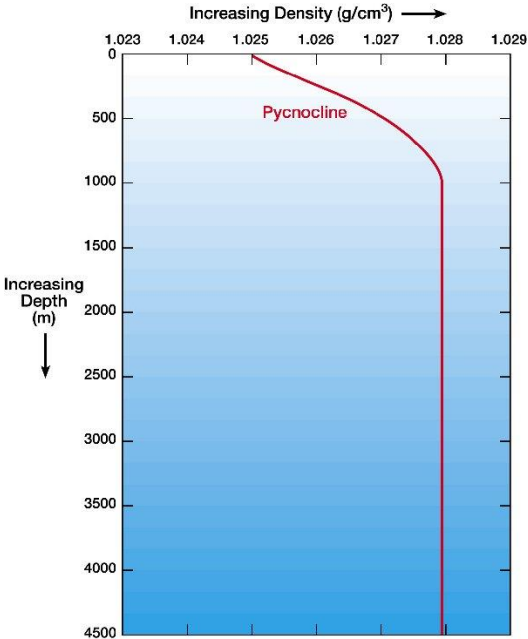


Figure 9: General water density profile of the ocean[6]

2.2.4. CWP Location Bathymetry

For the Curacao Eco Park location, the seabed mainly consists of sand. The slope of the seabed is approximately 1 meter of increase in depth for every 7 meters of distance, or 1/7. This bathymetry is assumed to be quite common in many tropical regions, and therefore likely to be similar to other future OTEC locations. For this research, when describing the performance of materials and installation methods seabed irregularities are considered. For simplification, the modelling and calculations are done under the assumption that the seabed is smooth.

Depending on the installation method, the seabed slope might have a large influence on the CWP installation procedure. Although a steep seabed is beneficial for requiring a shorter CWP to reach the same water depth, geophysical hazards such as submarine landslides could occur. Furthermore, a steep seabed can increase the difficulty of installing a CWP, as the CWP might have to be secured to the seabed, to prevent it from moving. In general, a steeper seabed is expected to bring larger risks for the stability and safety of the installed CWP. Similarly, a very uneven seabed may require physical removal of obstacles or different techniques.

2.3. Cold Water Pipe Parameters

The cold water pipe must meet several design criteria. The design life of the CWP is planned to be 25 years, during this period it must be able to operate without (or with minimal) maintenance. Furthermore, the internal pipe diameter is given, as well as the pipe length. The external pipe diameter is dependent on the material which is used and on the structural requirements of the pipe.

Parameters	Bathymetry & Metocean Conditions & Assumptions
Internal diameter of CWP	2.5 m / 4 m
CWP length	7000 m
Design life of CWP	25 years

Table 3: CWP Parameters

3. Cold Water Pipe Material Selection

3

As part of this thesis several materials are considered for the cold water pipe. The material which is used can have a great influence on both the installation process, as well as on the operational performance of the OTEC plants. It is therefore important that these materials are compared and evaluated so that the best material is used.

There are several aspects which should be considered when evaluating the performance of the materials. These main aspects are:

- Installation performance
 - Material flexibility
 - Material strength
 - Density
- Surface roughness
- Resistance to fouling
- Resistance to corrosion
- Sensitivity to fatigue
- Thermal conductivity
- Material availability
- Environmental impact
- Material costs
- Maintenance & repair costs

Other relevant considerations are where the materials are produced and how they can be transported. By investigating the materials, and by considering these aspects, the materials can be evaluated with a multi criteria analysis (MCA).

For the material selection in this thesis, it is important that the material can currently be produced in 2,5 meter diameter pipes. Considering this and looking at previously installed cold water pipelines and other industries with similar requirements, the following 4 potential materials have been identified:

- HDPE
- Steel
- Fibreglass reinforced plastic
- Concrete

For each of these materials the main properties are given. These have been either been given by suppliers, or by the CES Edupack [6] materials selection database, which is commonly used within the TU Delft. For some of these materials, such as HDPE and composites like fibreglass reinforced plastic (FRP), the properties can be greatly altered by including fibres and other materials. This is not taken into account in this thesis. The full list of material properties which are used can be found in Appendix C.

At the end of this chapter, the materials are evaluated using the established criteria. The best material is used for the rest of the modelling, as explained in chapter 4.

3.1. HDPE

High density polyethylene, or HDPE, is a thermoplastic polymer which is used extensively in a wide large range of applications; from light weight milk jugs to fuel tanks for cars. It is known for its high strength to weight ratio, and its high chemical resistance.

HDPE is already commonly used for wastewater outfall pipes and for drinking water transport pipes, and is the most commonly used material for outfalls with a diameter of under one meter[7]. Some of the favourable properties of HDPE are resistance to corrosion, marine growth & chemicals, high flexibility and low density. As the density of HDPE is lower than that of water, it can be installed using several methods, by either keeping the pipe buoyant, or by adding ballast to make it sink as seen in figure 10.



Figure 10: Installation of a ballasted HDPE Pipe

Pipelife, a company based in Norway, is one of the main producers of large diameter HDPE pipes. Currently, they produce solid wall pipe up to 2.5 meters OD, though they have stated that they can produce 3 meter diameter OD pipe. As HDPE is a thermoplastic material, Pipelife can produce single pipe segments in lengths of 500 meters, which can be floated out to sea. Due to the low density of HDPE, the pipe segments can be towed over the water surface to the project location as shown in figure 11. This reduces transport time, and installation time as only very few connections need to be made due to the long pipe segments.



Figure 11: Transport of HDPE Pipe Segments



Figure 12: Mirror Welding Technique

If a larger diameter HDPE pipe is required, there are several supplier options available such as Krah Pipes, which produces HDPE pipes with internal diameters of up to 4 meters. However these large pipes are only produced in segments of 6 meters[8].

HDPE can as most materials be connected with flanges. As HDPE is thermoplastic, it can also be connected by welding. One of the main welding techniques for HDPE is mirror welding, shown in figure 12. With mirror welding, a hot plate is first placed between the 2 segments that must be connected. The pipe ends are heated up, and then pressed together firmly so that the 2 segments melt together. This process is quick and creates strong connections. These welds are almost as strong as the pipe itself, and have proven to be one of the most trouble free joints in the marine environment[7].

Although HDPE has a high strength to weight ratio, the yield strength is low compared to the other materials which are considered. This is somewhat compensated by the fact that HDPE is quite flexible. Due to this flexibility and the low density of the material, it can be installed on slightly irregular surfaces without leading to large forces in the pipe. This possibly results in less seabed preparation, lowering costs. Sharp rocks and edges must still be avoided, as this could result in puncture of the pipe.

Material Property	Unit	HDPE (PE100)
Density	kg/m ³	961
Yield strength	MPa	23
Max available length	m	500/6
Max available internal diameter	m	2.5/4
Material price	EUR/kg	1.82-2.23

Table 4: HDPE properties

Furthermore, HDPE has some favourable properties for long time use. It has little influence of fatigue, is corrosion resistant, and marine growth is not able to grow on the material. As marine growth cannot grow in the pipe, this is very beneficial to the performance of the OTEC plant as internal flow friction is kept small without the requirement for regular cleaning. The strength of the material does degrade over time however. This is known, and suppliers such as Pipelife give the material specifications for long lifetime use[9]. This is relevant for decommissioning the pipe at the end of lifetime, as possibly more care should be taken. If the CWP is finally decommissioned, HDPE can be recycled, reducing the environmental impact.

Key advantages of HDPE	Main Disadvantages of HDPE
<ul style="list-style-type: none"> • Long segment lengths • Transport over water • Low density • Quick connections • Flexible • Fatigue resistant • Corrosion and chemical resistant • Recyclable 	<ul style="list-style-type: none"> • Low yield strength • Requires additional ballast for certain installation methods

3.2. Steel

Steel pipes are used extensively in the offshore industry for oil and gas transportation. There are many vessels built exclusively to lay steel pipes offshore such as illustrated in figure 13, and there is significant knowledge and experience with installation of steel pipes.



Figure 13: Allseas Solitaire pipelay vessel

Steel pipelines have often been laid in water depths of over 1000 meters. However, the maximum pipe size is limited. For example the Pioneering Spirit, which is the world's largest pipe laying vessel, can install pipes up to is 68 inches, or approximately 173 centimetres OD[10]. Furthermore, specialized installation vessels are very expensive.

Larger pipes cannot possibly be installed with these vessels, due to the size of the tensioners and specialized equipment on board of these vessels. In order to install larger pipes, the vessels would have to be completely modified, which is not feasible at this stage of OTEC development.

One of the reasons that steel is used, is due to the high strength of the material. If the wall thickness is chosen correctly, it can withstand high pressure and high axial loadings. Care must be taken however to prevent buckling, as it cannot withstand large amounts of bending.

In the offshore industry, usually seamless or single seam pipe is used. This is done as welds generally weaken the pipe, and result in higher risks of failure. These types of pipe are not available in the large diameters that are required for this study.

Spirally welded pipe, on the other hand, is made in sizes of up to approximately 4 meters OD. With this type of manufacturing, the pipe is welded in a spiral along the pipe. Spirally welded pipe has less ideal properties than other types of steel pipe. It is for example more sensitive to fatigue, due to the long welds.

Material Property	Unit	Steel (coated with TPU) AISI 1020 rolled
Density	kg/m ³	7800-7900
Yield strength	MPa	295-365
Max available length	m	12
Max available diameter	m	3.65[11]
Material price	EUR/kg	0.532-0.541

Table 5: Properties of steel

The main disadvantage however, is that these large diameter pipes can only be produced with small wall thicknesses of up to approximately 2.5 cm[12]. This is due to the size of the metal sheets from which the pipe is made.

This small wall thickness results in a large diameter over wall thickness ratio. In the offshore industry the DNV-OS-F101 code is often followed for the design of subsea pipelines. This guide is generally applicable for D/t ratios of up to 60[13]. With these ratios already large care must be taken when handling the pipe, to prevent buckling or ovalization. If a pipe diameter of 2.5 meters is used, the D/t ratio would be 100, going up to a 4m diameter pipe the D/t ratio becomes 160. Although the DNV

guide is focussed on the oil and gas industry, if pipes with these dimensions are installed failure is not unlikely. Buckling is expected to occur very quickly, and ovalization can also be expected, even during the handling of the pipe segments before the installation itself.

Welding these large diameter sections together is a very slow process, as there is a large amount of welding material that must be used to fill the gaps. Estimations have led to the conclusion that these welds will take between half a day and a full day per pipe connection, resulting in an extremely long process to complete a 7 km pipe as more than 580 welds are required.

Key advantages of Steel	Main Disadvantages of Steel
<ul style="list-style-type: none"> • High yield strength • A lot of engineering experience with the material 	<ul style="list-style-type: none"> • Small wall thicknesses for large diameters • Subjective to corrosion and marine growth • Pipe assembly takes a long time

3.3. FRP

Fibreglass reinforced plastic is a composite material made of a polymer matrix reinforced with glass fibres. The polymer is usually a thermosetting plastic such as epoxy, or polyester resin. FRP pipes are similar to HDPE pipes, often used for water transport. This includes transport of cooling water and sewage water. Like HDPE, it is corrosion resistant and can be treated to be UV resistant. FRP experiences very little fatigue, making it a good option for long term use. Due to the addition of the glass fibres, FRP is a very strong and stiff material, compared to HDPE. The density is higher than that of seawater, although it is still light compared to concrete and steel.



Figure 14: Preparing FRP pipes for installation

FRP is currently produced up to approximately 4 meters diameter, and is produced in 12 meter segments by suppliers such as Future Pipe Industries[14]. As the pipe is a composite of fibres and resin, it is usually produced with special machines which wind the strings of fibreglass into the pipe.

Material Property	Unit	FRP Polyester filament wound +-60deg
Density	kg/m3	2020-2200

Yield strength	MPa	50-55
Max available length	m	12
Max available diameter	m	4[14]
Material price	EUR/kg	1.68-1.86

Table 6: FRP properties

FRP pipe can be connected with usual bolted flanges, or by laminating the pipe segments together. FRP seems to be a very good option for methods where large pulling forces are exerted on the pipe, as especially longitudinally the material is very strong.

Considering environmental impact, FRP pipes have a major disadvantage as the material, being thermosetting, is difficult to recycle.

Key advantages of FRP	Main Disadvantages of FRP
<ul style="list-style-type: none"> • Strong material • High fatigue resistance • No corrosion or salt water degradation 	<ul style="list-style-type: none"> • Short pipe lengths • Difficult to recycle • Relatively expensive

3.4. Concrete

The final main material which is considered for this thesis is concrete. Like HDPE and FRP, concrete is often used in civil engineering projects for water transport. It is an inexpensive material, and pipes can possibly be produced locally using this material.



Figure 15: Connecting Concrete Pipe Segments

Concrete by itself is very brittle, and does not withstand tension and bending forces well. To improve this, a steel core can be used. The result is a strong pipe which can also withstand some tension forces, is corrosion resistant, impact resistant and can be made up to 4 meters ID[15]. These pipe segments are normally connected with spigot joints as illustrated in figure 15. The disadvantage of these joints is that they cannot withstand large tension forces. It would therefore be very difficult to install the CWP in one piece, as with most installation methods there will be internal tension forces in the pipe. Installing the pipe in segments could be possible, although it would still be a challenge to connect the pipe segments at the seabed. Furthermore, these joints could lead to friction losses in the pipe, decreasing the overall efficiency of the OTEC plant.

Due to the brittleness of concrete, it is unfavourable to use on irregular surfaces. Should subsidence or liquefaction due to seismic activities occur if a concrete pipe is used, it could easily get damaged. Finally, due to the large weight, as large wall thicknesses are often required, the segments which are produced are generally very short, leading to long installation times. Humes, a

large manufacturer of concrete pipes for example produces pipe with a diameter of 3.6 meters with a segment length of 2.44 meters[16].

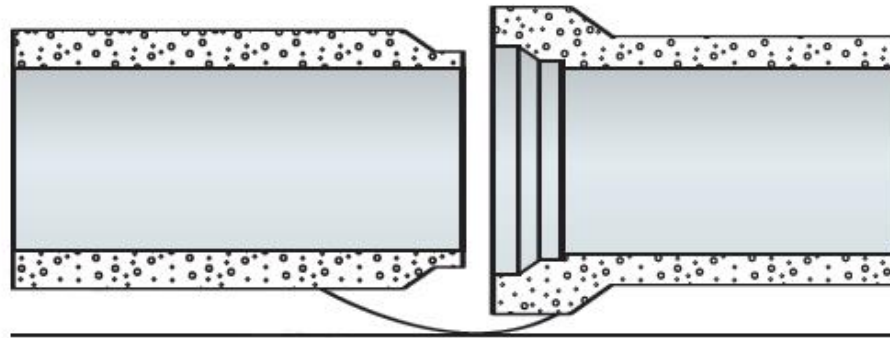


Figure 16: Spigot Joint

Material Property	Unit	Concrete (Portland standard)
Density	kg/m ³	2200-5500
Yield strength	MPa	1-1.2
Max available length	m	2.44
Max available diameter	m	3.6
Material price	EUR/kg	0.0367-0.055

Table 7: Concrete properties

Key advantages of Concrete	Main Disadvantages of Concrete
<ul style="list-style-type: none"> • Inexpensive material • Can be produced locally • Low environmental impact • Can be made up to very large diameters 	<ul style="list-style-type: none"> • In pure form, very limited resistance to bending and tension • Short segments • High wall roughness • Heavy • Joints are difficult to make underwater, and cannot resist pulling forces • Susceptible to fouling

3.5. Materials Multi Criteria Analysis & Evaluation

By comparing the material properties and by using the available experience from previous relevant pipe installation projects, the materials are evaluated. This evaluation is done based on important criteria which they must meet. The criteria are established in a manner such that the materials are evaluated on the lifetime performance of the OTEC plant, not only on the installation performance.

3.5.1. Multi Criteria Analysis

For each criterion, scores are given between 1 and 5, where 5 is the best score and 1 the lowest possible. The main criteria include aspects such as installation performance, thermal performance, durability and costs.

For evaluating the installation methods and materials in the MCA, the effect of weather conditions on the installation are taken into account, as the effect is included in factors such as installation time and installation risks.

For better results, the MCA has been filled in independently by Bluerise, INTECSEA and the author of this thesis, after which the results have been merged.

The shortened MCA is given in table 8, the full MCA is given in Appendix C.

Weight	Criteria	HDPE (PE100)	GFRP Epoxy lay-up	Steel	Concrete
0.15	Risks	3.7	2.3	2.0	3.0
0.2	Installation time	4.5	2.8	2.8	1.5
0.15	Installation technical performance	2.2	2.8	1.8	1.2
0.1	CWP performance	3.3	3.9	2.9	3.6
0.1	Durability	3.2	4.0	3.8	2.2
0.05	Material environmental impact	4.1	1.9	4.1	5.0
0.1	Technical scale up potential	1.6	2.6	1.6	3.4
0.15	Costs	4.0	3.0	3.0	2.0
1	Total score	3.4	2.9	2.6	2.4

Table 8: Shortened MCA of materials

3.6. Conclusion

From the MCA it is found that HDPE is clearly the best material. One of the main reasons for this is that it can be installed in much less time than a CWP made from the other materials. This is due to the long lengths in which it is produced, and thus the short amount of time which is required to connect the pipe segments. If HDPE is used, great care must be taken during installation however, as the material limits are quickly reached.

FRP comes in second place, and seems like a viable material. A significant downside compared to HDPE is that it is produced in small lengths. This results in longer installation times than HDPE, increasing the project costs. In addition, it has the least attractive characteristics from an environmental perspective.

Steel as a material for large diameter cold water pipes could be an option, yet the fact that large diameter steel pipes are only produced with small wall thicknesses greatly decreases the performance of the material, and increases the risks of failure when installing the pipe. Furthermore, as with FRP the connection of the segments takes much longer than with HDPE, resulting in high costs, and depending on the installation method a large required weather window.

Finally, concrete as a material for a CWP is found to be a poor option. Due to the brittleness and inability to bend or flex, and its weakness against pulling forces it can only be practically installed in segments. Furthermore, when installing these segments great care must be taken not to damage the pipe. The very short lengths of the large diameter concrete pipe segments create additional challenges. For very large diameter pipes, above the 4 diameter considered in this thesis, concrete might be the only currently available option.

4. Cold Water Pipe Installation Method Selection

4

As HDPE came out as the most suitable material for large diameter CWP's, this material has been selected for the evaluation of the various installation methods.

For the installation of a Cold Water Pipe many methods can be considered. So far, the most used installation method for existing OTEC plants is the float and sink method. This method has been proven to work well with smaller HDPE pipelines. As this method has been found to be inadequate for large diameter CWP's using HDPE, this installation method must either be modified, or a new method must be found.

In order to find the best installation method for a large diameter CWP, several installation methods are researched. Some of these methods have previously been used for pipe installations in other industries, and others have been newly developed. These installation methods are described independently of the pipe material that is used, although some installation methods are more suitable with certain materials, as the type of loading on the pipe that will occur corresponds with the material properties.

For the installation methods some brief calculations are done, to obtain an impression of the critical factors and limits of the installation methods. As HDPE was found to be the preferred material in chapter 3, this material is used for the calculations which are done in this chapter.

Similar to the materials analysis in chapter 3, the installation methods are evaluated with a MCA, where the criteria follow from the following important aspects for the CWP installation:

- Sensitivity to weather conditions
- Installation time
- Complexity of installation
 - Amount of vessels working simultaneously
 - Requirement for specialized vessels
- Safety
- Sensitivity to varying bathymetry
- Scalability for larger diameter pipes
- Costs

The installation methods which are considered are placed in the following 3 categories:

- Single segment installation methods
- Bottom/ Off-bottom tow installation methods
- Alternative installation methods

4.1. Pipe specifications

In order to compare and evaluate the installation methods, the dimensions and specifications of the CWP must be known. Thus specifications from Pipelife, one of the world's largest HDPE pipe suppliers are used[17]. As Pipelife does not produce pipes with a diameter of 4 meters, the wall thickness of the 2.5 meter pipe is linearly extrapolated.

The pipe specifications which are used are outlined in the table below.

Material	HDPE	HDPE	Unit
Pipe inner Diameter	2.5	4	m
Pipe Outer Diameter	2.738	4.381	m
CWP Density	961	961	kg/m ³
Young's modulus	1050	1050	MPa
Yield strength	21	21	MPa
Max allowed bending radius	30*OD	30*OD	m
Minimum CWP density for bottom installation	1036.7	1033.3	kg/m ³
Maximum section length	500		m

Table 9: HDPE CWP properties

Depending on the installation method, the CWP can be required to have a positive buoyancy, for example when it is floating slightly above the seabed, held in position with anchors. In this case, the HDPE CWP is not ballasted, as HDPE has a density lower than the seawater.

If the CWP is installed on the seabed, it must have a higher density, in order to have a negative buoyancy. Furthermore, after installation current forces will act on the pipe, resulting in drag and lift forces, which could displace the CWP over the seabed if the mass of the pipe is not high enough to withstand these forces.

By adding ballast, for example in the form of concrete blocks, it is ensured that the pipe will remain in position during its operational lifetime. For simplicity, after the amount of required ballast is found, this is included in the density of the CWP resulting in a minimum density for the CWP as seen in table 5. The equations to find the required amount of ballast can be found in Appendix B.

4.2. Single segment installation methods

The single segment installation methods are based on the principle that the entire CWP is installed in a single process. Initially the entire pipe is held at the water surface, either due to keeping the CWP filled with air, or with attached buoys or vessels. The pipe is then either sunk to the bottom by filling it with water, or pulled down to the seabed with cables attached to the seabed.

One of the key advantages of these methods is that the installation is very quick, as the entire pipe is installed at once. Furthermore, the pipe segments do not necessarily have to be brought onshore. The pipe can be transported overseas, and if long HDPE segments are used, it can then be connected as it is held into position near the installation location. One of the challenges with these installation methods is that the CWP will be influenced by weather conditions as it is installed. Calm weather is required, as well as monitoring of the lateral displacement of the pipe during the installation.

Although several vessels might be required for these installation methods, they are generally simple tugs or small crane vessels. Due to the short installation time these vessels are required, the costs are expected to be low for these installation methods. The main unknown is if these methods can be used for the large diameter CWP's considered in this thesis, without exceeding the material limits of the pipe.

The single segment installation methods which are considered are:

- Modified float and sink method
- Modified float and sink method with additional buoyancy and or ballast
- Brewers method
- Modified float and sink method in combination with Brewers method
- Hold and Sink method

4.2.1. Modified Float and Sink Method

As some of these methods are based on the F&S method, this method is described first. For this method, it is required that the CWP is buoyant when filled with air, and sinks when filled with water. The pipe is initially held at the water surface above the location where it must be installed, as a tension force is applied to the end of the pipe by a tug vessel to keep it straight. To install the pipe, it is slowly filled with water from the shore end, and the pipe starts to sink. Naturally, the pipe will start to bend, as the air filled part of the pipe remains floating at the surface. To prevent the pipe from bending too much, the tension force applied to the pipe end must be large. As the water depth increases, the forces in the pipe increase due to the mass of the suspended pipe, which is countered by a large tension force. The limit for this installation method, is when the combination of suspended pipe mass and water depth become too large. The tension must be high enough to prevent buckling, but will eventually become higher than the yield strength of the pipe material. Figure 17 depicts the float and sink installation procedure.

By decreasing the total submerged pipe mass, for example by adding buoys, or by decreasing the suspended pipe mass by holding the pipe end underwater for example, instead of on the water surface, it might be possible to increase the limits of the installation method enough for the large CWP's considered in this research.

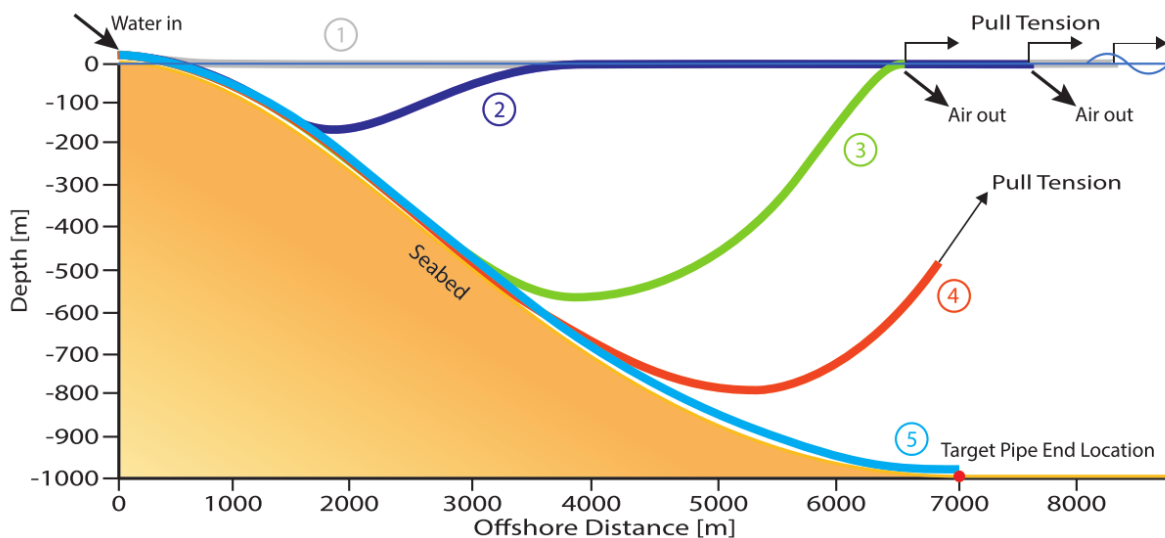


Figure 17: Depiction of the float and sink installation procedure

4.2.2. Modified Float and Sink with Buoyancy and/or Smart Ballasting

The idea is to use the F&S method, in combination with buoys or additional vessels to support the pipe, and thus decrease the amount of pull force which must be applied on the pipe end, and to decrease the amount of bending in the CWP as shown in figure 18. Additionally, near the end of the CWP additional ballast can be attached to bring the pipe end below the surface, to decrease the amount of bending in the pipe even more. As buoyancy modules are less expensive than using vessels, these are preferred. After the installation, the buoyancy modules are released, and the vessels are disconnected. Although these modifications add costs and complexity to the original float and sink method, this method might still outperform the other installation methods.

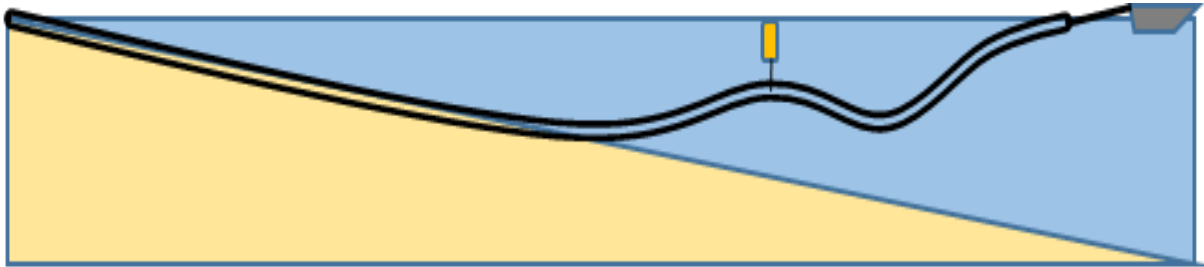


Figure 18: F&S with Lazy Wave / Smart Ballasting

The installation procedure could either be performed by having a load out from shore, where pipe ends are connected before the pipe string is launched into the water, or by attaching the segments offshore, in the case of large floating sections, as would be likely if HDPE is used.

As the pipe is being lowered by filling it with water, this also means that the pipe can be relocated if it is misaligned during the installation by pumping water out of the pipe. Still, due to the very long floating pipe string it is expected to be quite a challenge to locate the pipe precisely, as it will be affected by currents, waves and wind.

Some of the benefits and downsides of this installation method are shown below.

Positive	Negative
Inexpensive installation	Less accurate positioning of pipe
Small amount of vessels required	Large influence of weather conditions, when the pipe is held at the surface
Quick installation process	

Float and Sink Installation Limits

Previous research by K. Keesmaat has shown that the maximum diameter for an HDPE CWP which is installed in 1000 meters water depth using the conventional F&S method is approximately 2.3 meters[5]. It can be expected that this limit can be increased by modifying the installation method. The question is if it can be increased enough to install a 4 meter diameter CWP. Unfortunately the catenary model which he uses, cannot incorporate buoys and local ballasting. His research also shows that by increasing the applied tension, the installation limit can be increased as the bending stresses in the CWP are reduced, as shown in figure 19. In his research, the limit of the amount of applied tension force is assumed to be 390 mT. This value is also used in this thesis, as this is based on the bollard pull which some of the largest tugs can deliver[18].

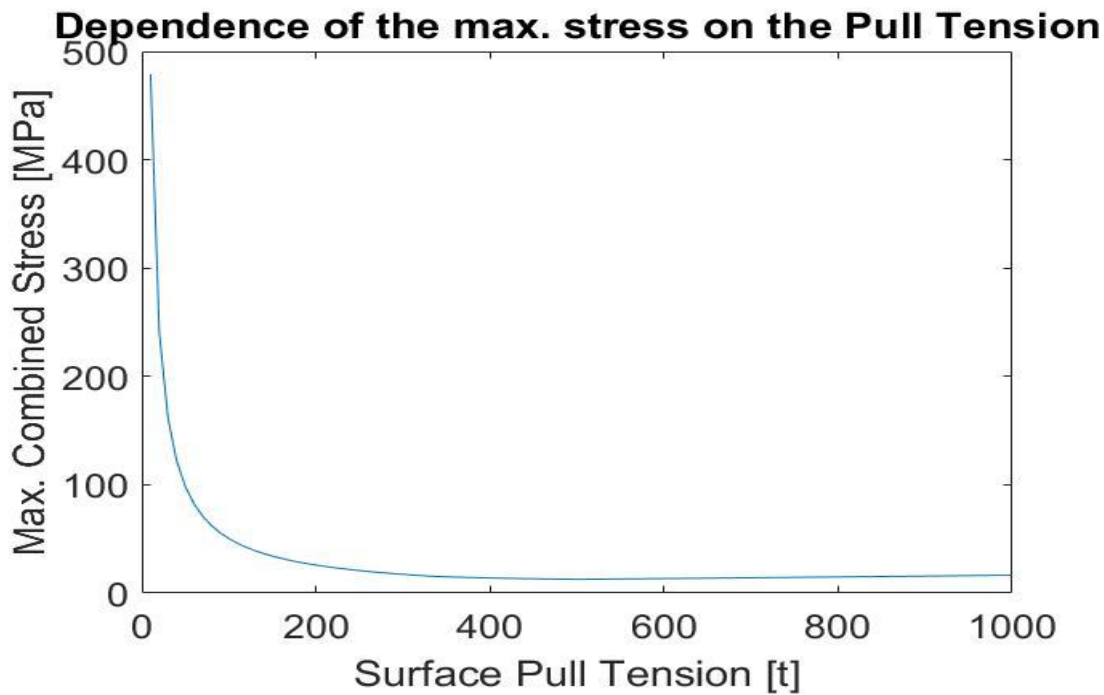


Figure 19: Dependence of the Maximum Stress on the Pull Tension

4.2.3. Brewers Method

The Brewers installation method was proposed by Brewer in 1979 as an installation method for OTEC cold water pipes[19]. As with the F&S method, Brewers method can also be used to install the entire CWP at once. With this method it is required that the CWP must be buoyant, even after being filled with water. The pipe is positioned above the installation location at the water surface, and is then pulled down to its location using cables connected to anchors on the seabed. The cables are guided through pulleys on the anchors, and then back up to the surface where they are connected to one or multiple vessels. These vessels use winches to pull the pipe down until it reaches its final position, suspended above the seabed. In order to minimize the costs, it might be possible to replace some of the vessels with buoys, as illustrated in figure 21, which is an original drawing by Brewer.

One of the benefits over the F&S method, is that the shape of the entire pipe can be manipulated very accurately. Bending can therefore be reduced, by using the correct amount of anchors. This will result in lower forces on the pipe, increasing the limit of pipe diameters that can be installed.

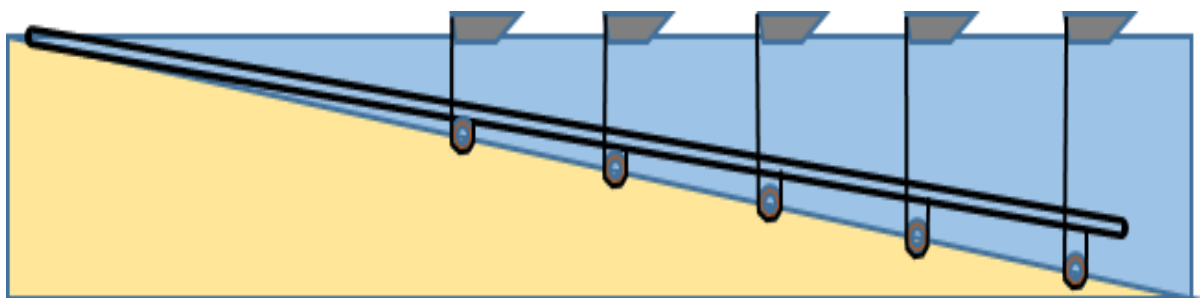


Figure 20: Brewers Method - Illustration of Replacement of Vessels with Buoys

The benefit of this method, is that the pipe is installed hovering above the seabed. Seabed irregularities are therefore not a problem, as these do not interfere with the pipe. Therefore, in locations with hard irregular rock bottoms, this installation method could be a good option. As the pipe end is also suspended above the seabed, there is no risk of sand and debris from the bottom being pumped up. A disadvantage however of installing the pipe in this manner, is that it is more exposed to currents, and can displace slightly, making the pipe, cables and anchors more susceptible to fatigue.

Due to this, and the constant stress acting system during its lifetime, there is a risk of anchors coming loose, or cables failing which could result in failure of the pipe.

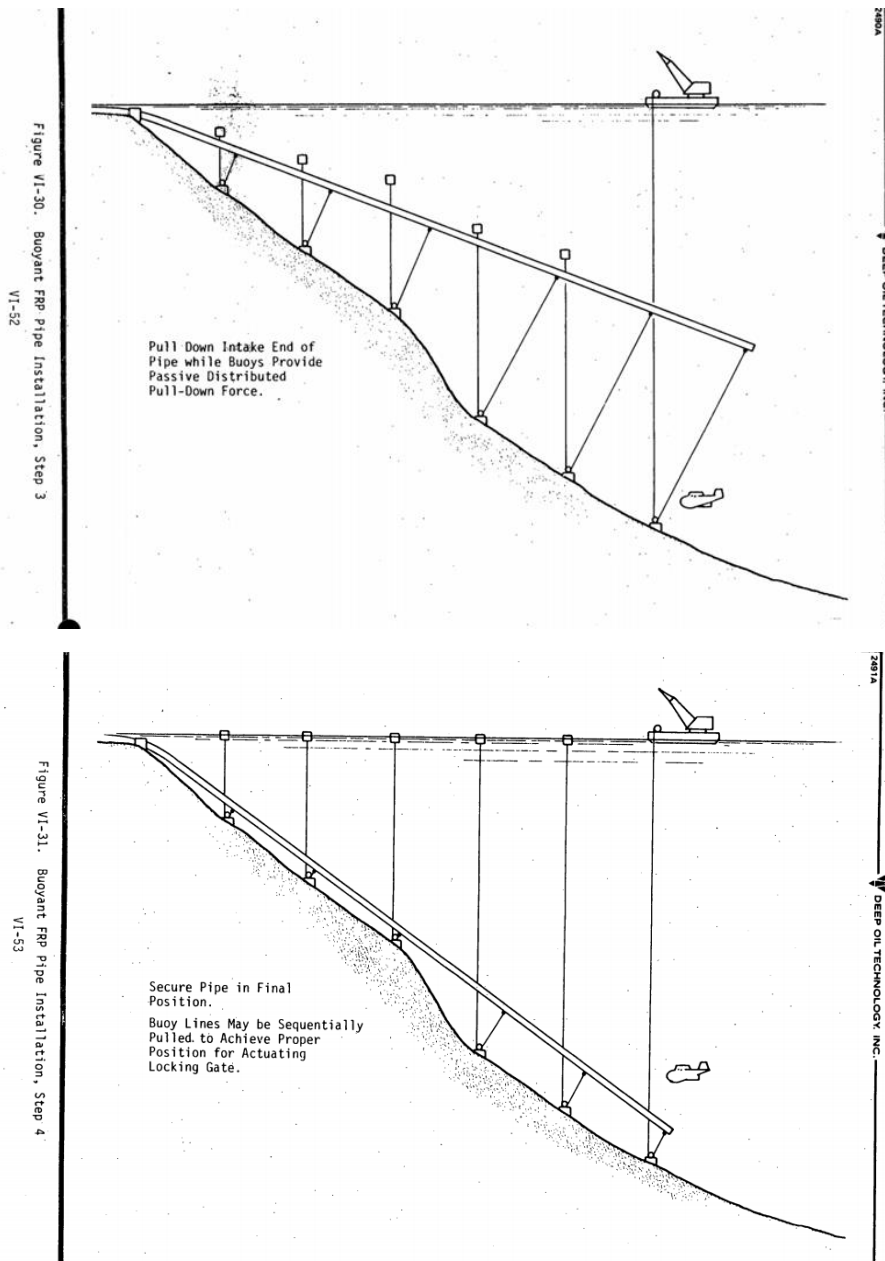


Figure 21: Buoyant FRP Pipe Installation (Deep Oil Technology Inc)

Positive	Negative
No influence of irregular seabed	Many vessels / buoys required
Suitable for large diameter pipes	Risk of failure of the system due to constant loadings during lifetime
Controlled installation and decommissioning	Installation of anchors at deep water depth. Long cables required for pull down

For Brewers method, it is assumed that the cost of the CWP installation is very dependent on the amount of anchors which is required. Therefore, a quick estimation can be made. , so the first step is to find the amount of required anchors.

For this, the CWP is assumed to behave as several fixed - fixed beams connected to each other, where the length of each beam is the distance between two anchors. This is under the assumption that the cables that pull on the CWP are equally distributed along the pipe, and exert an equal force on the pipe. Due to the buoyancy of the HDPE, the pipe will bend upwards as shown in figure 22. Due to the buoyancy force, a bending moment occurs in the CWP. The maximum allowable stress in the pipe determines the amount of required anchors. Besides the allowable stress, the overall bending of the CWP is also important. If a flexible material such as HDPE is used, the vertical displacement of the CWP can get quite large, resulting in impractical installation conditions.

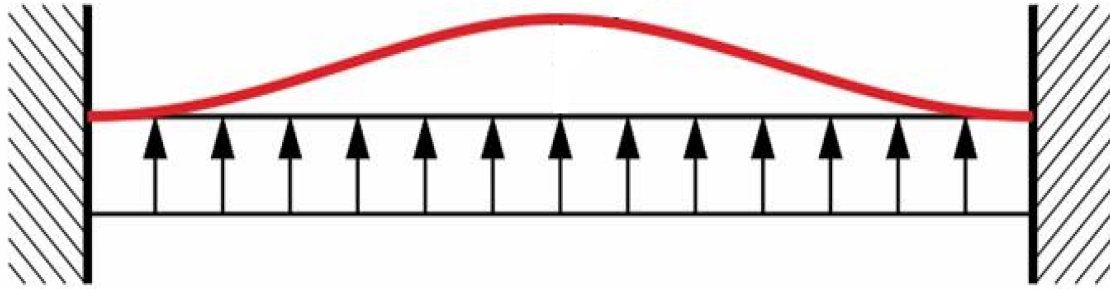


Figure 22: Illustration of Upward Pipe Displacement

The maximum displacement of the pipe will occur in the middle between the anchors. This can be found using formula 4-1.

$$w_{\max} = \frac{q_0 \cdot L^4}{384 \cdot EI} \quad (4-1)$$

Where

$$q_0 = (\rho_{CWP} - \rho_{seawater}) A_{CWP} \cdot g \quad (4-2)$$

And E is the Young's modulus, and I the moment of inertia of the pipe, which can be found using equation 4-3.

$$I = \frac{\pi}{4} \cdot (R_o^4 - R_i^4) \quad (4-3)$$

The maximum occurring bending moment in the pipe occurs in the fixed connections, and can be found with formula 4-4.

$$M_{\max} = \frac{q_0 \cdot L^2}{12} \quad (4-4)$$

As only stress in the pipe due to bending is considered for this calculation maximum allowable bending moment in the pipe can be found with formula 4-5.

$$M_{\lim} = \sigma_{yield} \cdot \frac{I}{R_o} \quad (4-5)$$

Where σ_{yield} is the yield strength of the pipe material.

Brewers Method	Max segment length HDPE 2.5m ID	Max segment length HDPE 4m ID
Max vertical displacement of pipe	58.3m	58.3m
Clamped-clamped	422.8	534.9m
Minimum amount of anchors required	17	14

Table 10: Maximum pipe segment length for Brewers method

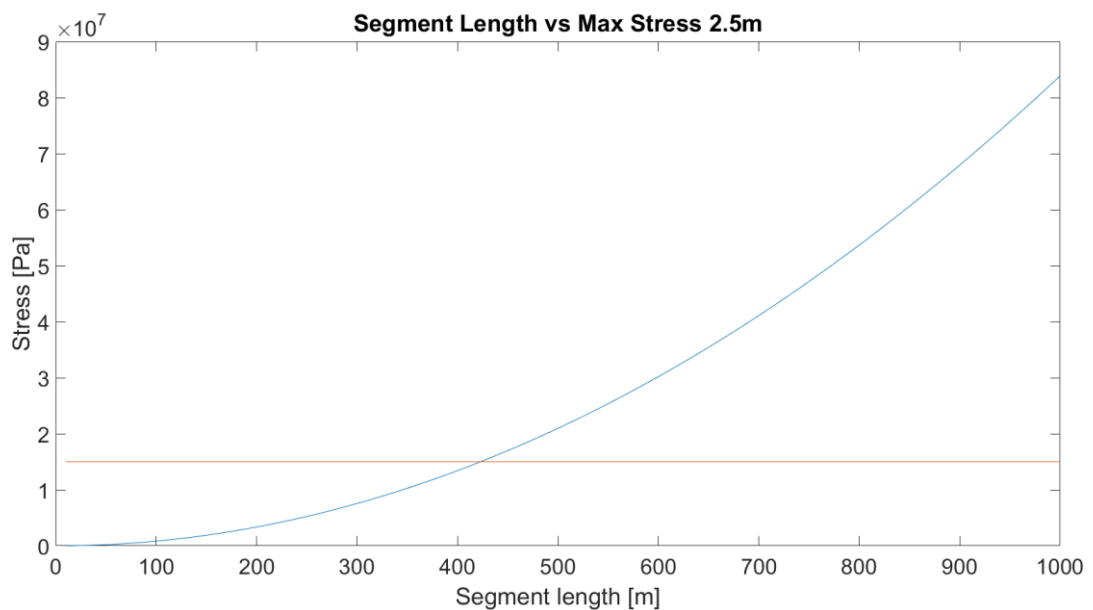


Figure 23: Comparison of Segment Length and Stress for a 2.5m CWP

4.2.4. F&S hybrid with brewers method

Due to the amount of anchors required for Brewers method, it is expected to cost more than an installation using the float and sink method. To minimize costs, these 2 methods can be combined as illustrated in figure 24. The first part of the CWP is ballasted, so that F&S is used until the water depth becomes critical for the pipe stresses. From this point, the pipe is unballasted. Brewers method is then used to pull down the remaining pipe length. By doing this, the bending stresses can be decreased compared to the conventional float and sink method.

Due to the use of Brewers method, the height of the pipe end can accurately be determined, and is installed slightly above the seabed, in order to make sure no sand or sediment will flow through the pipe end during operation.

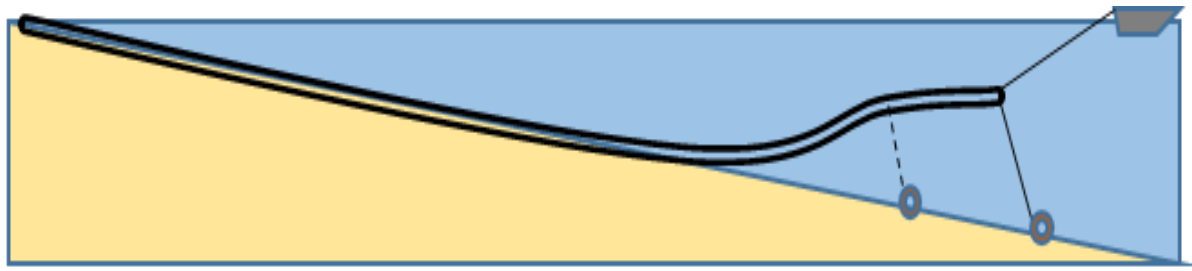


Figure 24: F&S Hybrid with Brewers

Positive	Negative
Relatively few vessels required	Risk of breaking loose of CWP end
Precise and simple locating of pipe end compared to conventional float and sink	Fatigue on CWP end and components
Quick installation	Installation of anchors at large water depth
	Long cables required for pull down

4.2.5. Hold and Sink installation method

The hold and sink (H&S) method is the final installation method which is considered where the pipe is installed as a single segment. Initially the CWP held at the water surface where it is kept into position with several ships and possibly buoys. For this installation method, the pipe must have a negative buoyancy, so that it can sink to the seabed. The pipe is filled with water, while still being held at the water surface. As the entire pipe is filled, it is slowly let down, where the shape of the pipe is controlled by the vessels and buoys holding it from the surface, as well as by a tension force applied on the pipe end.

The result is that the pipe can be installed with less bending than with the float and sink method, although more vessels are required. There are similarities to Brewers installation method, as multiple lowering points are used. Using this method however, it is possible to apply a tension force on the pipe end during installation, which can result in less required lowering points on the pipe.

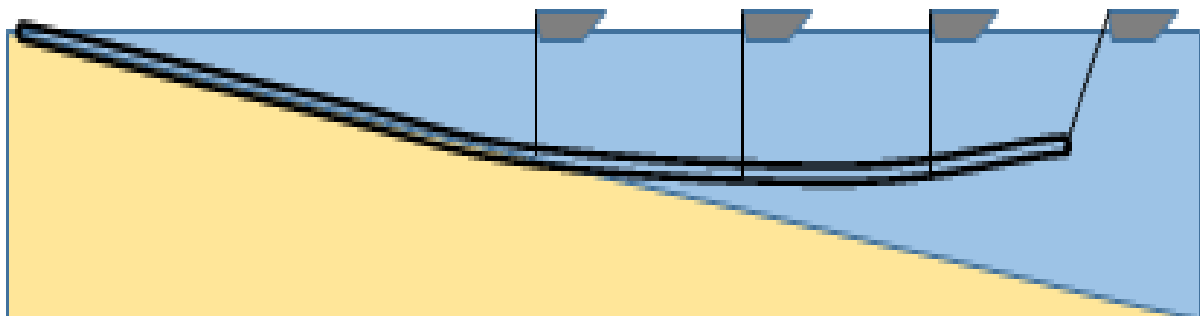


Figure 25: Hold and Sink Method

Positive	Negative
Limited bending of CWP	Many vessels/ buoys required
Highly adjustable installation method	
Quick installation	

In a similar manner to the calculations done for evaluating Brewers method, the minimum amount of lowering points is found for the hold and sink method. The main difference is that the pipe now has negative buoyancy, resulting in downward bending, shown in figure 26.

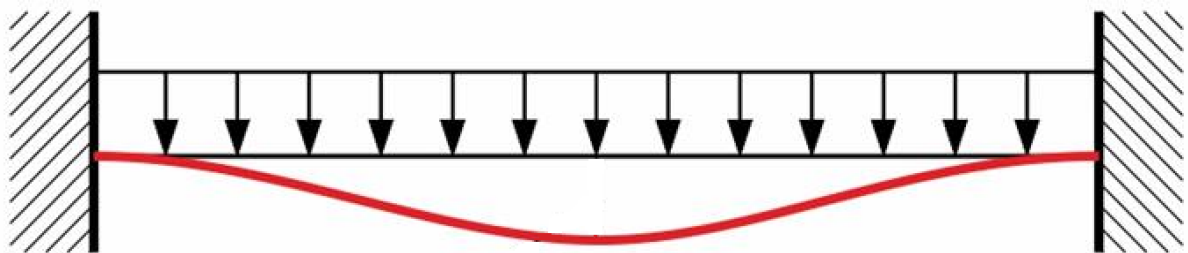


Figure 26: Illustration of Downward Pipe Displacement

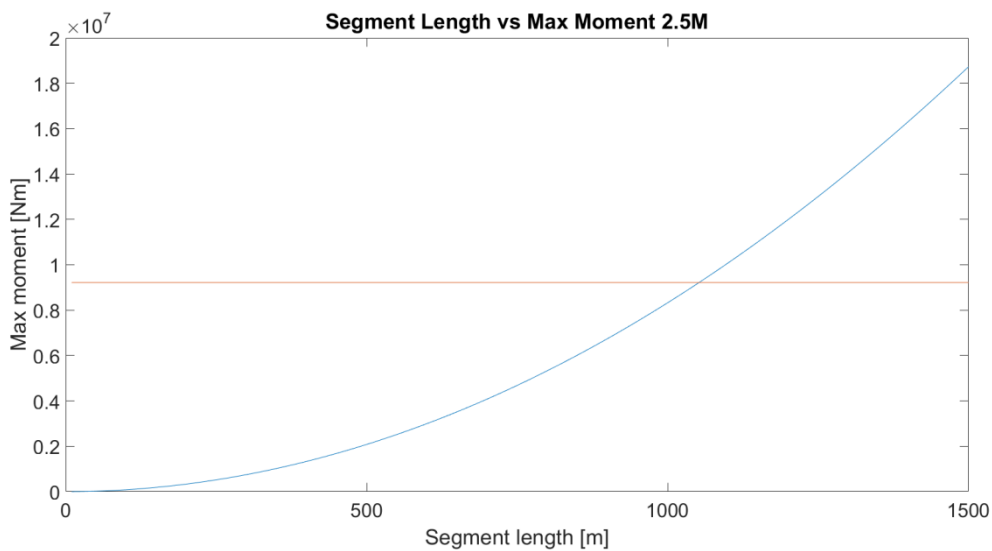


Figure 27: Comparison of Segment Length and Bending Moment

The results are given in table 11. For these calculations, the minimum required ballast is used to keep the CWP stable on the seabed during operation. As seen, the resulting pipe lengths are longer than when using Brewers installation method. This is due to the fact that the buoyancy force of unballasted HDPE is larger than the total negative buoyancy force of the ballasted HDPE pipe, when installed using the H&S method. As seen, the vertical displacement is very large, if the minimum amount of lowering points would be used. This is impractical, so therefore the maximum vertical displacement due to bending is limited at 75 meters. This gives more reasonable results for a pipe installation procedure. These values do not include the tension force, which can decrease the amount of bending in the pipe and therefore the amount of required lowering points.

Hold and sink method	Max segment length 2.5m ID HDPE	Max segment length 4m ID HDPE
Max vertical displacement of pipe	361m	603m
Max distance between lowering points	1052m	1689m
If limited to 75 meters	710m	1002m
Minimum amount of lowering points required.	10	7

Table 11: Maximum segment length for H&S

4.3. Bottom Tow installation methods

The second category of installation methods consists of the bottom tow methods, the off-bottom tow and the bottom-tow method.

Both installation methods are similar. The installation starts from shore, where the pipe is pulled out over the seabed until it is installed at the required position. As the installation starts from shore, the pipe segments can be connected onshore, as the pipe is slowly pulled out into the ocean. If the weather conditions change, the pipe installation can be stopped, and continued again if the weather calms down. The advantage of these methods is that the bending of the pipe is reduced to a minimum. This is beneficial if materials are chosen that are not allowed to bend much, but can resist large axial stresses. These installation methods are sometimes used in the offshore industry for transporting steel pipes short distances.

The major downside of these installation methods is that the pipe can get damaged, or even potentially stuck if the seabed is not smooth. It can be expected that for some OTEC project locations, extensive seabed preparation would be required.

4.3.1. Off-bottom tow

The off-bottom tow installation method can be used if the cold water pipe has a positive buoyancy. The CWP segments are connected onshore, and then pulled into the ocean. To lower the forces on the pipe, a guide track can be built which reaches into the water. The pull out is then done by a large tug, which pulls on the end of the pipe. The cable can go either directly to the pipe, or via a pulley on the seabed.

As the pipe is buoyant, large metal chains are connected to the CWP, to prevent it from floating. Due to the mass of the chains, the pipe will be in equilibrium at a certain distance from the seabed.

One of the risks is that the chains will catch on the seabed during the installation, or the drag of the chains becoming too high to complete installation. Therefore, a detailed metocean survey must be done to identify a safe route for installing the pipe. Furthermore, a possible risk is that as the pipe will move under strong currents, as the chains will not be secured to the seabed.

As the CWP must be built from shore, the installation is expected to take longer than with the single segment installation methods.

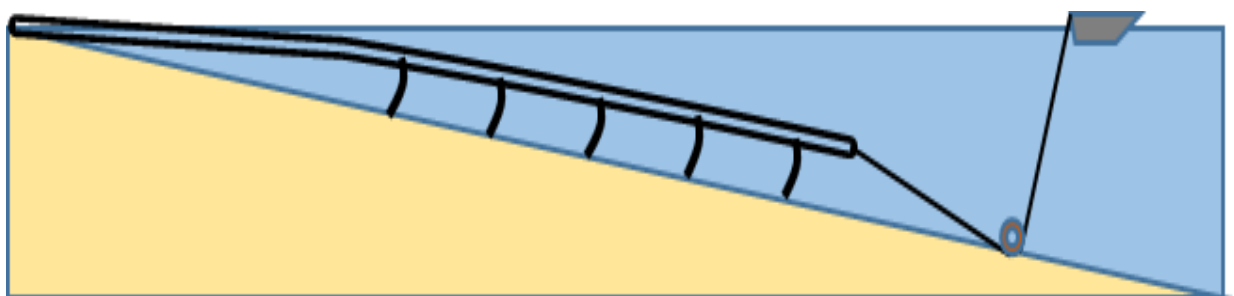


Figure 28: Illustration of Off-bottom Tow

Positive	Negative
Good for free spans	Risk movement of pipe during operation
Segments are connected from shore	Risk of catching on the seabed during installation
Minimal bending of the pipe	Bottom preparation possibly required
Limited influence of waves during installation	Fatigue/ VIV's

4.3.2. Bottom tow

The bottom tow method is nearly identical to the off-bottom tow method. The pipe segments are connected on shore, and then pulled and/or pushed out into the water.

The main difference with the off-bottom tow method for using this method, the pipe must have a negative buoyancy. Due to this, there are no chains required to prevent the pipe from floating. The pipe is towed directly over the seabed. As the pipe is installed directly on the seabed, it will experience less influence from currents. This also brings risks for the installation, as the pipe can damage as it is in direct contact with the seabed.

Bottom tow is a method that has been used in the offshore industry several times for steel pipelines, with pipe lengths up to 16 kilometres [20].

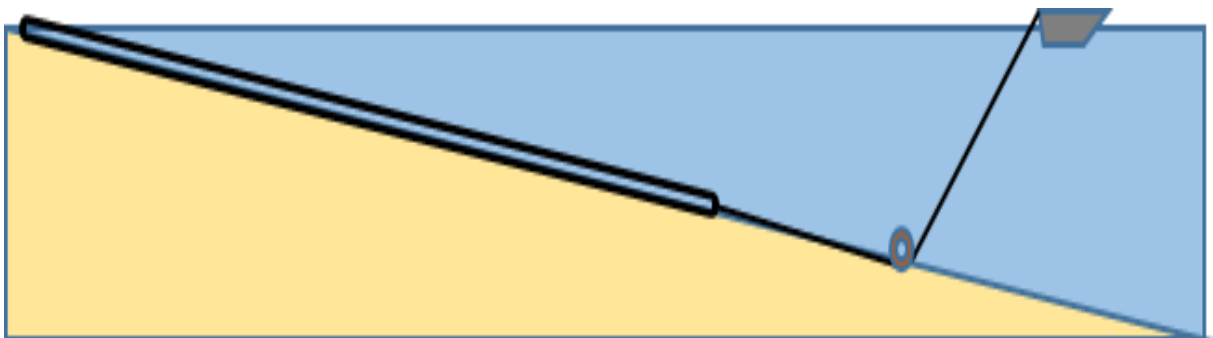


Figure 29: Illustration of Bottom Tow

Positive	Negative
Segments are connected on shore	Potential risk of damage during installation due to contact with seabed. Large pulling force required.
Minimal bending during installation	Extensive bottom preparation and surveys required
Small influence of weather during installation	

For evaluating the bottom tow installation methods, it is important to have an impression of the required pull force to install the cold water pipe.

The friction coefficient of the seabed has a large influence on this force. In literature a friction coefficient of 1 [20] has been found for a seabed consisting of sand. It is stated that this value is occasionally used for transport and installation of pipes using the bottom tow method.

Theoretically, the total friction forces do not differ for a bottom tow or off-bottom tow, as the required downward force on the seabed is the same, in order for the pipe to be stable. This is if the influence of currents is assumed to be the same. For this reason, the results are the same for this check. It is also assumed that the CWP does not drag on rocks or coral, which could potentially severely increase loads on the CWP and damage the CWP.

Table 12 shows that both 2.5 and 4 meter diameter cold water pipes can be installed under ideal circumstances based on these calculations. The maximum stress is well under the material limit if HDPE is used. The pull force is also within the range of what can be provided by large tugs.

Bottom tow installation methods	2.5m HDPE	4m HDPE
Max axial stress within pipe for 1000m WD	1.53 MPa	1.30MPa
Required pulling force for installation	153mT	331mT

Table 12: Axial stress and pull force for bottom tow installation methods

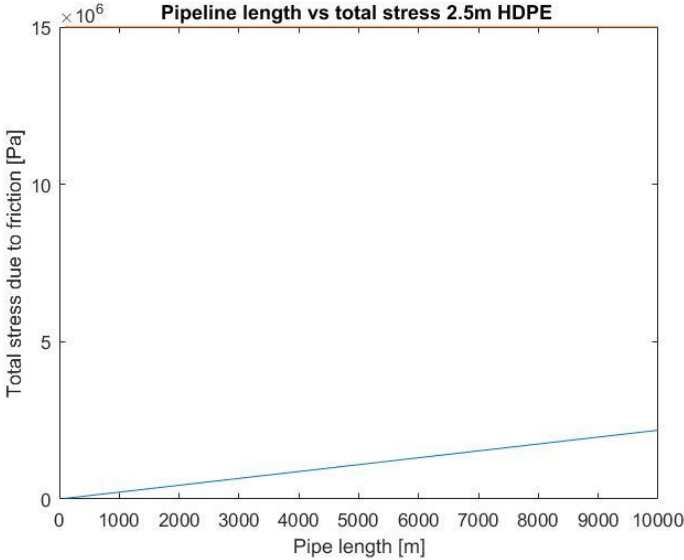


Figure 30: Pipeline Length versus Total Stress (2.5m HDPE)

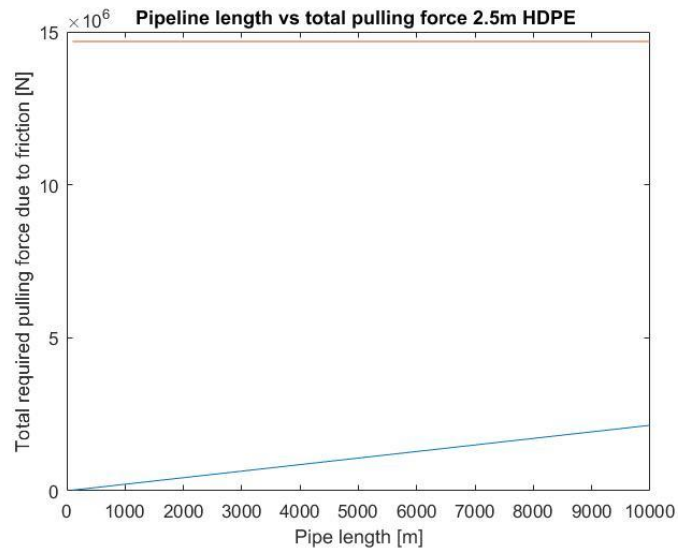


Figure 31: Pipeline Length versus Total Pulling Force (2.5m HDPE)

4.4. Alternative installation methods

In this chapter the final two installation methods are discussed, installation by sections, and tunnelling.

4.4.1. Installation by sections

Instead of installing the entire pipe in a single complex procedure, the pipe can also be installed in pieces, using relatively simple crane vessels. The segments are lowered to the seabed, where they are connected with the help of ROV's. The main advantage of this method is that the installation is spread out in small steps, where the pipe segments are individually installed.

Using this method, the installation will take longer than with the single segment methods. To decrease the installation time, it should be checked what the maximum segment length is which can be installed per time. The main advantage of this method is seen for very large diameter CWP's, which cannot be installed in any other manner.

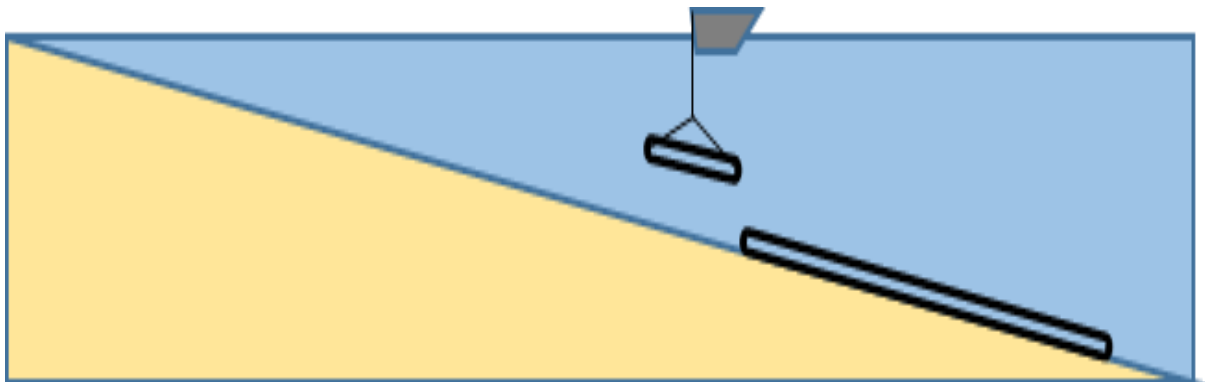


Figure 32: Installation by Sections

Positive	Negative
Can be used for very large diameter CWP's	Long installation time
Small forces in the pipe during installation	Not good for free spans
Work can be stopped and proceeded rapidly if required	Difficult connections on the seabed

To find the maximum length of the segments which can be installed, similar calculations are done as for the hold and sink installation method. As the segments are installed individually, they are better described as a pinned-pinned beam, as shown in figure 33.

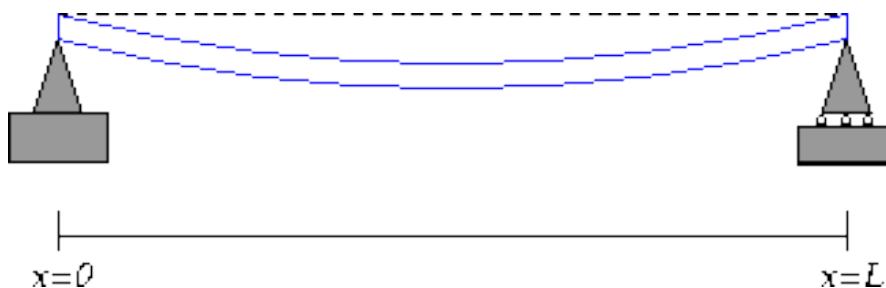


Figure 33: Calculation to Determine the Maximum Length

Therefore, the maximum displacement of the middle of the pipe segment is described with formula 4-6.

$$w_{\max} = \frac{-5 \cdot q_0 \cdot L^4}{384 \cdot EI} \quad (4-6)$$

The maximum occurring bending moment in the pipe is now found using formula 4-7.

$$M_{\max} = \frac{q_0 \cdot L^2}{8} \quad (4-7)$$

As seen in table 13, the displacement becomes very large if the material limits are reached. As this is very impractical, the maximum displacement is again limited to 75 meters, as in chapter 4.2.5.

Installation by segments	Max segment length 2.5m ID HDPE	Max segment length 4m ID HDPE
Pinned-pinned assumption	859m	1354m
Max displacement	-802m	-1246m
Displacement limited at 75m	475m	671m

Minimum amount of segments required	15	11
-------------------------------------	----	----

Table 13: Segment length limit for installation by segments

4.4.2. Directional Drilling

Besides installing the CWP on the seabed, an alternative is to drill a tunnel through the seabed up to the required water depth. For the CWP, directional drilling is currently not possible, the limit is at approximately 36 inches in diameters, with distances achieved of up to approximately 4.5 kilometres. Alternatives to directional drilling are tunnelling using a Tunnel boring machine (TBM), or micro tunnelling which are very similar. Tunnel boring machines are widely used, and go up to diameters of 17.5 meters[21]. A distance of 7km would not be an issue for a large TBM. TBM's are only used relatively close to the surface such as under rivers, so they are never exposed to the large amounts of hydrostatic pressure at 1000m water depth.

Currently the deepest tunnel in the world is the Eiksund tunnel, of which the deepest point below sea level is 287 meters. The length of the tunnel is 7765 meters. This tunnel was constructed using the drill and blast method, and cost approximately 500.000.000,- NOK, or 53 million euros[22].

At this point it is considered unrealistic to tunnel to these large water depths, however in the future this could prove to be an efficient manner to create a cold water inlet for OTEC, especially if large diameters are required.

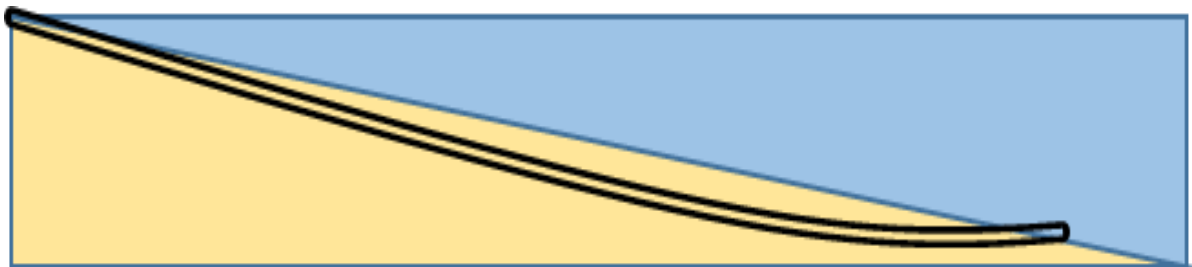


Figure 34: Directional Drilling

Positive	Negative
No pipe transport/ installation	There are no machines capable of going to these depths
Concrete for wall support can be made locally	After punching through into the ocean at the end of the tunnel, the machine must be recovered
Minimal interaction with marine life/ coral	There is a risk of getting the machine stuck, leading to a complete failure
No influence of currents	Risks of tunnel collapse
No risk of dropped anchors or other forms of human interference	

4.5. MCA

As with the evaluation of the materials in chapter 3, the installation methods are compared and evaluated with a multi criteria analysis. The criteria are not only based on the installation, factors which affect the lifetime performance of the pipe, are also taken into account. These are factors such as ease of decommissioning, which is dependent on how the pipe is connected to the seabed, and risks of failure before the end of lifetime for example.

Focus is laid on finding an installation method which is applicable in locations with varying metocean conditions, as it is important that the installation method is generally applicable for any given OTEC project.

While scoring the different installation methods, the attempt is made to score the methods independently of the used material.

Although these parameters are fixed, the influence of these on the installation process is still taken into account.

As with the materials MCA, the installation MCA has been filled in independently by Bluerise, INTECSEA and the author of this thesis, after which the results have been merged. For each criterion, scores are given between 1 and 5, where 5 is the best score and 1 the lowest possible. The summarized MCA with the highest scoring installation methods is given in table 24. The complete MCA can be found in Appendix C.

Weight factor	Criterion	F&S with lazy wave	F&S hybrid with brewers	Hold & Sink	Brewers with ships	Bottom tow	Off-bottom tow
0.15	Installation conditions	3.8	3.3	3.3	3.0	3.8	3.4
0.2	Sensitivity/adjustability	3.0	3.0	3.3	4.0	1.9	2.5
0.1	Environmental impact	2.7	2.7	3.0	3.0	1.3	2.7
0.2	Risks	3.4	3.5	3.6	3.2	2.9	2.7
0.1	Technical scale up potential	1.9	1.9	2.7	1.6	2.8	2.4
0.1	Safety	3.3	3.3	2.7	3.7	3.3	3.3
0.15	Costs	4.0	3.3	3.5	2.3	3.7	3.3
1		3.2	3.1	3.2	3.0	2.8	2.9

Table 14: Summarized installation method MCA

4.6. Conclusion

From the MCA it follows that the single piece installation methods are seen as the best method for a CWP installation. The short installation time when using these methods distantiates these methods from the other installation methods. As discussed previously, one of the main challenges for the single string installation methods is to limit bending, which has been identified as the limiting factor for the float and sink method. The MCA shows that it is still thought that by improving and optimizing the installation method, be it with buoys, additional ballast, or by pulling the pipe down these large diameter cold water pipes can be installed. It is thought that by using the hold and sink installation method, the shape of the pipe can be controlled even more precisely, to minimize bending even further. The material properties of HDPE correspond well to the best installation methods, as it is relatively flexible.

In order to confirm that these installation methods can indeed be used for the installation of a large diameter cold water pipe, a model is made in which these installation methods can be compared, and where the influence of various loadings on the pipe can be found.

If we look at the F&S method in combination with Brewers method, it can be seen that instead of pulling the CWP end down, it might be better to attach a large mass to it, and to guide it down with a vessel from the water surface. This makes it simpler to apply a tension force on the end of the pipe, using a vessel at the surface.

As the modified float and sink method and the hold and sink method are seen as the best installation methods, the rest of the thesis focusses on evaluating these installation methods. To further evaluate these methods, a model is created in which the installation process can be simulated using these different installation methods.

5. Numerical Modelling of the CWP

5

From the materials and installation methods analysis it is found that overall, the single segment installation methods, in combination with an HDPE pipe are considered to be the best. It is still not certain however if an HDPE pipe can be installed without exceeding the material limits using these methods. Therefore, it is important to know how the pipe will behave during the installation, and what the stresses in the pipe will be. Furthermore, there are many different factors which have an influence on the stresses in the pipe during the installation, such as the tension force, the amount of ballast, and the amount of buoys which are attached to the pipe. For this reason, a model has been developed in which the pipe installation using these different methods can be simulated. In order to model these different installation methods, it must be possible to apply external forces which resemble buoys or ballast attached to the pipe.

The entire pipe installation is modelled, and the stresses in the pipe are calculated throughout the entire installation. Within the model, parameters of the installation can be changed to find the influence on the installation procedure.

In order to be able to analyse the entire installation process, independent of the installation method, it's chosen to make a numerical model in which the pipe is modelled dynamically in the vertical direction. Numerical modelling is chosen as it is simple to adapt to different installation scenarios. The model is made in such a manner that it can be adjusted so that all relevant single piece installation methods can be modelled.

In a real life situation, there are forces acting on the pipe in all directions during installation. Due to the fact that weather conditions are neglected, it is assumed that the model gives representative results by only describing the pipe in the vertical plane.

The purpose of this model is to do comparisons of different installation scenarios, to find if the pipe bending can be kept small enough for the pipe installation to succeed. After obtaining results, the final preferred installation method should be modelled with a more accurate validated engineering software package, to find the exact stress in the cold water pipe.

5.1. Model Theory

For modelling the cold water pipe installation, several theories can be used. Each theory has its own benefits and downsides, and the accuracy of the theory is based on the assumptions which are made, and the problem which is solved. For this research, it is chosen to describe the CWP using Euler-Bernoulli beam theory, which is solved numerically using a finite difference method.

Euler-Bernoulli beam theory is accepted for small amounts of bending, and for beams with a large length over diameter ratio. When the bending of the pipe becomes large, the theory is inaccurate and is known to underestimate the displacement of the pipe. One of the assumptions for this theory is that the cross section of the pipe does not change due to bending, so that the cross section of the pipe remains perpendicular to the bending line. A second main assumption is that there is no shear strain in the pipe.

The CWP has a length of 7000 metres, with a maximum outer diameter of 4.381 meters. As this results in a length over diameter ratio of over 1500, the CWP can be considered to be thin. Due to this, and the fact that the purpose of this model is to find an installation method where the bending of the pipe is minimized, Euler-Bernoulli beam theory is accepted.

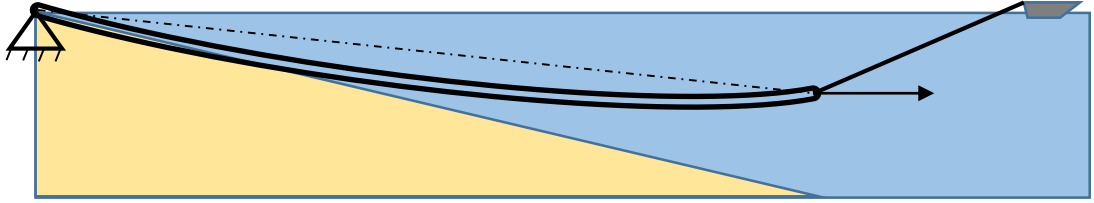


Figure 35: Illustration of the basic pipe configuration

5.2. Equation of Motion

The CWP is modelled as a nonlinear Euler-Bernoulli beam, of which the equation of motion, equation 5-1, is a 4th order differential equation. This equation is used, and describes the CWP only in the vertical plane.

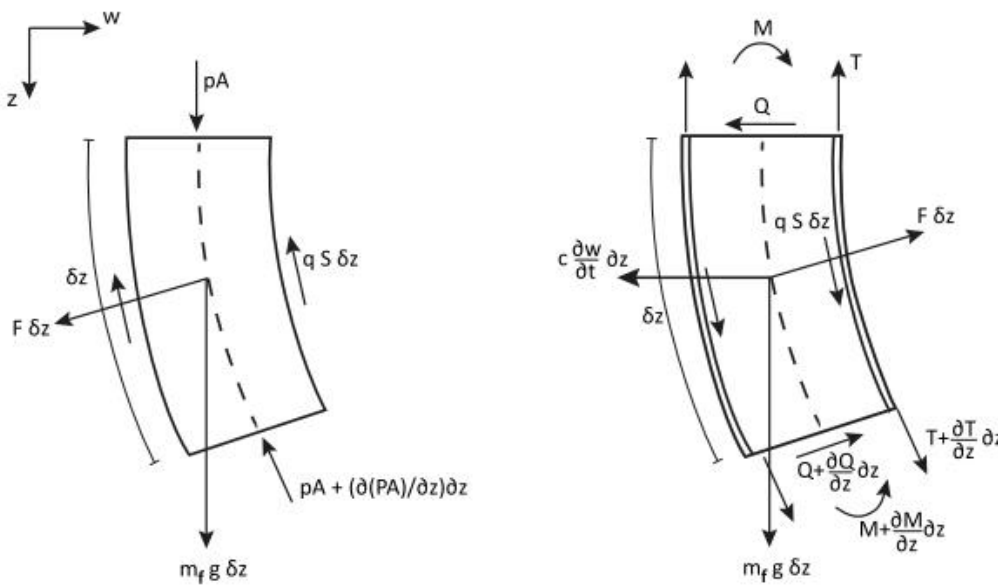


Figure 36: Euler-Bernoulli beam theory

$$\begin{aligned}
 & EI \frac{\partial^4 w}{\partial x^4} - T \frac{\partial^2 w}{\partial x^2} + \underbrace{(m_p + m_a)}_3 \frac{\partial^2 w}{\partial t^2} + \underbrace{k_d(x)(w - d_{sb}(x))}_4 + \underbrace{c_d(x) \frac{\partial(w - d_{sb}(x))}{\partial t}}_5 \\
 & = \underbrace{\tau_{Morison}(x, t)}_6 - \underbrace{q_{gravity}(x)}_7 + \underbrace{f_{vessel}(x)\delta(x-a)}_8
 \end{aligned} \tag{5-1}$$

The equation of motion is a fourth order differential equation, which consists of the following terms:

1. Restoring force due to the bending stiffness of the beam
2. Restoring force due to tension in the CWP, applied by tug
3. Inertia forces of the pipe and added mass
4. Stiffness of the seabed
5. Damping of the seabed
6. Distributed force due to hydrodynamic drag
7. Distributed load along the CWP due to gravity

8. External load such as a lifting force from a vessel

The tension force is assumed to be constant throughout the entire pipe, as the force is applied by a tug continuously and slowly.

During installation, the CWP will be affected by drag from the water as it is lowered or raised. The resulting drag is due to water flowing around the pipe. This drag force is approximated using Morisons equation, shown in equation 5-2. This equation has been found empirically, and is accepted to be valid for slender pipes, generally when $\frac{D_o}{L_{CWP}} \leq \frac{1}{20}$, which is the case for the CWP dimensions discussed in this thesis.

$$\tau_{Morison}(z,t) = \frac{1}{2} \rho C_D D_o \dot{w}^2(z,t) \quad (5-2)$$

Morisons equation describes the drag acting on the pipe, which is a result of the relative velocity of the CWP moving downwards or upwards through the water. As weather conditions are assumed to be zero during the installation, the drag force acting on the CWP entirely results from the velocity of the pipe.

The added mass is an inertia term which is a result of the acceleration of the CWP, displacing the water surrounding the pipe. This force is dependent on the diameter of the pipe, the acceleration of the pipe and the shape of the pipe.

$$m_a = \frac{\pi}{4} \cdot \rho_{sw} C_a D_o^2 \quad (5-3)$$

The gravity force consists of the mass of the submerged pipe, multiplied with the gravitational acceleration, as shown in equation 5-5, where the gravity force is a distributed load.

$$q_{gravity}(x) = m_{sub} \cdot g \quad (5-5)$$

$$m_{sub} = \frac{\pi}{4} \cdot (\rho_{cwp} - \rho_{sw})(D_o^2 - D_i^2) \quad (5-6)$$

In order for the pipe to slow down and stop as it reaches the seabed, it must be modelled. This is done by describing the seabed as a visco-elastic foundation, shown in figure 37. This is included in the equation of motion, with terms 4 and 5 describing the seabed, where w_{sb} is the distance from the surface to the seabed. By correctly choosing the stiffness and damping coefficients the seabed can be modelled accurately. These values are zero if the pipe is above the seabed.

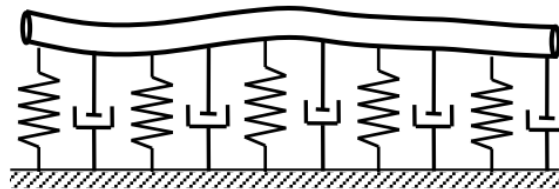


Figure 37: Illustration of visco-elastic foundation

5.3. Boundary conditions

The CWP is restricted by two boundary conditions, one on the left hand side and one on the right hand side.

The boundary at the left hand side of the pipe is modelled as a pinned connection at the location of the shore crossing. The pipe can freely rotate around this connection, though it cannot displace, nor can there be a bending moment in the pipe at the boundary. This results in the following 2 boundary conditions:

$$x = 0; w = \frac{\partial^2 w}{\partial x^2} = 0 \quad (5-7)$$

At the right hand side, at the end of the CWP, there are again 2 boundary conditions. Due to the pull force which is applied by the tug there is tension in the pipe, aswell as a vertical force acting on the pipe end. This vertical force acts as a shear force on the pipe end. The bending moment at this end is zero, this results in the following boundary conditions:

$$x = L; EI \frac{\partial^3 w}{\partial x^3} - T \frac{\partial w}{\partial x} = -F_{tensvertical} \quad (5-8)$$

$$x = L; \frac{\partial^2 w}{\partial x^2} = 0 \quad (5-9)$$

5.4. Finite Difference Discretisation

In order to numerically solve equation of motion of the pipe, the continuous equation of motion is discretised using the finite difference method. With this method, the CWP is divided into several nodes, connected with elements. Each node is described with its own equation of motion. Each node is able to move vertically, and is connected to the nodes nearby. By giving the nodes properties that correspond to those of the CWP, the displacement of the CWP can be described. As the amount of nodes is increased, the accuracy of the model becomes higher, as the CWP is described better.

The following equations are used to approximate the derivatives of the displacement of the CWP:

$$\frac{\partial w_n}{\partial y} = \frac{w_{n+1} - w_{n-1}}{2l}$$

$$\frac{\partial^2 w_n}{\partial y^2} = \frac{w_{n+1} - 2w_n + w_{n-1}}{l^2}$$

(5-10)

$$\frac{\partial^3 w_n}{\partial y^3} = \frac{w_{n+2} - 2w_{n+1} + 2w_{n-1} - w_{n-2}}{2l^3}$$

$$\frac{\partial^4 w_n}{\partial y^4} = \frac{w_{n+2} - 4w_{n+1} + 6w_n - 4w_{n-1} + w_{n-2}}{l^4}$$

The full discretization of the equation of motion is given in Appendix D.

By substituting these equations into these equation of motion of the pipe, and into the boundary conditions, an equation of motion for each node can be found. These equations of motion can then be solved in Matlab using an ODE solver. In this case ode45 is used.

5.5. Pulling force from tug

As a pulling force acting on the pipe is modelled, it is assumed that the tug which applies the tension force remains at a fixed distance from the CWP. As the pipe is lowered, the angle of the pulling force on the pipe changes, which changes the amount of tension in the CWP, and results in a vertical force on the end of the CWP. For simplicity, the mass of the towing cable is neglected, so that the cable remains straight between the tug and the pipe end.

The tension force and the vertical force on the pipe end are approximated using the following equations:

$$\alpha = \tan^{-1}\left(\frac{D_{tensionvessel}}{w_{end}}\right) - \tan^{-1}\left(\frac{w_{end}}{L_{CWP}}\right) \quad (5-11)$$

$$T_{CWP} = T_{cable} \cdot \sin(\alpha) \quad (5-12)$$

$$F_{tensvertical} = T_{cable} \cdot \cos(\alpha) \quad (5-13)$$

Where:

$D_{tensionvessel}$	Distance from the vessel to the pipe end
w_{end}	Water depth of the pipe end
L_{CWP}	Length of the CWP
T_{CWP}	Effective tension in the CWP
$F_{tensvertical}$	Vertical force on the CWP end
T_{cable}	Tension force applied by the tug

5.6. Displacement in the horizontal plane

As the pipe is installed, it will also displace in the horizontal plane. Although this is not described in the equations of motion, it is still partially taken into account. There are 2 types of horizontal displacement that are taken into account, displacement due to rotation, and due to tension in the pipe.

5.6.1. Due to rotation

As the pipe is lowered, it rotates around the pinned connection at the shore line, and therefore moves horizontally towards the pinned connection. This horizontal displacement is taken into account in the following manner. As the slope of the seabed is known, the angle of the seabed is found with formula 5-14. Using this angle, the horizontal displacement of the CWP end is found with equation 5-15.

$$\angle_{seabed} = \tan^{-1}\left(\frac{1000}{L_{CWP}}\right) \quad (5-14)$$

$$x_{end} = L - L \cdot \cos(\angle_{seabed}) \quad (5-15)$$

As the slope of the seabed is 1:7, the total horizontal displacement of the end of the pipe is approximately 70 meters after installation.

Re-initialisation

As the theory assumes that the displacement of the pipe is small, an error is introduced as the pipe is installed. This is due to the fact that the model assumes that the forces are either in the vertical or horizontal direction, while as the pipe rotates around the shore, the components of these forces also change slightly. As the angle of the seabed slope is small, approximately 8 degrees, the error is relatively small. Still this error is removed by re-initializing the model after a certain chosen time step. With the re-initialisation, an imaginary straight line is taken between the two boundaries of the CWP, as illustrated with the dotted line in figure 35, and as calculated. New initial conditions for the displacement are then used, determined by the distance of the nodes to this line.

$$IC_{line x_n} = \frac{w_{end}}{x_{end}} \cdot x_n \quad (5-16)$$

$$IC_{displacement} = w_{x_n} - IC_{line x_n} \quad (5-17)$$

Where:

x_n	Distance from the vessel to node n
$IC_{line x_n}$	The imaginary point where the initial condition for displacement is zero
$IC_{displacement}$	The new initial conditions for displacement, of node n

5.6.2. Due to tension

Furthermore, tension in the pipe results in a certain amount of strain. This is included in the model. As the tension is assumed to be continuous in the pipe, the strain in the pipe is equal for each element. The strain is found using formula 5-19, which is then used to determine the amount of elongation of the pipe.

$$\sigma_{axial} = \frac{F_{tens}}{A} \quad (5-18)$$

$$\varepsilon = \frac{\sigma_{axial}}{E} \quad (5-19)$$

5.7. CWP Stresses

During the installation process, the CWP will encounter stresses due to the forces which are applied, due to bending and due to the hydrostatic pressure.

There are 3 types of stresses considered in the pipe:

- Axial stress
- Radial stress
- Hoop stress

5.7.1. Axial stress

Axial stress is a result of both the tension force applied to the CWP, as well as of the bending which occurs in the CWP.

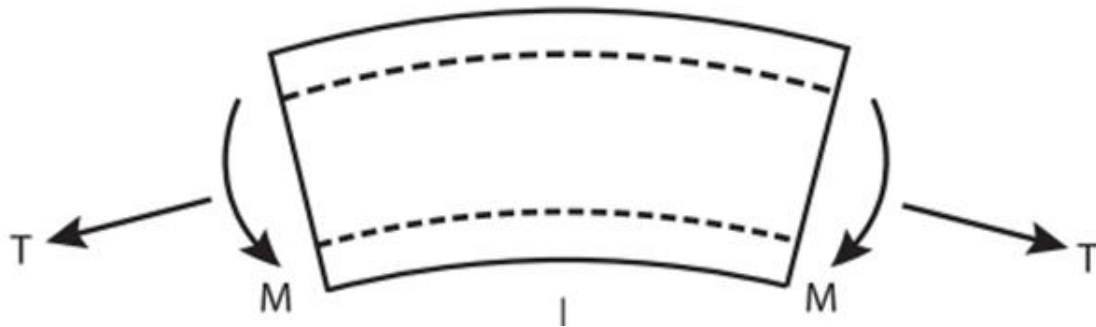


Figure 38: Illustration of Axial Stress

As the tension is considered constant throughout the pipe, the axial stress due to tension pipe is calculated using formula 5-20.

$$\sigma_{at} = \frac{T}{A_{CPW}} \quad (5-20)$$

For finding the axial stress due to bending, first the bending moment in the CWP must be found. This is done by multiplying the curvature of the CWP with the bending stiffness of the pipe:

$$M = EI\kappa \quad (5-21)$$

Where the bending stiffness is:

$$\kappa = \frac{\partial^2 w}{\partial x^2} \quad (5-22)$$

Finally, the axial stress throughout the CWP due to bending can be found with equation 5-23.

$$\sigma_{ab} = \frac{Mr}{I} \quad (5-23)$$

Where r is the stress calculation radius, from the middle of the pipe.

By summing up the axial stress due to bending and due to the tension the total axial stress is found.

5.7.2. Hoop Stress & Radial Stress

The hydrostatic pressure which act on the CWP, especially at large water depths, creates stresses in the pipe, as shown in in figure 39. This pressure results in both hoop stress, as well as radial stress.

Hoop stress is a circumferential stress in the pipe, while radial stress is a stress in the radial direction of the pipe.

Considering an HDPE cold water pipe, the diameter over wall thickness ratio is equal to 20. This is the limit for which the pipe is considered to be thick walled, and thus the thick walled pressure vessel equations are used, although for materials such as FRP the thin walled assumptions would likely be valid.

It is assumed that the CWP is open-ended and filled with water during installation. Therefore the internal and external pressure on the CWP will be equal. As the pipe is open-ended no axial stress is generated due to the hydrostatic pressure.

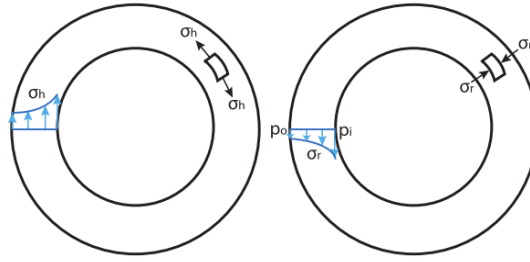


Figure 39: Illustration of hoop and radial stress

For finding the hoop and radial stress in the pipe, the thick walled pressure vessel equations are used:

$$\sigma_h = \frac{p_i r_i^2 - p_o r_o^2}{r_o^2 - r_i^2} - \frac{r_i^2 r_o^2 (p_o - p_i)}{r^2 (r_o^2 - r_i^2)} \quad (5-24)$$

$$\sigma_r = \frac{p_i r_i^2 - p_o r_o^2}{r_o^2 - r_i^2} + \frac{r_i^2 r_o^2 (p_o - p_i)}{r^2 (r_o^2 - r_i^2)} \quad (5-25)$$

As the internal and external pressure are equal, the equations are reduced to:

$$\sigma_h = \frac{p_i r_i^2 - p_o r_o^2}{r_o^2 - r_i^2} \quad (5-26)$$

$$\sigma_r = \frac{p_i r_i^2 - p_o r_o^2}{r_o^2 - r_i^2} \quad (5-27)$$

Therefore it is found that the hoop stress and radial stress are equal in the CWP, and at all times equal to the hydrostatic pressure.

To find the combined stress in the pipe, which must remain below the yield strength of the material, the Von Mises theorem is used:

$$\sigma_v = \sqrt{\frac{(\sigma_h - \sigma_r)^2 + (\sigma_r - \sigma_a)^2 + (\sigma_a - \sigma_h)^2}{2}} \quad (5-28)$$

5.8. Model verification

Before using the model, it must be verified that it functions properly under the assumptions on which it is based.

Furthermore, the influence of the amount of nodes must be checked, to find the amount of required nodes which must be used for modelling. More nodes should result in a more accurate model, yet increase the computational time.

The first verification which is done, is a free fall (FF) test. The entire pipe is held at the surface, and released. There are no external loadings or forces acting on the pipe, except for the hydrodynamic drag. As gravity acts on the pipe, it should reach a velocity where it is in equilibrium with the hydrodynamic drag, described by Morison's equation. This velocity can be found using equation 5-29.

$$\dot{w}(x,t) = \sqrt{\frac{\rho_{sub} A_{CWP} \cdot g}{\frac{1}{2} \rho C_D D_o}} \quad (5-29)$$

This test is done with 40 and with 60 nodes, where the same velocity should be reached. Furthermore, a node chosen at 75% of the pipe length is looked into, and it is checked how long it takes for the node to reach the seabed. As seen in table 15, the velocity reached in the model precisely matches the theoretically calculated velocity, showing that this is implemented correctly. Looking at the time to reach the seabed, there is a 6 second difference. This can be accounted for by the fact that the pipe bends as it reaches the seabed, which is more accurately described if more nodes are used, giving slightly different results. Figure 40 shows the velocity of node 45, when 60 nodes are used.

At x=5250 from shore	60 nodes	40 nodes	Theory
Max velocity at L=75% [m/s]	0.2434	0.2434	0.2434
Time to reach seabed [s]	3111	3105	-

Table 15: Free Fall velocity verification

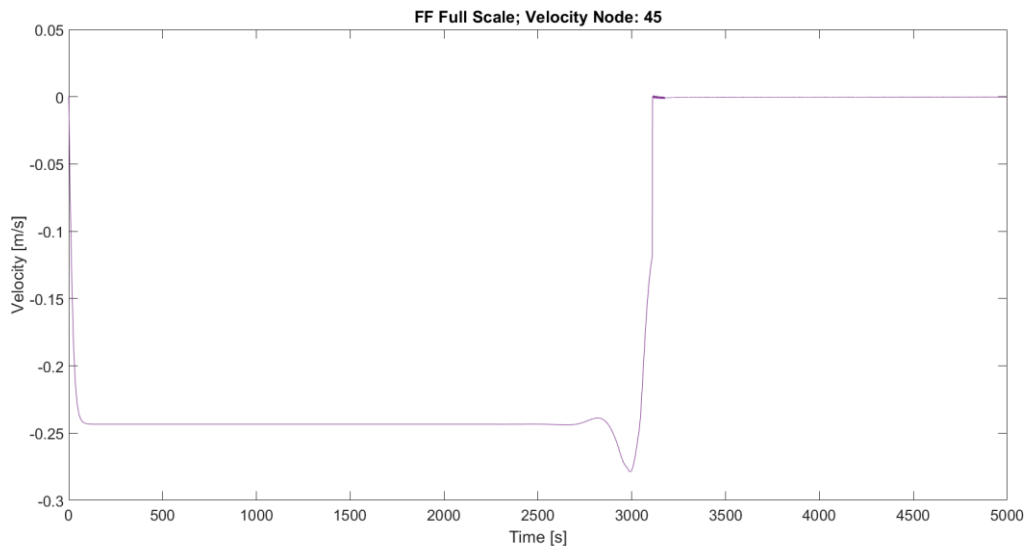


Figure 40: Velocity of the pipe at L=75% with 60 nodes

The next verification step which is done focusses on the amount of nodes, under some bending of the pipe. For this, the pipe is held at the surface and released, while a tension force of 390mT is applied to the pipe end. The pipe sinks, and the vertical force on the end of the pipe increases, until the pipe is held in equilibrium as shown in figure 41 (for illustration purpose only). By looking at the pipe end, and at L=75% in table 16, it is shown that the displacement is nearly identical if both 40 or 60 nodes are used. The velocity which the pipe reaches is also similar. Figure 42 and figure 43 show how similar the displacement and velocity are, when 40 or 60 nodes are used. These results imply that if local bending of the pipe is small, the amount of nodes which is required is not very large.

Applied tension=390mT	60 nodes	40 nodes
Displacement at L=75% [m]	263.5	265
Displacement at pipe end [m]	192	193
Max velocity at L=75% [m/s]	0.2446	0.2451
Max velocity pipe end [m/s]	.0.2141	0.2054

Table 16: Displacement and bending verification

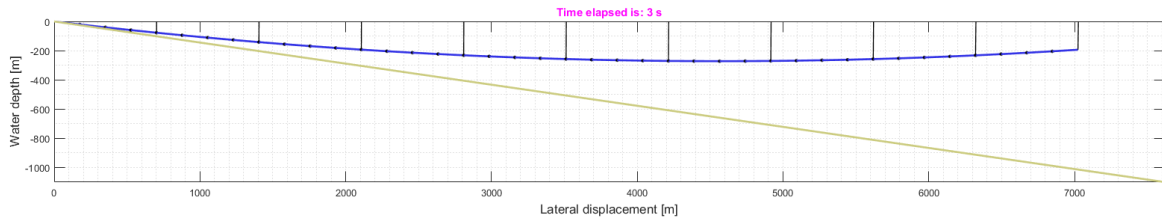


Figure 41: Maximum displacement of pipe with 390mT tension

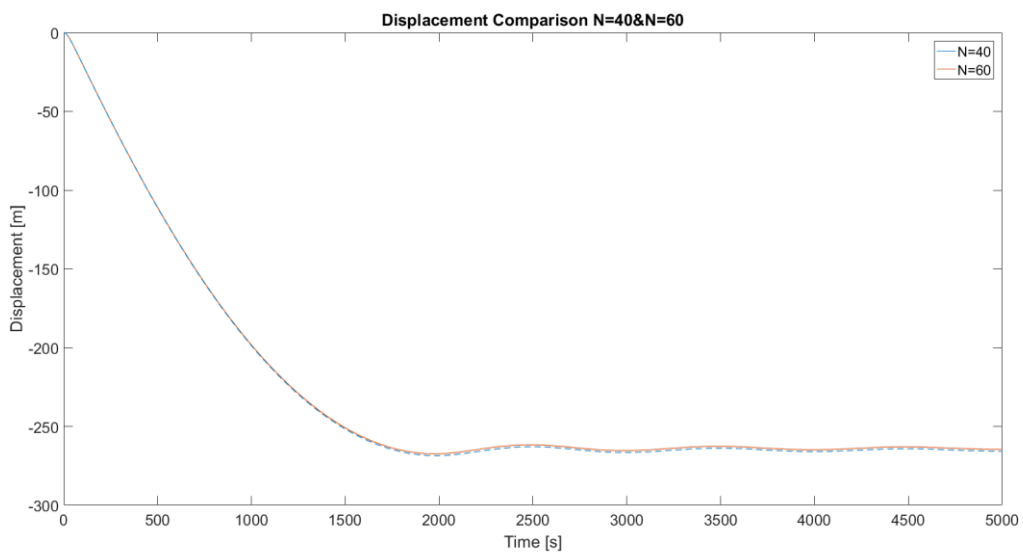


Figure 42: Displacement comparison for 40 and 60 nodes

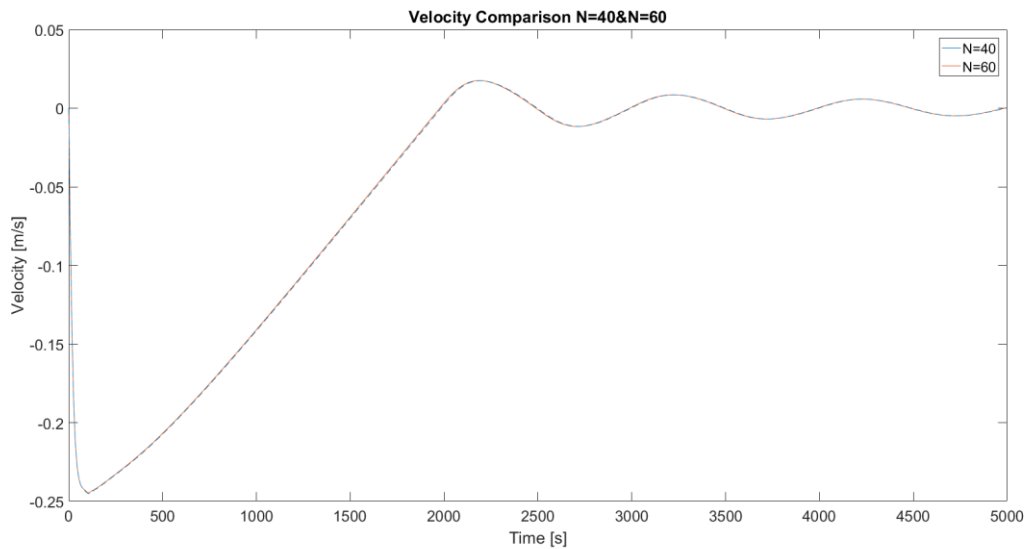


Figure 43: Velocity comparison for 40 and 60 nodes

Local bending

If local bending occurs, it is expected that the accuracy of the model decreases. Furthermore, the amount of nodes which is used becomes more important. This is shown by holding the pipe at the surface with buoys every 700 meters, where the local bending in between the buoys is discussed. Due to the way the pipe is held at the surface, in it can be approximated by describing it as a fixed-fixed beam, as done in chapter 4 when approximating Brewers installation method. Using the rules of thumb for the displacement of a clamped beam the deflection can be found. This test is done with 40, 60, 80 and 100 nodes.

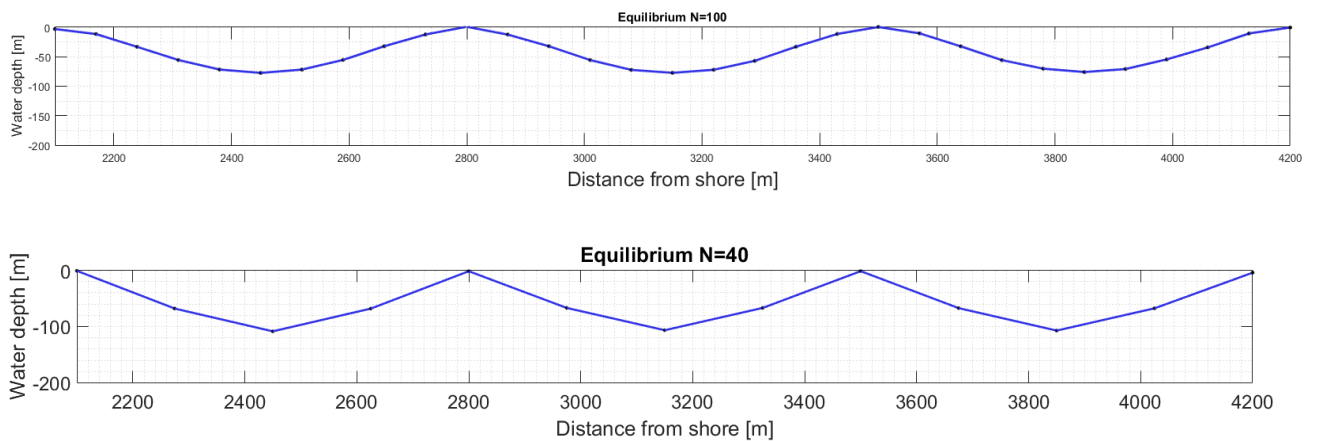


Figure 44: Displacement comparison for 40 and 100 nodes

As seen in figure 44 , visually there is a large difference between the shape of the pipe if 40 or 100 nodes are used. As seen in figure 45, as the amount of nodes is increased, the displacement of the model approaches the theoretical displacement under the fixed-fixed beam assumption.

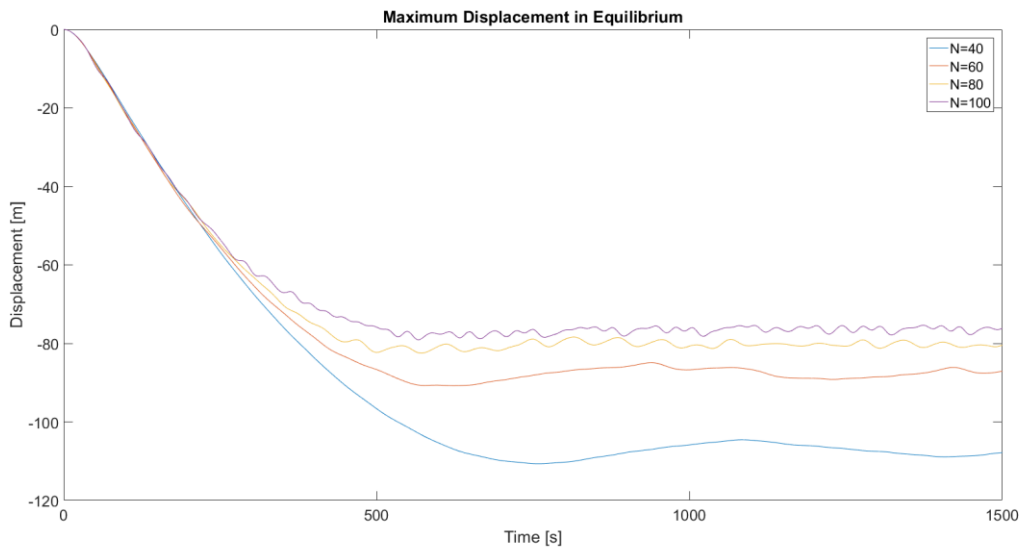


Figure 45: Displacement comparison for an increasing amount of nodes

The values of the displacement are given in table 17. This tests shows that for local bending, it is important to use enough nodes. Due to computational power limitations however, the amount of nodes which is used is 60. Under the assumption that the goal is to minimize local bending, and that Euler-Bernoulli beam normally underestimates bending, this should give reasonable results. Eventually, the choice can be made to run the final installation method with more nodes.

	Matlab N=40	N=60	N=80	N=100	Theory
Maximum deflection in equilibrium [m]	108	87	80	76	71

Table 17: Local bending verification

5.9. Conclusions

The main benefits of this model are that it is quick, adjustable for several installation methods, and that it simulates the entire installation of the pipe, as opposed to most previous static models.

This makes this model very useful for comparisons. It must be realized however when using the model, that results become inaccurate if large bending in the pipe occurs, this is partially due to the fact that the model is only solved in the vertical direction, as well as due to the fact that the general Euler-Bernoulli beam theory does not take strain due to shear into account. Furthermore, an error is introduced due to the fact that only the vertical displacement is solved, while results would be more accurate if the CWP displacements would also be solved in the horizontal direction.

One aspect which differentiates this model from many others, is that it does not look for a static equilibrium. Most installation models Bluerise has used so far are quasi-static, meaning that they constantly search for a static equilibrium. This means that an installation procedure for example would require a certain tension and lifting force, which is then constantly adjusted during the installation process. With this model, a static equilibrium is not necessary. A constant force can be applied to the CWP which is smaller than the gravity force, resulting in an acceleration of the pipe. The thesis model can be used to investigate many more different installation procedures than using conventional models.

As the model is 1 dimensional, this gives different results than a 2 or 3 dimensional model.

6. Marin Tests

6

In order to get a better understanding of the installation process and to validate the numerical model, 2 weeks of model tests have been done at the research facility of MARIN in Wageningen in January 2017. A detailed report which describes the tests has been written, and is available for more information by request from Bluerise. The main goals of the tests regarding this thesis were the following:

- Performing experiments to validate the Matlab installation model
- Establish the impact of different forces and loadings on the CWP, to eventually be able to optimize the CWP installation process.
- Get a basic comprehension and visualization of the pipe installation process, in order to understand real life CWP installation challenges and possibilities.

6.1. Test Setup Overview

The tests have been done in the Concept Basin, which has a water depth of 3.6 meters, and is 220 meters long with a width of 4 meters. A small area of this tank was used for the test setup. A setup was built which resembled the parameters which are used in the numerical model on a small scale. The setup had a length of approximately 6 meters, and reached a water depth of 2 meters. In order to see the influence of different loadings on the pipe and according to scaling laws, it was important that the CWP model was very flexible. The CWP was therefore made of flexible silicon, and had a length of just under 5.5 meters. The CWP was setup as in the Matlab model, with a pinned connection at the shore line, a tension cable attached to the end on the right hand side. Figure 46 gives an impression of the setup.

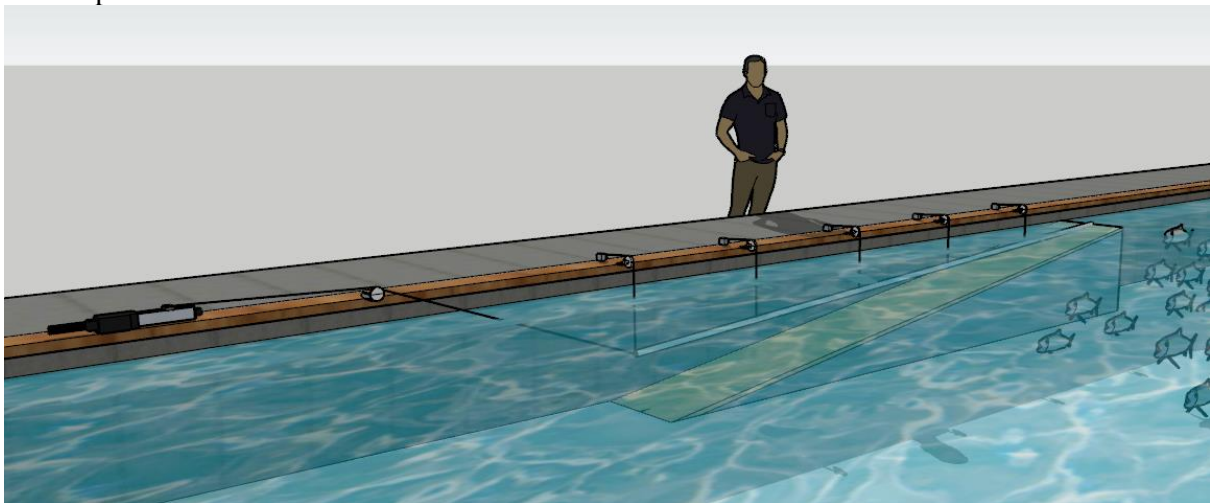


Figure 46: Artists impression of the tank test setup

In order to control the CWP, it could be lowered and raised using 5 stepper motors equally distributed along the CWP model. Instead of using the motors, a force could also be applied by attaching a mass to these 5 lifting points, to apply a constant tension.

The pipe displacement was measured using 5 rotational potentiometers, connected to these 5 lifting points. Besides measuring velocity, the friction of the potentiometers as well as the mass of the pipe was measured using load cells mounted underneath the potentiometers. This setup is shown in figure 47. For visualisation a calibrated high resolution underwater camera was used to record the installation tests. With additional programming work, these videos can be used to measure displacement along the entire pipe.

The setup was built with the goal of being able to vary all relevant installation parameters. Therefore parameters such as pipe mass, tension force, and installation speeds could be varied.



Figure 47: Photograph of the lifting points

6.2. Tests

At Marin, 2 different type of tests have been done. These are:

- Free-fall tests
- Hold and Sink tests

6.2.1. Free Fall Tests

The Free Fall tests have been done specifically for validation of the Matlab model. As with the FF test described in chapter 5, the pipe is held at the water surface and released, while a tension force is applied at the pipe end.

By doing the tests with various amounts of tension, several datasets are obtained. By using the same parameters in the Matlab model, comparisons can be made. By comparing values such as acceleration of the CWP, maximum velocity and the time to reach the seabed, the accuracy of the hydrodynamics in the model can be checked.

6.2.2. Hold & Sink tests

As it is found that the H&S installation method is one of the best methods in chapter 4, tests have been done with this installation method. By doing several H&S installation tests with varying forces and loadings on the pipe, the influence of these could be established.

With the H&S installation method, one of the questions is if multiple vessels are required for lowering the pipe, or if buoys can be used along the pipe. For this, first tests were done where the pipe was installed using the stepper motors, which resemble vessels with winches. The pipe was installed, where all vessels deploy the pipe with the same velocity, shown in figure 48. As can be seen, the pipe remains straight during the installation, and bends as it touches the seabed. The advantage of this installation, is that the amount of suspended pipe decreases as it is installed.

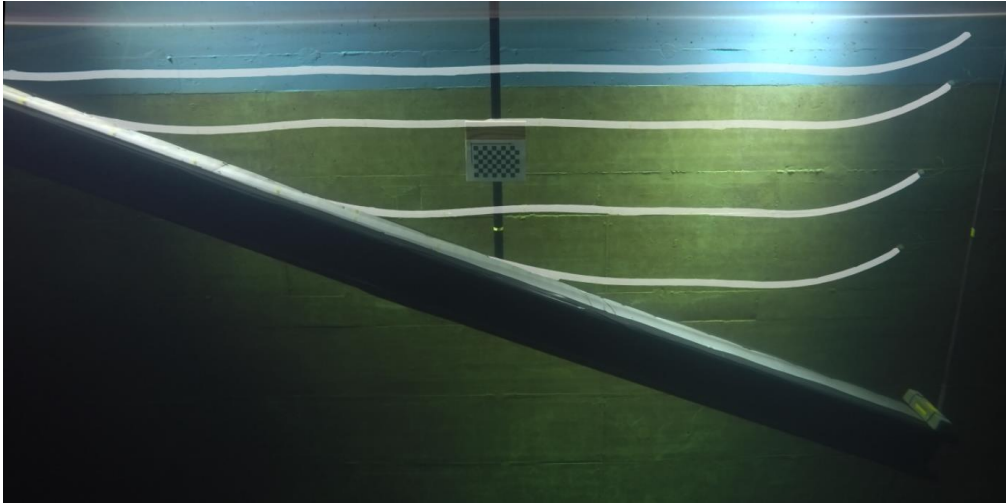


Figure 48: Installation with constant velocity of the pipe

For decreasing the bending in the pipe even more, the pipe can also be installed using different velocities, where the pipe is rotated around the shore connection, shown in figure 49.

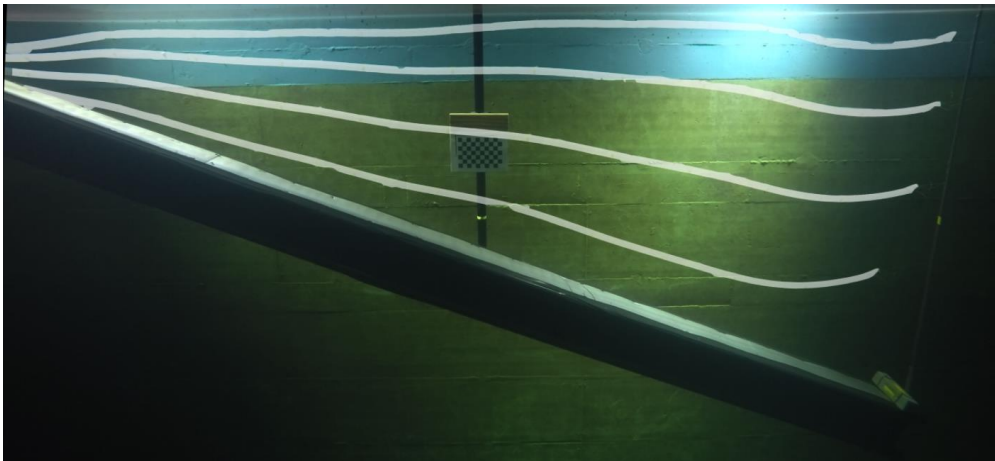


Figure 49: Installation with minimized pipe bending

Constant tension

Besides using the motors as winches, H&S tests have been done where a constant lifting force was applied, as would be the case if buoys are used instead of vessels. These constant tension tests are also used for validation of the numerical model.

6.2.3. Test Results

The tests results with regards to this thesis consist of observations which have been done, and data which is used for validation of the numerical model. The tests have been done with the goal of obtaining accurate data, although there are several factors which have an impact on the accuracy of the results. An important factor is that due to the manner in which the CWP model was produced, there was an internal bending moment in the pipe, even without external loading. This can be seen in figure 48, as the pipe end curves up steeply. Furthermore the displacements have been measured quite accurately, yet due to the sampling rate of the data the velocity of the pipe is less accurate, and has large peaks as can be seen in figure 54. The numerical parameters which are used are given in Appendix A, including the most relevant parameters of the test setup at Marin.

6.3. Matlab Model validation

In order to validate the Matlab model some of the tests done at MARIN are recreated in the Matlab model. The parameters from the MARIN tests are used in the model, after which the results are compared.

For the validation, the model is compared to the free-fall tests, and to the constant tension tests. By comparing different tests, with differences in tension, lift force, and lifting points, it can be seen if the Matlab model takes these parameters into account correctly.

For comparing the results, the overall pipe displacement is discussed, aswell as the specific displacement of the pipe at the position of motor 4, shown in figure 50. As the displacement of the pipe has been measured at this location, the data can be compared. Due to the bending moment in the pipe, the results from motor 5 are considered less accurate, while motor 4 gives the most detailed results, as it reaches the largest water depth compared to the other pipe locations.



Figure 50: Illustration of investigated pipe location

Free Fall test comparisons

The first test which is compared is the free-fall test. The free-fall test is done without external loadings, except for a tension of 100 grams –force.

Test name	Mass per point [g]	Lift points used	Tension on pipe end [g]
FF.100	-	-	100

As figure 52 shows, as the pipe is released, it remains nearly horizontal, as the applied tension does not yet have a vertical component. As the pipe sinks deeper, the vertical components increases, and the pipe tip starts deflecting vertically.

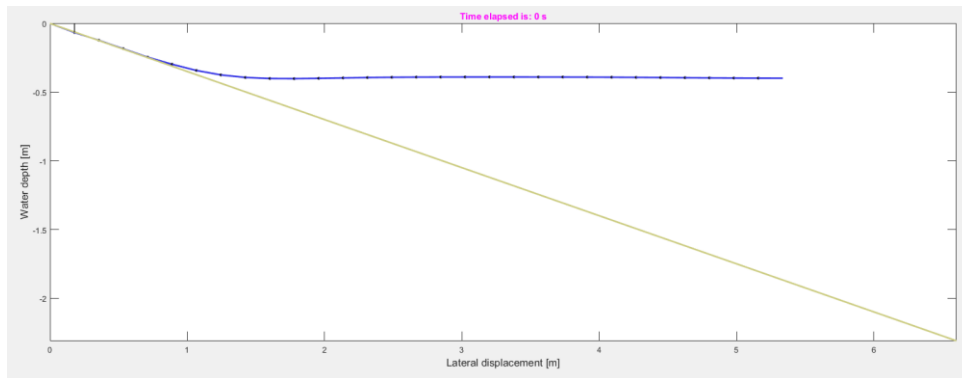


Figure 51: Simulation of the FF experiment in Matlab

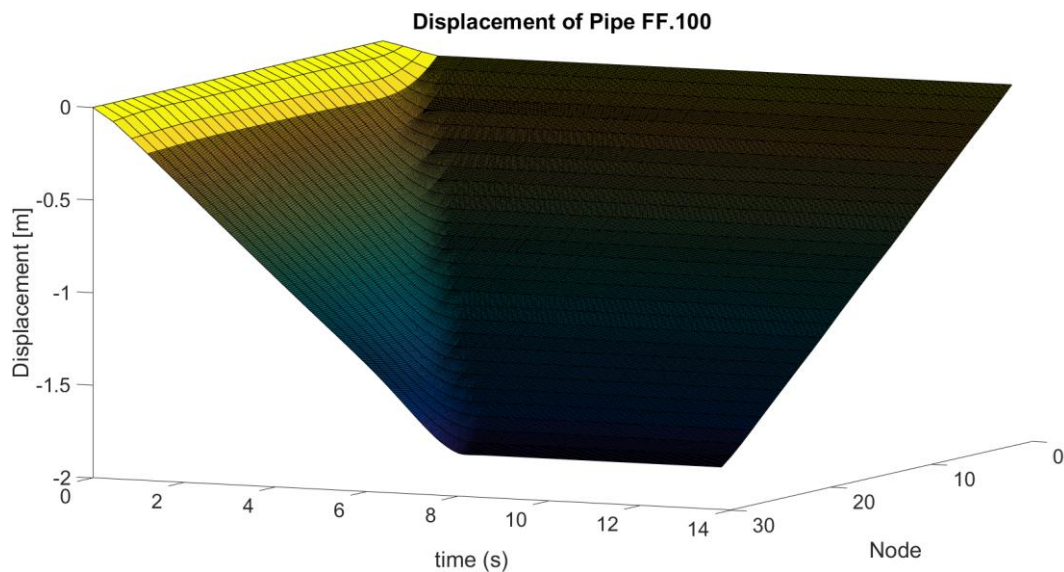


Figure 52: Displacement of the pipe over time

If we look at the velocity and displacement shown in table 18, it is clear that the velocity of the real CWP is lower than in the numerical model. Therefore, the time to reach the seabed is also longer. The velocity profile however is quite similar. The CWP accelerates to a maximum velocity, after which it decelerates slightly, as it reaches a velocity at equilibrium. Then due to the bending of the pipe at the seabed, it accelerates again slightly, until it decelerates as it touches the bottom.

CWP at sensor 4	Matlab	Low density, High drag coefficient Matlab	MARIN
Time to reach seabed [s]	6.8	11.6	12
Max velocity [m/s]	0.247	0.142	0.175

Table 18: FF test validation

Instability/ vortex shedding

As seen in table 18, an additional test is included. It was observed several times that large horizontal vibrations (from a top view) occurred in the CWP during the FF tests, in the order of several centimetres. This seems to be a case of instability, similar to flutter, or possibly vortex shedding.

In order to see if vortex shedding could be the reason for the vibrations, the Strouhal number can be calculated. The Strouhal number relates the frequency of shedding to the velocity of the flow and a characteristic dimension of a body. For pipes a value of 0.2 is valid in most situations[23].

Using equation 6-1 for the Strouhal number and a range of velocities of the CWP tests gives a frequency of vortex shedding of between 1.75 and 0.85 Hertz. This order of magnitude seems to visually correspond with the videos made, although this must still be verified.

$$St = \frac{f \cdot D}{V} \quad (6-1)$$

The result of these vibrations is that energy is transferred to the water, resulting in a larger amount of drag. This seems to correspond with the comparisons between the Matlab data and the test results. As the numerical model does not take 3-dimensional effects into account, an additional test is done where the drag coefficient is increased, to account for this effect.

Besides this, a possible explanation for the difference in results is that the density or shape of the silicon CWP model does not correspond to the values which are used. The density has not been stated by the pipe supplier, and therefore has been taken from a materials database. It is possible that the compound of the pipe has a slightly lower density, which would result in lower pipe velocities.

For this reason, an additional scenario is modelled in Matlab, where as an initial guess the density of the pipe is decreased by 4%, from 1250 kg/m³ to 1200 kg/m³, and the drag coefficient is increased greatly, from 1.2 to 2.8.

As seen in figure 53 and figure 54, the difference between the numerical model and the physical tests is already much smaller. They still do not match exactly, as only these 2 parameters are adjusted, whilst in reality the difference is likely dependent on more factors, as explained in the discussion in chapter 6.4.

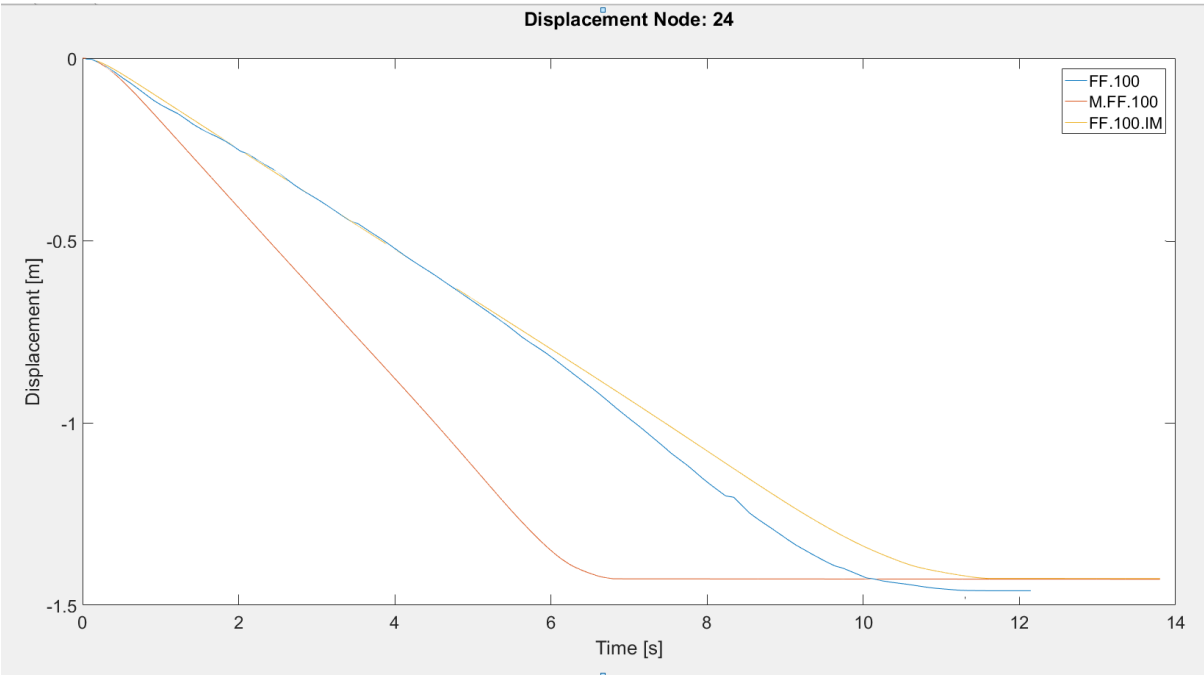


Figure 53: Displacement comparison between the numerical and physical model

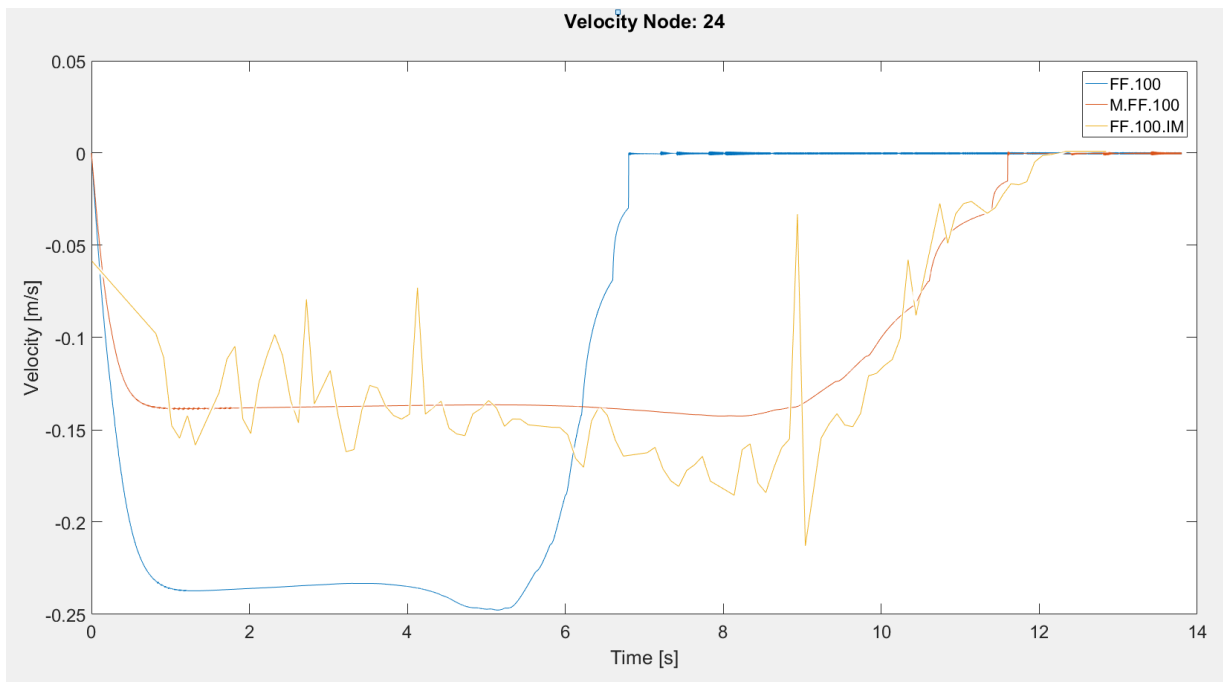


Figure 54: Velocity comparison between the numerical and physical model

Constant tension tests

In order to validate that the applied forces on the pipe in the model correspond to a real installation, several constant tension tests are compared.

T.2.50.50 & T.2.50.100

The first two tests are done where 3 lifting points are used, and the tension is varied from 50 gf to 100gf as shown in table 19. This is done to validate that the effect of pipe tension is taken into account properly.

Test name	Mass per point [g]	Lift points used	Tension on pipe end [g]
T.2.50.50	50	1,3,5	50
T.2.50.100	50	1,3,5	100

Table 19: Installation test description

Figure 55 shows the displacement of the pipe, where it is seen that the pipe indeed sinks slower at the points where the lifting force is applied.

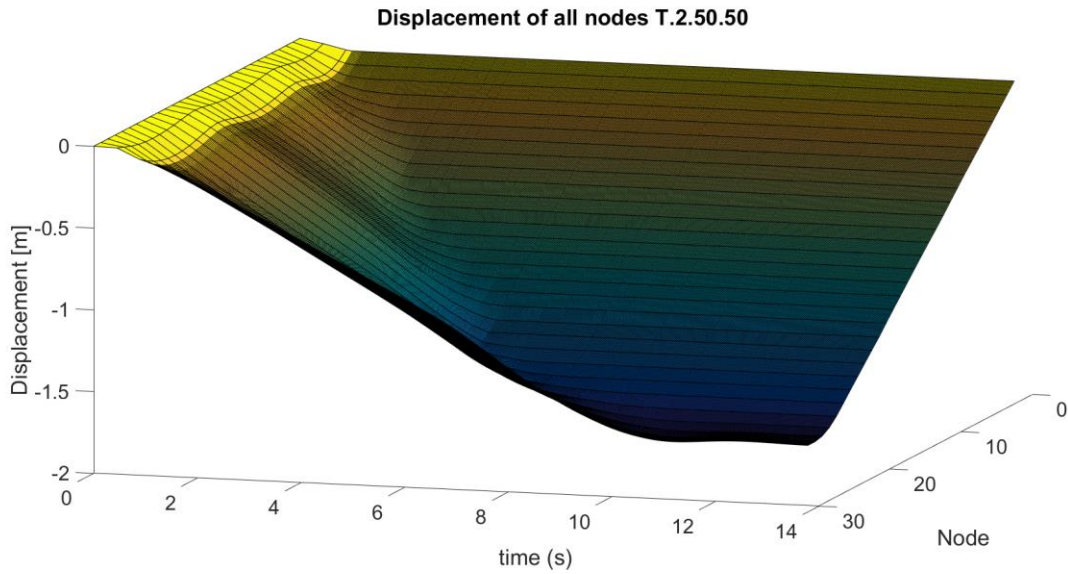


Figure 55: Displacement of the pipe with constant tension

Figure 56 shows an overlay of the numerical model with the physical model, where the vertical deflections are clearly larger in the real model. An explanation for this is the internal bending moment in the physical model, which causes it to curl upwards, resulting in larger vertical bending than a perfect CWP model.

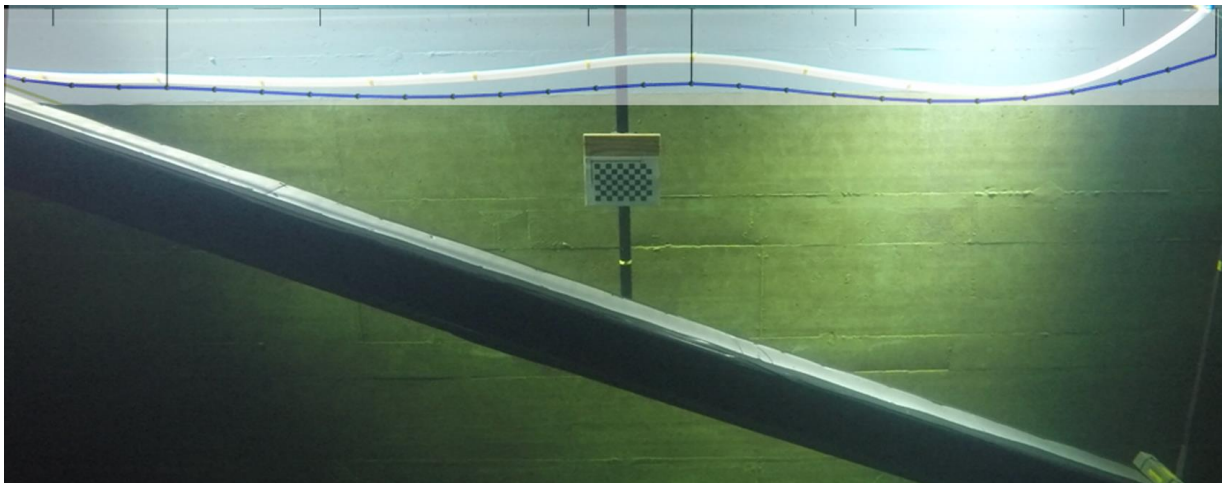


Figure 56: Comparison of numerical model with physical model

By looking at the displacement and velocity, shown in figure 57 and figure 58, it is again seen that trend wise the displacement of the numerical model corresponds to the physical tests.

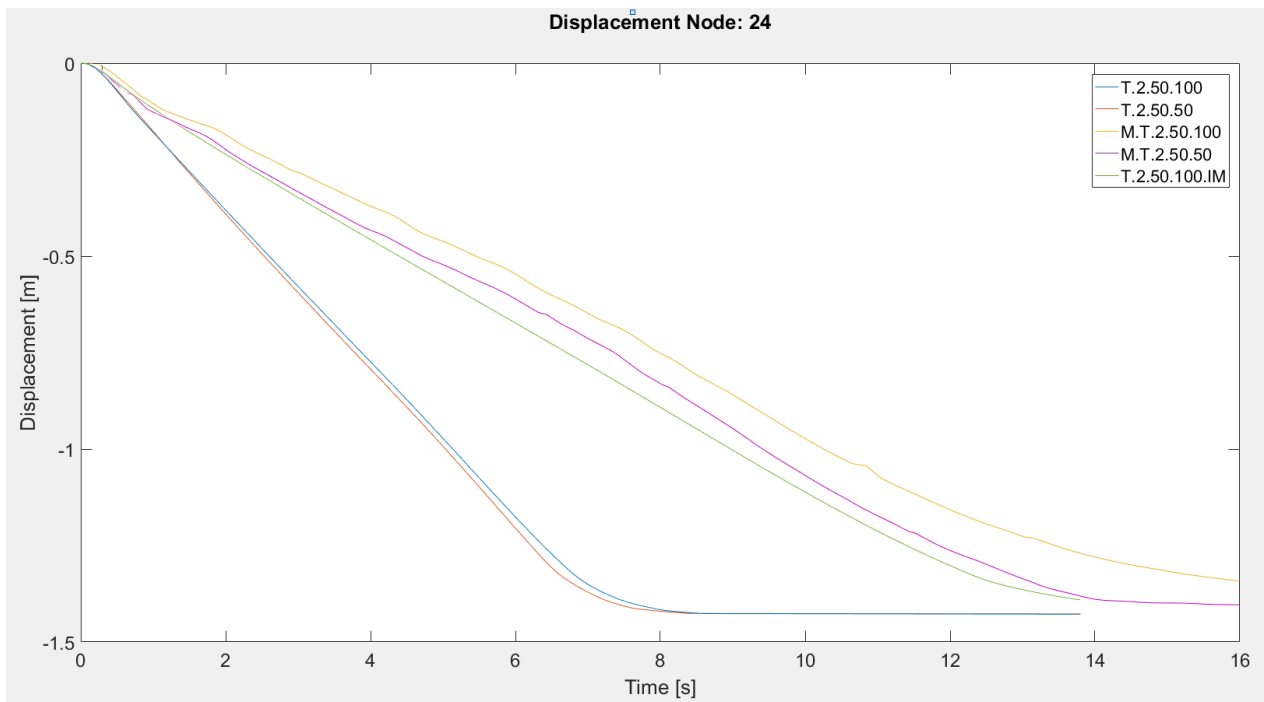


Figure 57: Displacement comparison between the numerical and physical model for CT tests

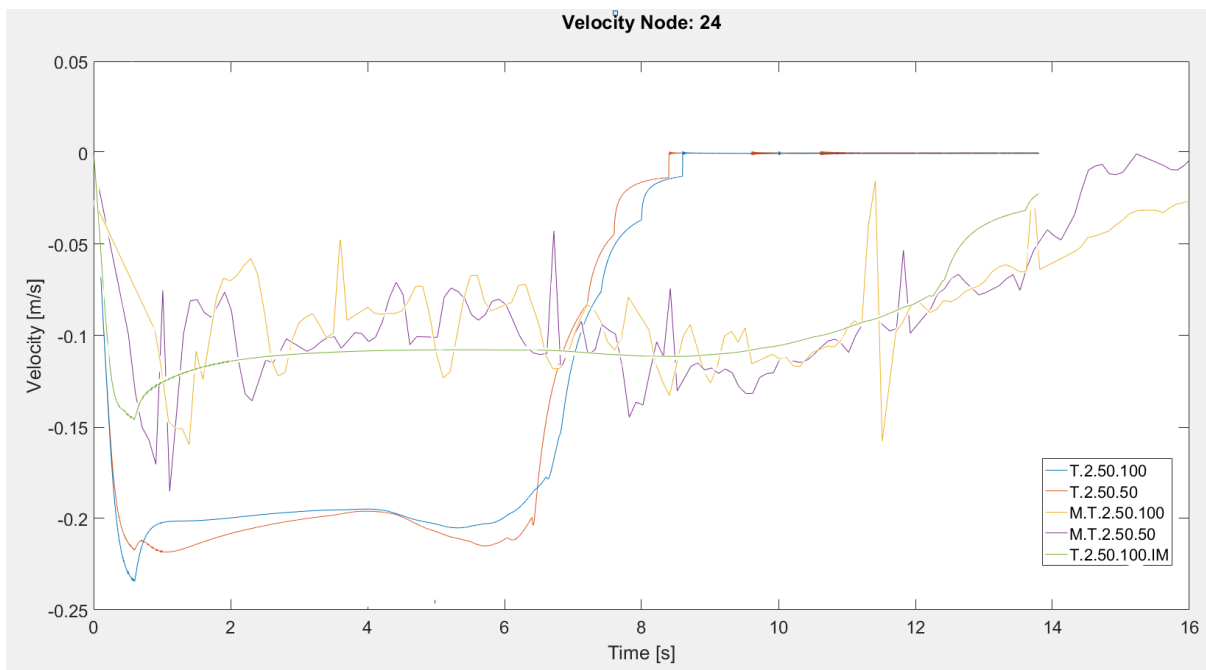


Figure 58: Velocity comparison between the numerical and physical model for CT tests

The exact values for sensor 4 are given in table 20. Here it is seen that as with the free-fall tests, the velocity of the real pipe is lower than that of the numerical model.

CWP at sensor 4	T.2.50.50 (Matlab)	T.2.50.100 (Matlab)	T.2.50.100.IM (Low density, high drag)	M.T.2.50.50 (Marin)	M.T.2.50.100 (Marin)
Time to reach seabed [s]	8.4	8.6	15	14.2	17.8

Max velocity [m/s]	0.22	0.23	0.175	0.16	0.15
--------------------	------	------	-------	------	------

Table 20: Constant tension validation

T.7.50.100 & T.7.100.100

The final tests which are used for the model validation are 2 tests where the amount of lifting force is varied, from 50gf per lifting point to 100gf per lifting point as seen in table 21. With these test, only 2 lifting points are used.

Test name	Mass per point [g]	Lift points used	Tension on pipe end [g]
T.7.50.100	50	2,4	100
T.7.100.100	100	2,4	100

Table 21: Test description

Looking at the displacement and velocity, given in table 22, similar results are obtained. The Matlab model reaches higher velocities than the physical tests. Trendwise, it can be seen in figure 59 and 60 that the model reacts correspondingly to the change in tension which is applied on the pipe end.

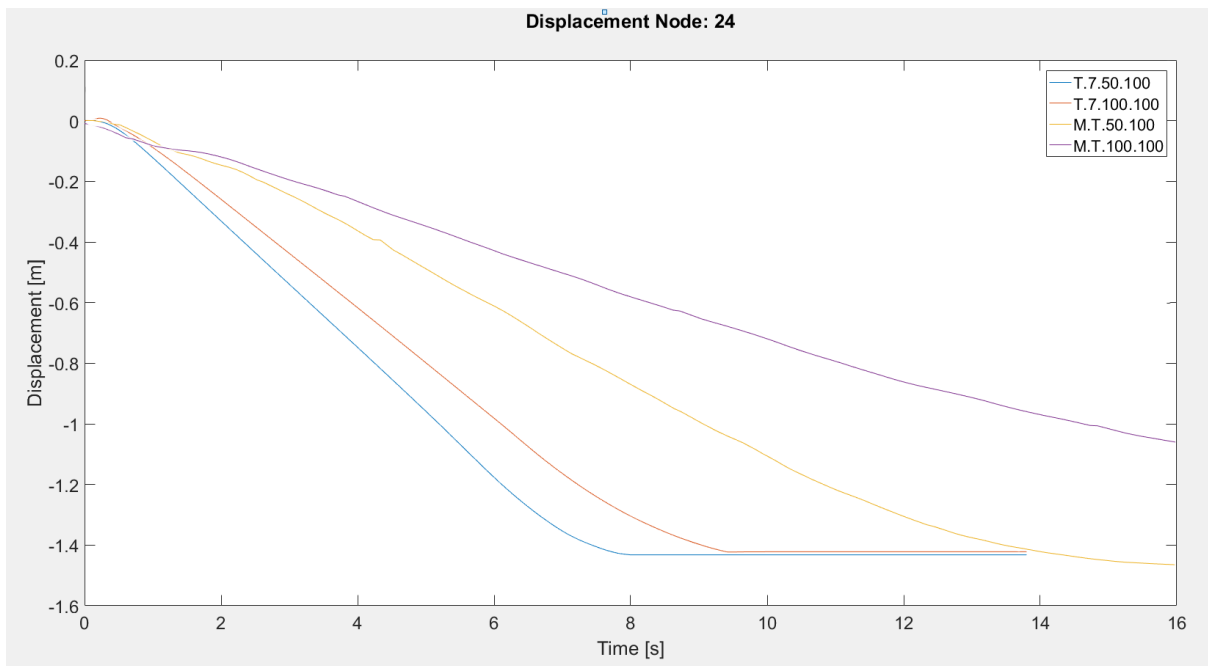


Figure 59: Displacement comparison between the numerical and physical model

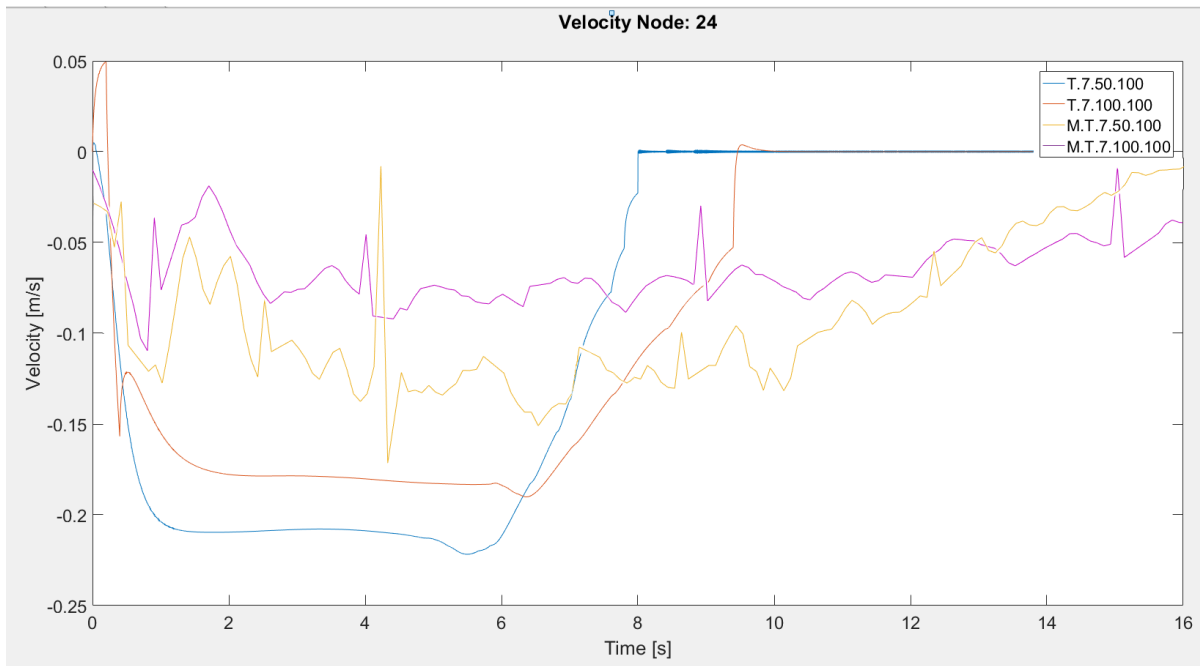


Figure 60: Velocity comparison between the numerical and physical model

CWP at sensor 4	T.7.50.100	T.7.100.100	M.T.7.50.100 (Marin)	M.T.7.100.100 (Marin)
Time to reach seabed [s]	8	9.5	16.2	20
Max velocity [m/s]	0.23	0.19	0.14	0.09

Table 22: Constant tension test data

6.4. Discussion

It is clear that the pipe in the Matlab model reaches higher velocities, and thus reaches the seabed in less time. There are several factors which can attribute to this, of which the most logical are:

- The CWP mass and or density of the real model is not correct. This explains why the Matlab model gives better results is a lower density is used.
- The CWP dimensions are not exactly correct. As the pipe model is made from food grade silicon, which is made for the food industry, the tolerance of the dimensions of the CWP might not be as high as thought. If the wall thickness varies, or the inner or outer dimensions are not exactly as assumed, this has an influence on the mass and thus the velocity of the CWP, giving similar results to the model where the pipe mass is decreased
- 3-Dimensional effects. It has been found that especially with the FF tests, strong vibrations occur in the CWP.
- Cushioning. It is possible that as the pipe is installed, it is cushioned by the water between the pipe and the seabed. This would slow down the pipe, resulting in an increase in installation duration.

From the numerical model checks and the validation with the physical tests, it can be concluded that the model behaves consistently under various types of loading, and accordingly to the equations and assumptions that it is based on. From the tests, it is concluded that from a practical aspect, it is likely that the shape of the CWP can be controlled precisely enough by attaching buoys to the pipe, while using the Hold and Sink method. During the tests which have been done at MARIN, the pipe was not held at equilibrium. Therefore the pipe would sink without having to decrease the tension on the pipe, or using a clump weight. The result of these tests was that the impact of the pipe with the seabed was therefore quite large, and the installation procedure could not be considered controlled. In a real life pipe installation procedure it is necessary to have full control over the pipe at all phases of the installation. This might be possible, by using a variable tension force for example.

7. Final Installation Method Analysis

7

From the installation methods comparison in chapter 4, it was found that both the modified Float and Sink method and the Hold and Sink installation method are found to be the preferred installation methods in combination with an HDPE cold water pipe. In this chapter, both methods are further discussed, to find if a conclusion can be made what the best installation method is, and if this method can be used to install the cold water pipe.

7.1. Modified Float and Sink Method

The modified Float and Sink method seems to have a large potential. It is a very controlled method for installing a CWP, as the installation can be stopped and continued at any time by controlling the amount of water in the pipe. By applying a large tension force on the pipe and adding additional buoyancy, it can be thought that the pipe can be installed using this method. If we look at the model verification in chapter 5 however, it is seen that if a tension force of 390mT is applied, even without additional buoyancy the pipe will find an equilibrium position, where it is not yet on the seabed. This means that it is not possible to install the pipe with the traditional float and sink method without increasing the amount of ballast on the pipe, or decreasing the amount of tension. Both scenarios are unfavourable. Instead, the hold and sink method is first further evaluated.

7.2. Hold and Sink Installation Method

It is thought that by using the hold and sink installation method the HDPE cold water pipe can be installed. By applying a tension force on the pipe end, and possibly attaching buoys, the pipe can be deployed. It is important that the installation process must be controlled, and therefore, by increasing and decreasing the tension on the pipe, it must be possible to lower or raise the pipe. If we look at the model verification in chapter 5, it is seen that if a tension force of 390mT is applied, even without additional buoyancy the pipe will find an equilibrium position where it is not yet on the seabed. This is due to the fact that the minimum amount of ballast which is required to hold the pipe on the seabed after installation is very small. This also shows that if the pipe is brought into this position, it must be possible to lower the pipe further by decreasing the pipe tension. As in the verification in chapter 5 it is seen that with a tension force of 390mT the local bending is small. It is checked if it is possible to install the CWP by letting the pipe reach this equilibrium position, and then decreasing the tension on the pipe until it lies on the seabed.

For this, the following parameters are used:

Simulation time	12000s
Number of lifting points with buoys	0
Clump weight on end of pipe	2000 kg
Distance tension vessel from pipe end	5000 m
Initial Tension	390 mT
Tension decrease rate	$1/(1+\text{time in seconds}/1000)$ after $t=1500\text{s}$
Final Tension	30 mT

Table 23: Hold and sink installation parameters

As seen in table 23, a clump weight is added to the end of the pipe. This is done to counter the vertical force component acting on the pipe, which should decrease local bending slightly.

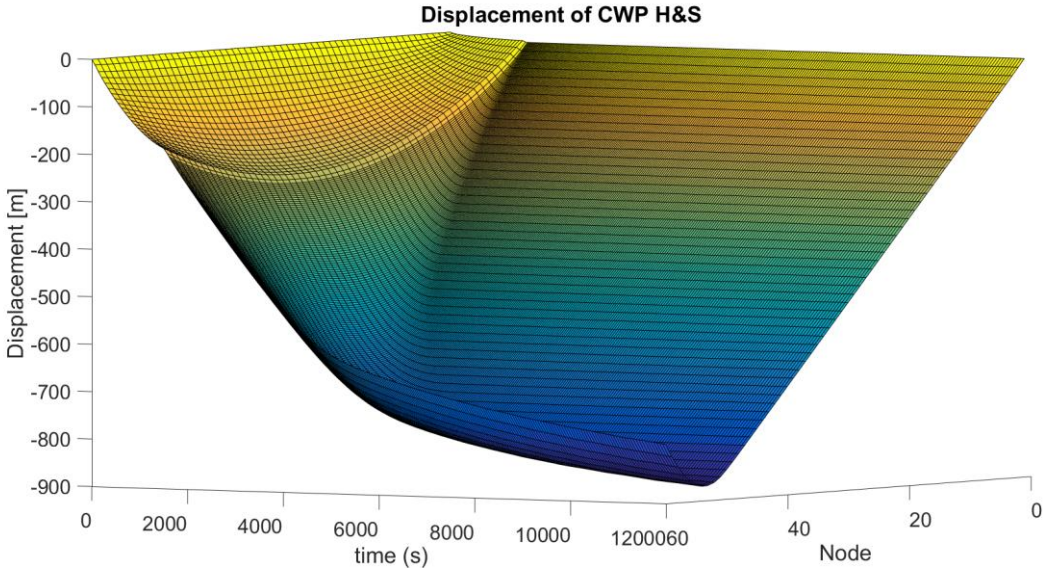


Figure 61: Displacement of 2.5m CWP with the Hold and Sink test

Figure 61 shows the displacement of the pipe during the installation. It can be seen that the pipe reaches the equilibrium position at approximately 1500 seconds. After this, the pipe tension is decreased and the pipe is installed. At the end of the simulation the pipe end is still above the seabed at a water depth of 774 meters. This is due to the simulation time. If the simulation would be run longer, or if a larger clump weight would be used, the pipe end would reach the seabed at the end of the simulation.

If we now look at the Von Mises stress in the pipe shown in figure 62, it is found that the maximum occurring stress in the pipe is approximately 9.5 MPa, which is well under the material yield stress of 21 MPa. A major contribution to this is due to the hydrostatic pressure, as at a water depth of 1000 meters this is approximately 10MPa.

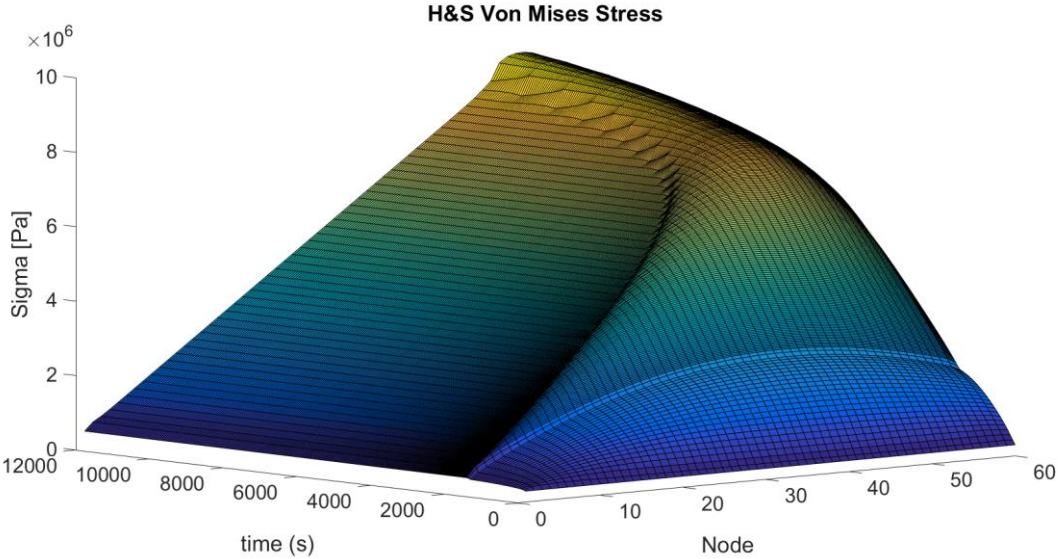


Figure 62: Von Mises stress in the CWP during H&S installation

By filtering out the hydrostatic pressure, we can see stress in the pipe due to bending and tension, shown in figure 63.

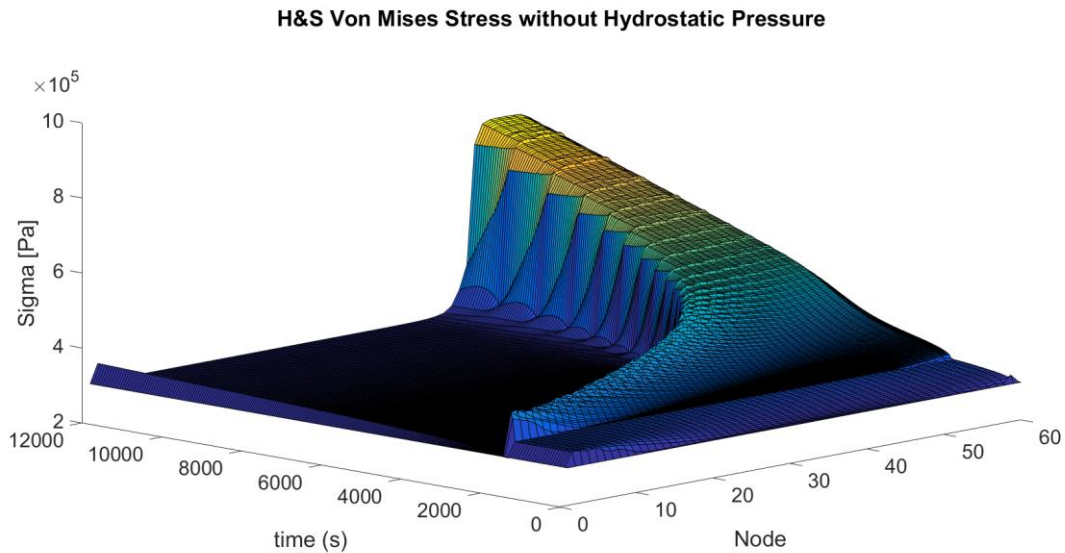


Figure 63: Von Mises stress without hydrostatic pressure

The maximum stress occurs near the end of the pipe and is approximately 0.8 MPa. This is due to the fact that the most bending occurs there, and increases with time as the tension is lowered.

In a real installation the loads on the pipe would be slightly higher, as the pipe would be installed slower. Still, due to the high tension the difference would be small. From this, it can be concluded that the 2.5 meter HDPE CWP can be installed in the assumed configuration with the hold and sink method. This is for a large part due to the low density of the pipe.

7.3. Hold and Sink with additional ballast

Although the previous installation simulation shows that the CWP could be installed using the hold and sink method without additional buoys, in reality additional ballast would be added to the pipe, to be sure that if any ballast would fall off during installation or operation, or if weather conditions would be different than expected, the pipe would not fail.

To investigate this, another simulation is done where the ballast is increased with 25%. This results in a new average CWP density of 1056kg/m³. The rest of the parameters are kept identical.

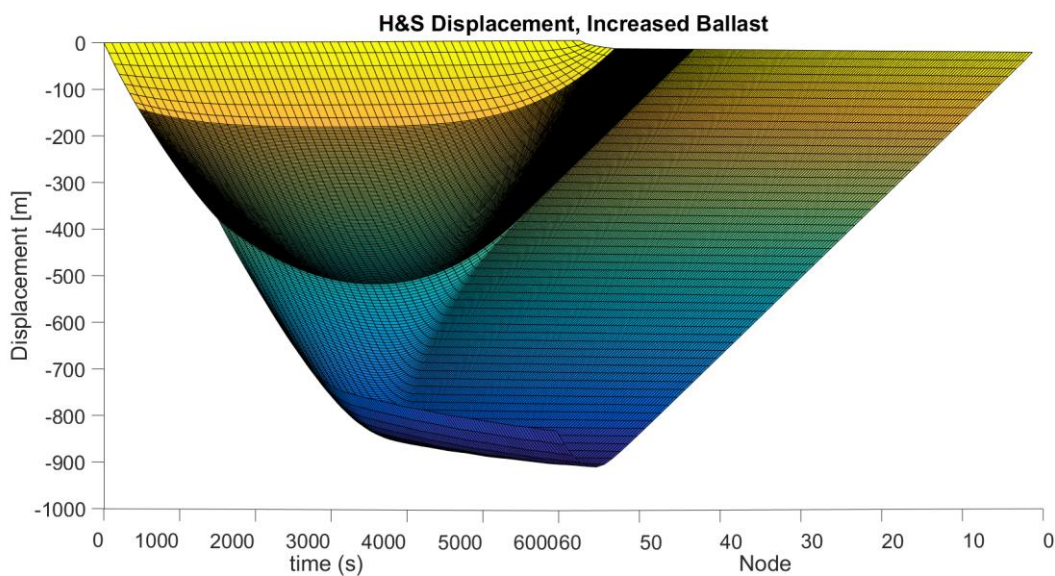


Figure 64: Hold and Sink installation with increased ballast

Figure 64 shows the displacement of the pipe during the installation. Due to the increased mass, the velocity of the pipe is much higher on average, and the bending is more severe. A major issue which can be seen is that with the initial equilibrium condition, part of the pipe is already on the seabed. This means that if this method would be used, part of the pipe would hit the seabed with a high velocity and thus would likely get damaged. This can also be seen in figure 65, where it shown that the pipe approaches the seabed with a velocity of approximately 0.3m/s.

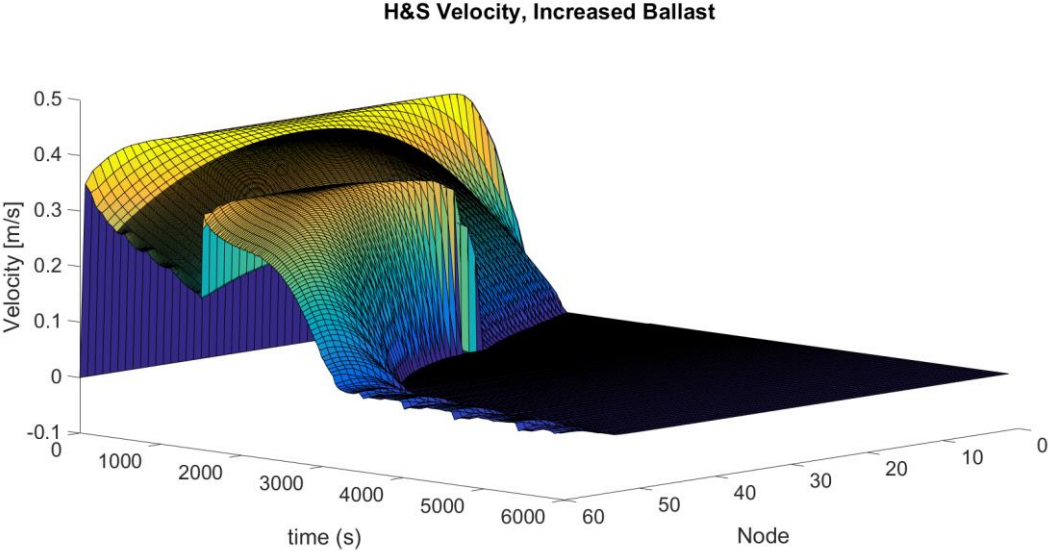


Figure 65: Velocity of the CWP during installation

Table 24 gives the maximum occurring Von Mises stress in the CWP. This is still well under the limit, although it does not accurately represent this installation as it does not take impact with the seabed into account.

Maximum stress in pipe during installation	10.4 MPa
Max stress without hydrostatic pressure	1.3 MPa

Table 24: Von Mises stress in CWP

7.4. Hold and Sink with additional ballast and buoys

In order to be able to install this pipe, either vessels or buoyancy modules must be used to support the pipe. As buoyancy modules are expected to be less expensive and easier available, an attempt is made to use these for installing the pipe.

As seen in the model verification in chapter 5, if buoyancy modules hold the pipe every 700 meters, maximum displacement between the modules is approximately 71 meters, which seems acceptable. In this scenario however, additional ballast is added to the pipe, which will increase the displacement. As the vertical resultant force from the tension will still lift a large part of the pipe, it is not necessary to make the pipe neutrally buoyant with buoyancy modules. Instead, enough buoys are used to counter 85% of the gravity force acting on the pipe. These modules are located every 700 meters along the pipe, excluding the pipe end. As seen in table 25, the simulation time is increased, and the rest of the parameters are kept the same as with the previous installation simulations.

Simulation time	14000 s
Submerged pipe mass per meter	28.8 kg
Gravity force acting on submerged pipe per meter	282.4 N

Number of lifting points with buoys	9
Clump weight on end of pipe	2000 kg
100% of buoyancy for equilibrium without tension	219.6 kN per lifting point
85% of buoyancy for equilibrium without tension	186 kN of lift force per lifting point
Distance tension vessel from pipe end	5000 m
Initial tension	390 mT
Tension decrease rate	$1/(1+\text{time in seconds}/1000)$ after $t=1500\text{s}$
Final Tension	26mT

Table 25: H&S with additional ballast installation parameters

The displacement of the pipe during this installation is shown in figure 66.

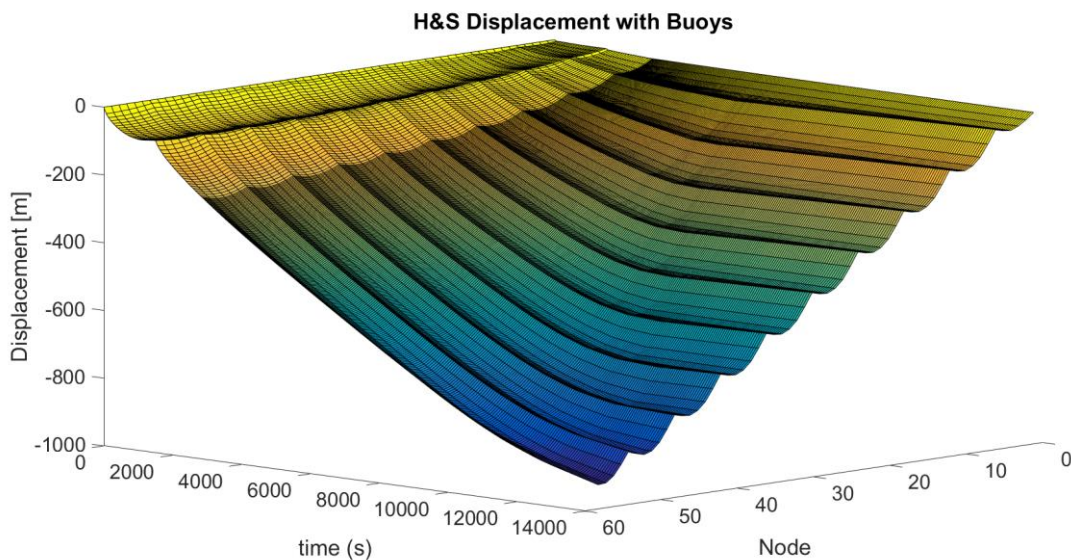


Figure 66: H&S installation with buoys

Clearly, the buoys have a large impact on the displacement of the pipe. It can be seen that the pipe reaches an equilibrium position where the entire pipe is still suspended, after which the tension is decreased and the pipe is lowered. The impact which was observed in the case without attached buoys does not occur during this installation. It can be seen that the pipe bends locally between the buoys, and as seen in figure 67 the velocity is much lower than if no buoys are attached.

H&S Velocity with Buoys

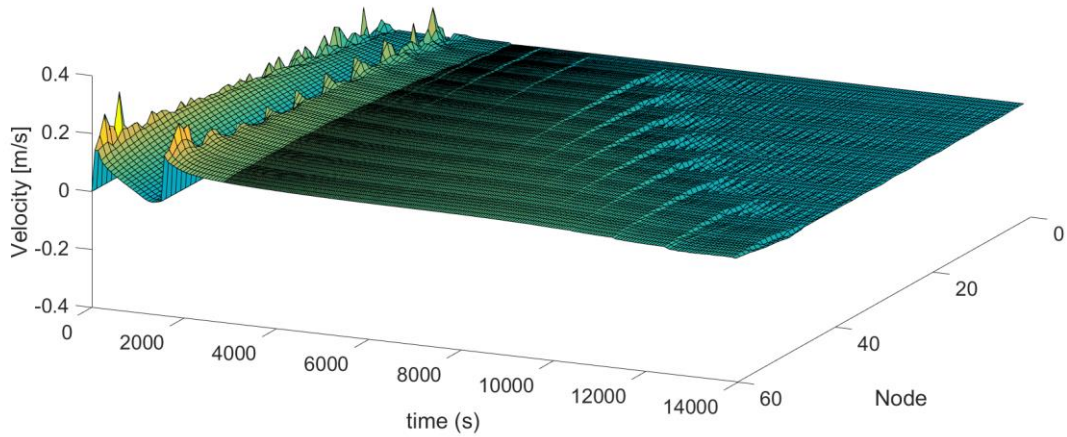


Figure 67: Velocity of the pipe with buoys attached

As shown in figure 68 the maximum stress in the pipe during this installation is 13.6 MPa. Without hydrostatic pressure, the maximum stress is 5.2 MPa as shown in figure 69. It can be seen that as the tension is decreased, the stresses increase due to the increased amount of bending in the pipe. This is clearly higher than in the previous case, and is much more representative of a real installation scenario. The buoys clearly have an impact on the bending stress, although even with the added ballast the pipe can still be installed safely according to the model.

H&S Von Mises Stress, with Buoys

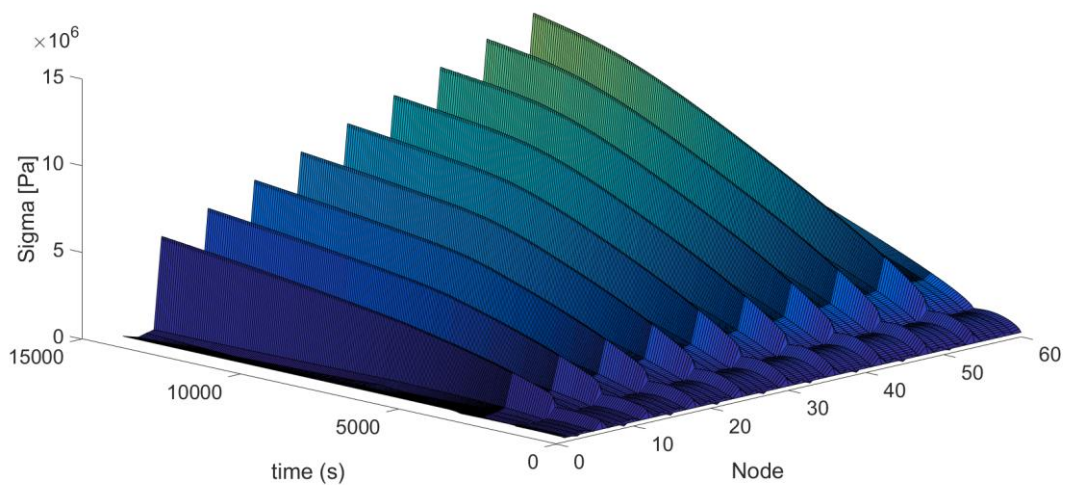


Figure 68: Von Mises stress

H&S Von Mises Stress without Hydrostatic pressure, with Buoys

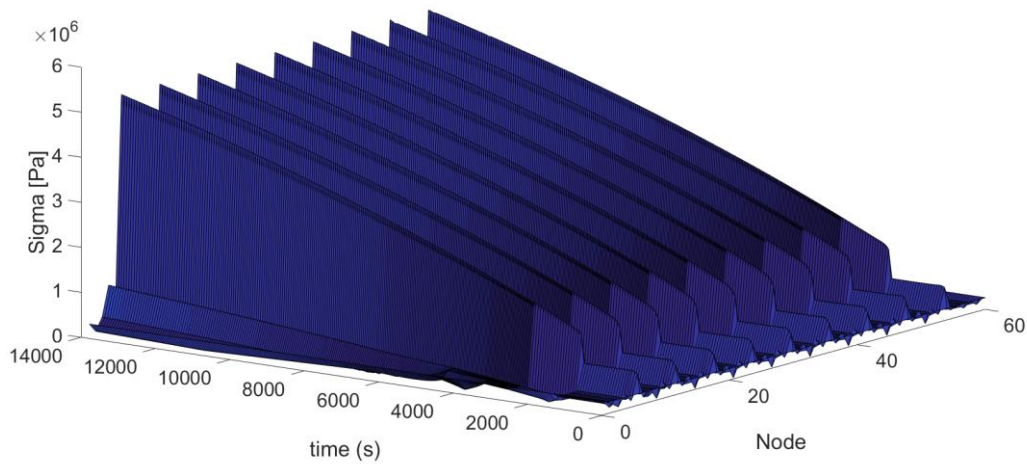


Figure 69: Von Mises stress without hydrostatic pressure

The results of the H&S methods are summarized in the table below:

Results	H&S	H&S with increased ballast	H&S with increased ballast and buoys
Max stress [MPa]	9.5	10.4	13.6
Max Stress without HP [MPa]	0.8	1.3	5.2
Allowable Limit [MPa]	21MPa		

Table 26: Von Mises stress comparison between H&S installation scenarios

7.5. Hold and Sink method for 4 meter diameter CWP

As it has been shown that the hold and sink method can be used for installing a 2.5 meter diameter cold water pipe, it now investigated if the same method can be used for a 4 meter CWP. A similar approach is used as with the 2.5 meter pipe installation simulations as these gave satisfactory results. Table 27 shows that the 4 meter diameter pipe with the minimum amount of required ballast has a similar mass underwater as the 2.5 meter pipe with additional ballast which was previously discussed. Again buoys are spaced apart 700 meters, and enough are used to counter 85% of the gravity force acting on the pipe.

Simulation time	14000 s
Submerged pipe mass per meter	26.08 kg
Gravity force acting on submerged pipe per meter	255.9 N
Number of lifting points with buoys	9
Clump weight on end of pipe	2000 kg
100% of buoyancy for equilibrium without tension	199 kN per lifting point

85% of buoyancy for equilibrium without tension	169 kN of lift force per lifting point
Distance tension vessel from pipe end	5000 m
Initial tension	390 mT
Tension decrease rate	$1/(1+\text{time in seconds}/1000)$ after $t=1500\text{s}$
Final Tension	26 mT

Table 27: 4m CWP installation parameters

As seen in figure 70, the displacement is similar to the displacement of the 2.5 meter diameter pipe with added ballast.

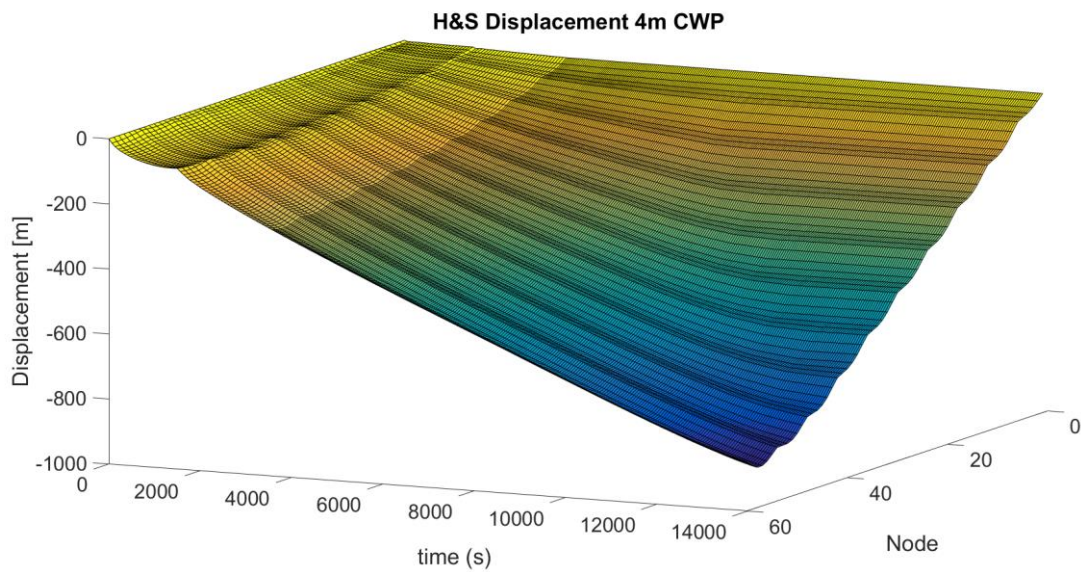


Figure 70: 4m CWP installation

Due to the tension in the pipe, and the buoys, the velocity of the pipe remains very low; approximately 0.05 m/s. This can be seen in figure 71.

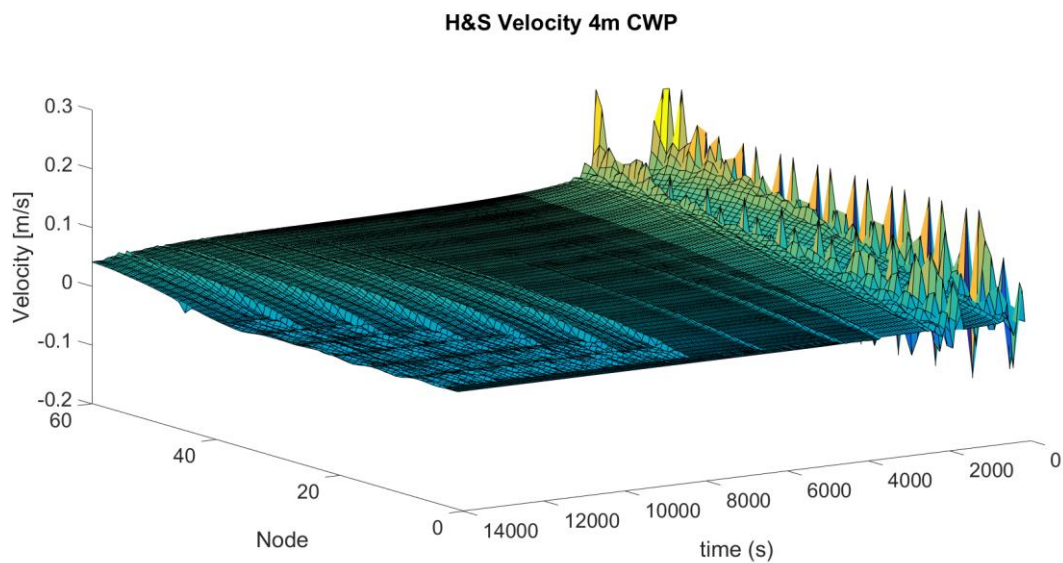


Figure 71: 4m CWP velocity

Due to the larger diameter and wall thickness, the 4 meter diameter CWP can resist even larger forces than the 2.5 meter diameter pipe. Looking at the Von Mises stress in figure 72, it is found that the maximum stress in the pipe is almost precisely 11 MPa, again well within the material limits.

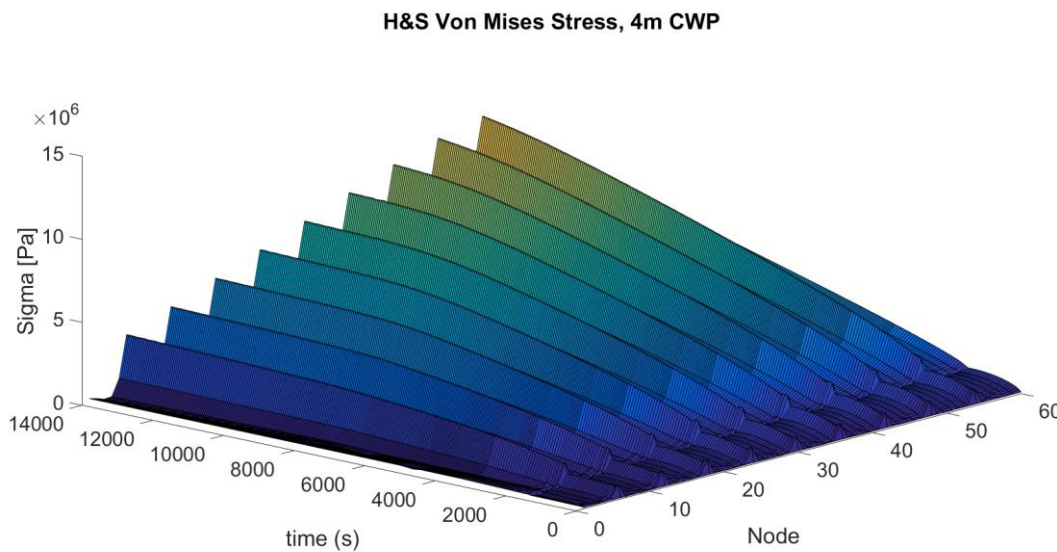


Figure 72: Von Mises stress 4m CWP

7.6. Final installation method

It is found that the hold and sink installation method gives satisfactory results. The stresses in the pipe remain within the material limits, including during the installation of a 4 meter diameter CWP. The main disadvantage of this method, is the initial step where the pipe is released at the seabed, where it sinks until it reaches and equilibrium condition, as this is an uncontrolled procedure. The final proposed installation method combines the float and sink method with the hold and sink method. This is proposed as follows. First the float and sink method is used to let the CWP sink until it is in equilibrium due to the tension force applied on the pipe end. For the parameters used in this thesis, the pipe is then suspended at approximately 200 meters below the water surface. This is well within the limits of the float and sink method. After this, the tension is lowered and the installation method becomes the same as the hold and sink method. This should result in a practical installation method, where the pipe is first held on the water surface filled with air, and installed in a controlled manner. By combining these installation method, there is full control over the pipe during the entire installation. Furthermore it results in a very limited amount of vessels which are required, which results in low installation costs. The maximum loads which occur during this installation are the same as in the previously discussed hold and sink simulations, as the largest stresses occur as large water depths due to the hydrostatic pressure.

This page is intentionally left blank

8. Conclusion and Recommendations

8

8.1. Conclusion

This thesis was started as it is was unknown what the best method was for installing a large diameter cold water pipe, and which material should be used. The goal was to find an installation method, and pipe material which can be using for installing a cold water pipe in most potential OTEC project locations.

By considering the Curacao Eco Park OTEC project location, parameters have been obtained which could be used for evaluating the performance of different materials and installation methods.

For finding the best material, a detailed analysis has been performed, where all relevant aspects of a cold water pipe lifecycle have been taken into account. It was quickly found that the only viable materials at this point in time are HDPE, and FRP as a second choice. These outperform the other considered materials in nearly every aspect.

Continuing with the installation method analysis, a large amount of installation methods was considered. Some of these methods are new and have never been used, while other methods have been used in previous OTEC projects, or in industries with similar requirements. These installation methods have then been described and evaluated. In the evaluation, installation aspects as well as operational aspects of the cold water pipe have been taken into account. Furthermore, to gain a feeling of the critical limits of these installation methods, some basic calculations have been done. Although many different types of installation methods were considered, it became clear from the multi criteria analysis that the advantages of installing the pipe as a single segment outweigh any possible disadvantages. The difference in installation speed is the main factor which sets these methods apart from the other considered methods.

To further evaluate these installation methods, a numerical model based on Euler–Bernoulli beam theory has been made. The model is made so that it can simulate an entire pipe installation process, as this is useful for finding the maximum occurring stress in the pipe. Although the model becomes less accurate if large amounts of bending occur, the goal is to find an installation method where the bending is minimized. Under this assumption, the model gives acceptable results. The model is seen as a tool, which is used to compare installation methods, and to investigate the influence of different types of loading on the pipe.

Besides the numerical model, physical model tests have been done at MARIN. From these tests it has been found that 3-dimensional effects have a large influence on the pipe behaviour. Possible instability or vortex shedding resulted in more drag than expected from using Morison's equation. The data from the MARIN tests has been used to validate the Matlab model, and it has been found that trend wise the numerical model gives similar results to the physical model.

The numerical model has been used to simulate several Hold and Sink scenarios. Using the established parameters for the CWP, it has been found that for the installation of a 2.5 meter diameter CWP additional buoys or vessels are not necessarily required. By applying a tension of 390mT to the pipe end, the pipe can be held at an equilibrium position at approximately 200 meters below the water surface. By then decreasing the tension force, the pipe can be installed while the Von Mises stress remains well under the material limits. This result was found by using the minimum amount of ballast which is required for the CWP. For more realistic results, the amount of ballast has been increased with 25%. Another simulation was done, showing that the increase in ballast has a very large influence on the CWP installation. It has been found that by adding buoys along the pipe, even with this additional ballast the pipe can be safely installed. The installation of a 4 meter diameter CWP has also been investigated, where it was found that again by adding buoys to the pipe results in a satisfactory installation.

Some attention has also been paid to the float and sink method, yet it was found that this method can only be used with the established pipe parameters if either a large amount of ballast is added, or if the amount of tension on the pipe is greatly reduced. Both options are not preferred.

The final proposed method combines the float and sink method with the hold and sink method. The hold and sink method has two large disadvantages. The first disadvantage is that the pipe must initially

be held at the water surface using multiple vessels or additional buoys, which are then no longer required when the pipe is released. By keeping the pipe filled with air on the water surface, these vessels or buoys are not required. The second disadvantage of the hold and sink method, is that as the pipe is released it is difficult to control as it sinks rapidly until it reaches its equilibrium position. This can be solved by using additional vessels or detachable buoys, yet this results in additional costs. By initially using the float and sink method, with an applied tension of 390mT, the pipe can be filled with water until it has reached the equilibrium position in a very controlled manner. As soon as the pipe is completely filled with water and in equilibrium, the tension is decreased as with the hold and sink method until the pipe reaches the seabed.

This final installation method results in a costs effective installation method, where the shape of the pipe during the installation can be precisely controlled. It can thus be concluded that the goal of this thesis has been reached, where the best installation method and material has been found for the installation of a large diameter cold water pipe.

8.2. Recommendations

This thesis has provided new insight in the installation of large diameter cold water pipes. Still, there is plenty of room for more work.

As observed during the tests at MARIN, it should be investigated if the vibrations in the pipe model where indeed caused by instability or vortex shedding. The influence of this effect on a full scale pipe must be found, as it could potentially influence the installation procedure as loadings are not as expected, as well as result in damage or failure of the pipe.

Furthermore, it is essential that the results from the numerical model are compared with 3rd party software, to see how accurate the model is. Due to the Euler- Bernoulli beam theory, it can be assumed that the numerical model underestimates bending stresses in the pipe.

Considering the final installation method, more optimisation can be done. In the method described in this thesis, the tension force is lowered to install the pipe on the seabed. This results in unnecessary bending of the pipe. By keeping the tension constant and adding a large clump weight to the pipe end, while using an additional vessel to control the vertical force at this end, it should be possible to install the pipe while keeping the tension on the pipe end large. This should result in less bending, and thus smaller stresses in the pipe.

The final installation method should be investigated further to find the influence of weather conditions in three dimensions. These weather conditions include currents, as well as waves and wind which act on the pipe. These will possibly introduce large dynamic loads on the CWP during the installation, which must be taken into account.

Also, as with the final proposed installation method the entire pipe is held at the surface, it can be expected that the pipe will be displaced due to currents and second order wave drift. It must be investigated if additional vessels will be required to hold the pipe above the installation location to counter these forces.

It is expected that by following up on these recommendations and using the results presented in this thesis, brings us one step closer to the realisation of commercial large scale OTEC plants.

Bibliography

1. *United Nations Framework Convention on Climate Change*. 2017 May 12; Available from: http://unfccc.int/paris_agreement/items/9444.php.
2. Forsythe, M. *China Aims to Spend at Least \$360 Billion on Renewable Energy by 2020*. 2017 January 5]; Available from: https://www.nytimes.com/2017/01/05/world/asia/china-renewable-energy-investment.html?_r=0.
3. Kleute, B.J., *Feasibility Study of a 10MW Installation*. 2014, TU Delft: Delft.
4. *OTEC History*. 2014; Available from: <http://www.oteci.com/otec-at-work/test-page/>.
5. Keesmaat, K., *Installation Limits of Large Diameter Cold Water Pipes in Deep Water for Land-Based OTEC Plants*. 2015, TU Delft.
6. *Granta Design Main Page*. [cited 2017; Available from: <http://www.grantadesign.com/education/edupack/>].
7. Roberts, P., *Marine Wastewater Outfalls and Treatment Systems*. 2010
8. *Krah Manufacturer Website*. [cited 2016; Available from: <https://www.krah.net/>].
9. *Technical Catalogue for Submarine Installations of Polyethylene Pipes*. 2002: Pipelife Norge AS.
10. *Allseas Pioneering Spirit Information*. [cited 2016; Available from: <https://allseas.com/equipment/pioneering-spirit/>].
11. *Saginaw Steel Solutions Reference Handbook*. [cited 2016; Available from: http://www.saginawpipe.com/Saginaw_Steel_Reference_Handbook.pdf].
12. *Arcelor Mittal Spirally Welded Steel Pipe Datasheet*. Available from: http://sheetpiling.arcelormittal.com/uploads/files/AMP_Spirally%20welded%20steel%20pipes%202010.pdf.
13. *DNV-OS-F101*. 2013; Available from: <http://rules.dnvgl.com/docs/pdf/DNV/codes/docs/2013-10/OS-F101.pdf>.
14. *Future Pipe Industries Fiberstrong Catalogue*. Available from: <http://www.futurepipe.com/images/Catalogues/fiberstrong/Fiberstrong%20Product%20Information.pdf>.
15. *Summary Bonna Pipe Brochure*. 2013; Available from: <http://www.stanton-bonna.co.uk/wp-content/uploads/2013/08/Summary-Bonna-Pipe-Brochure-small.pdf>.
16. *Humes Concrete Pipe Manual*. [cited 2016; Available from: http://www.humes.com.au/fileadmin/templates/HUMES/doc/Brochures/Humes_ConcretePipeManual.pdf].
17. *Pipelife Technical Brochure*. 2012.
18. *Kl Sandefjord breaks bollard pull record*. Maritime Journal, 2011.
19. Brewer, J.H., *Feasibility Design Study Land-Based OTEC Plants*. 1979: Long Beach, California.
20. Palmer, C., King, R.A., *Subsea Pipeline Engineering*.
21. *Tunnel Talk Forum Discussion*. [cited 2016; Available from: <http://www.tunneltalk.com/Discussion-Forum-Mega-TBMs.php>].
22. *Eiksund Tunnel*. Roadtraffic-Technology.
23. Resvanis, T.L., *REYNOLDS NUMBER EFFECTS ON THE VORTEX-INDUCED VIBRATION OF FLEXIBLE MARINE RISERS*. July 1 2012, Massachusetts Institute of Technology Cambridge: Cambridge, Massachusetts, USA.

Appendix A: Test Setup Parameters



Tend	14		
tlinstep	0.2		
densp	1250		
densw	1000		
E	3.00E+06		
do	0.035		
di	0.025		
cd	1.2		
ca	0.8		
L	5.345		
N	30		
Max load Load cells	10	N	
Resolution Load cell	0.01	N	
No Stepper Motor	5		
Moment Stepper motor	0.34	mNm	
Spacing between measurement sensors	100	Cm	
Diameter pulley Stepper	3	cm	
Diameter pulley POT	6	cm	
Width of Marin Bassin	4.02	cm	
Distance truss to wall	80	cm	
Distance Gopro to wall	21.5	cm	
GOPRO Hero 5 Black FOV			
Medium	94.4	deg	
Linear	-10	%	
Wide (above water)	118.2	deg horizontal	
	69.5	deg vertical	
	133.6	deg diagonal	
Eq Focal length(above water) Wide	17.2	mm	
Slope			
length of slope	6	m	
Depth of slope end	2	m	
pipe			
Distance between yellow stripes	40	cm	
distance between motors	1	m	
Length of pipe suspended in water	5.345	m	
length of pipe above water	0.155	m	

Table 28: Relevant MARIN test setup parameters

Appendix B:

Minimum CWP Mass and Air Fill Ratio

B

Parameters		units	
g	9.81	m/s^2	Gravitational acceleration
$\rho_{concrete}$	2400	kg/m^3	Density of concrete
ρ_{HDPE}	961	kg/m^3	Density of HDPE
μ	$1.3 \cdot 10^{-6}$	m^2/s	Kinematic viscosity of water
C_d	0.7	-	Drag coefficient as specified by Pipelife Technical Design Guide
C_l	0.5	-	Lift coefficient as specified by Pipelife Technical Design Guide
$\eta_{ballast}$	0.7	-	average for rectangular, starred or trapezoidal concrete ballasts in sand.

Table 29: Minimum pipe ballast parameters

As the CWP is installed on the seabed, it can displace if there is not enough ballast attached to the pipe, or if the mass of the pipe is too low. As it is on the seabed, a drag force and a lift force will occur on the pipe due to currents. For calculating the required minimum mass of the CWP, first the surface area of the CWP is found using formula B-1.

$$A = \frac{\pi}{4} \cdot (D_o^2 - D_i^2) \quad (B-1)$$

The Reynolds number of the installed CWP partially determines the drag and lift coefficients of the CWP, and is found:

$$Re = \frac{v_{current} \cdot D_o}{\mu} \quad (B-2)$$

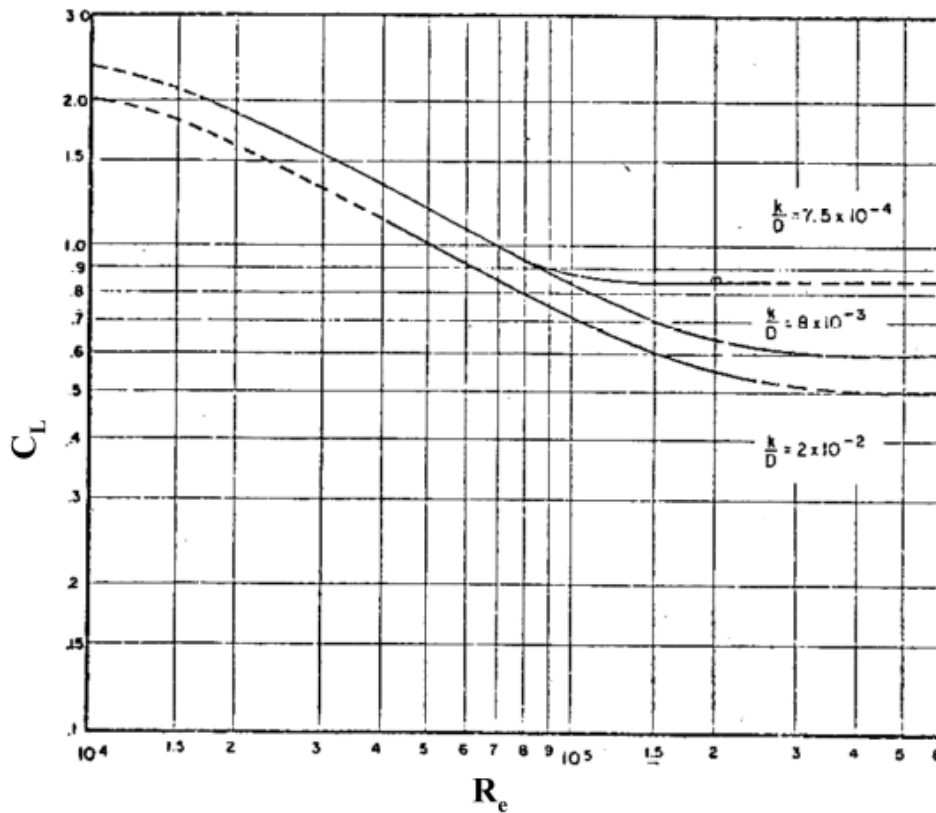
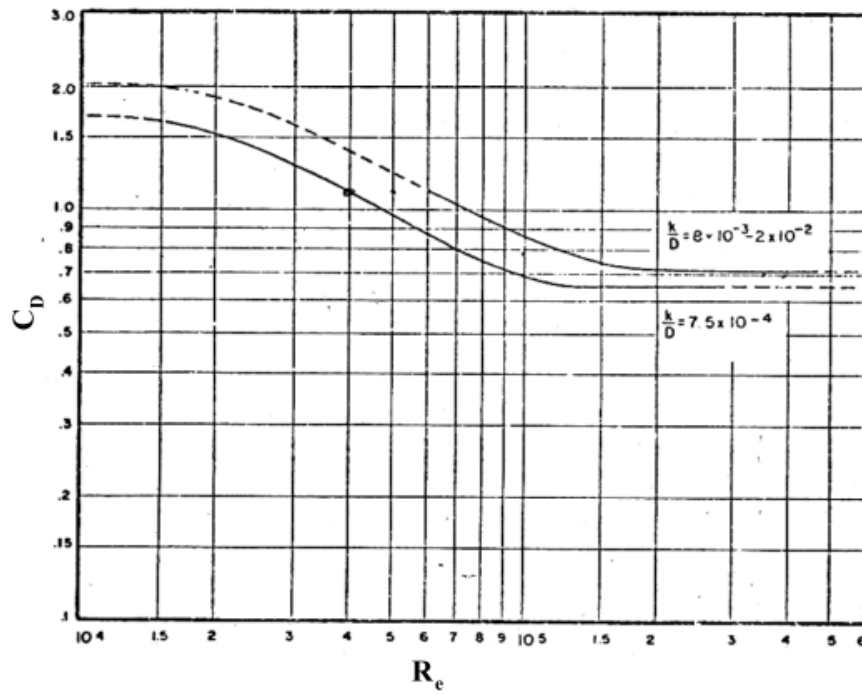


Figure 73: Drag and lift coefficient vs Reynolds number

Using the figure 73, which is taken from the Pipelife design guide[9], the lift and drag coefficients corresponding to the Reynolds number are be found.

Using these coefficients, the drag and lift force due to currents is calculated using equation B-3 and B-4.

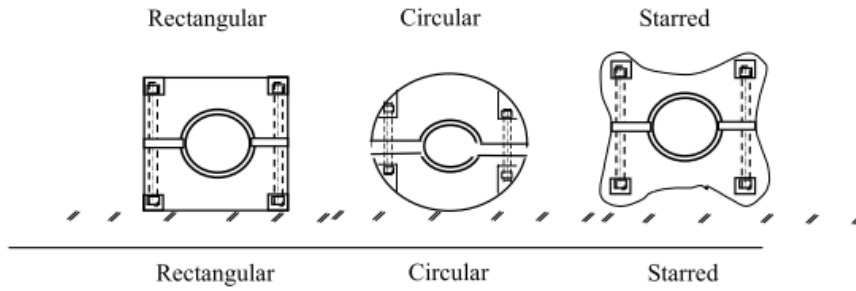
$$F_{drag} = \frac{C_D \cdot \rho_{swbottom} \cdot v_{current}^2}{2} \quad (B-3)$$

$$F_L = \frac{C_L \cdot \rho_{swbottom} \cdot v_{current}^2}{2} \quad (B-4)$$

In order to counter this drag force, the normal force resulting from the mass of the CWP must be large enough. This can be found with the following equation.

$$F_N = F_{drag} \cdot \mu_{concrete} \quad (B-5)$$

In this equation, the coefficient of friction is dependent on the type of ballast used, as shown in below.



The volume of the CWP results in a buoyancy force as water is displaced. This is taken into account in the final required mass.

$$F_B = \frac{\pi}{4} \cdot (D_o^2 \cdot \rho_{swbottom} \cdot g) \quad (B-7)$$

The total force which must be resisted is the sum of the buoyancy force, the drag force and the lift force, as shown in equation B-8.

Equation B-8 is then used to find the resulting CWP density for which it is stable.

$$m_{filled} = \frac{F_B + F_N + F_L}{g} \quad (B-8)$$

This method results in a homogenous CWP, where the mass of the concrete ballasting is distributed over the length of the pipe and is assumed to have no volume. This is done for the ease of modelling and for simplifying calculations. The impact on the results is small, in a real installation the bending is kept limited, so the concrete ballasts will not be restrictive, and as they are distributed evenly and relatively closely spaced, the local stresses due to these ballast blocks are expected to be small.

$$\rho_{stableCWP} = \frac{m_{empty}}{\frac{\pi}{4} \cdot (D_o^2 - D_i^2)} \quad (B-9)$$

Appendix C: Material Properties & MCA's



In order to compare materials, the properties must be known. Many suppliers do not directly give all the required specifications, though some have been found. CES Edupack has been used to find material properties. These are quite accurate, and are simple to use with solid wall structures. As some suppliers use altered materials and specific shapes for their pipes, it is not possible to use these properties. Therefore table 30 shows the material properties from CES Edupack, as well as some properties given by suppliers.

Material Property	Unit	HDPE High molecular weight	FRP Polyester filament wound +- 60deg	Pipelife HDPE PE100	Steel (coated with TPU) AISI 1020 rolled	Concrete (Portland standard)	Corrugated Pipe Krah HDPE (PE100)
Density	kg/m ³	947-955	2020-2200	961	7800-7900	2200-5500	960
Youngs modulus	MPa	1070-1090	15000-16500	1050	205000-215000	15000-25000	-
Yield strength	MPa	26.2-31	50-55	23	295-365	1-1.2	25
Tensile Strength	MPa	22.1-31	50-55	Modulus=1100	395-500	1.1-1.3	38 Modulus=1200
Shear modulus	GPa	0.377-0.384	6-6.6	-	79-84	6.5-10.9	-
Compressive strength	MPa	18.6-24.8	28-33	-	295-365	13.3-30	-
Flexural strength	MPa	30.9-43.4	50-55	-	295-365	1.7-2.4	-
Fatigue strength at 10 ⁷ cycles	MPa	8.84-12.4	30-33	10 (at 50 years 20degC)	223-264	0.54-0.84	-
Thermal conductivity	W/m.C	0.461-0.502	0.655-0.713	-	50-54	0.7-2.6	-
Poisson's ratio	-	0.41 – 0.427	0.13-0.15	0.4-0.5	0.285-0.295	0.1-0.2	-
Average coefficient of thermal expansion	mm/m 0 C	0.106-0.198	0.0579-0.0807	0.2	0.115-0.125	0.05-0.12	0.18
Max available length	m	500	12	500	12	2.44	18
Max available diameter	m	2.5/3	4	3 OD	3.65	3.6	4 ID
Joint type	-	Mirror welding/ Flanged/spigot	Laminating/ Spigot coupling with rubber	Mirror welding/ Flanged/spigot	Welded/ flanged/ coupled with seal	Spigot coupling	Mirror welding/ Flanged/spigot

			seal/ Flanged				
Salt water resistance	-	Excellent	Excellent	Excellent	Limited use	acceptable	-
UV Resistance	-	Fair	Fair	-	Excellent	Excellent	-
CO2 footprint averaged	kg/kg	4.06	6.93	-	3.18	.185	-
Recyclable	-	Yes	No	-	Yes	Yes	-
Price	EUR/kg	1.82-2.23	1.68-1.86	-	0.532-0.541	0.0367-0.055	-

Table 30: List of material properties

Materials MCA

The full materials MCA is given below.

			Weight factor in group	HDPE (PE100)	GFRP Epoxy lay-up	Steel	Concrete
0.15	Risks	Proven material in offshore	1.00	3.7	2.3	2.0	3.0
0.2	Installation time	Section lengths	0.67	5.0	3.0	3.0	1.0
		Availability	0.17	2.7	2.0	2.7	3.7
		Joinability	0.17	4.0	2.7	2.3	1.3
0.15	Installation technical performance	Density	0.30	4.0	3.3	1.3	2.0
		Youngs modulus	0.10	4.0	3.0	2.0	3.0
		Yield strength	0.15	2.0	5.0	4.0	1.0
		Tensile strength	0.15	2.0	5.0	4.0	1.0
0.1	CWP performance	Thermal conductivity	0.50	5.0	4.0	1.0	3.0
		Thermal expansion	0.40	1.0	4.0	5.0	5.0
		Surface roughness	0.10	4.0	3.0	4.0	1.0
0.1	Durability	Salt water resistance	0.40	5.0	5.0	3.0	2.0
		UV resistance	0.20	2.0	2.0	5.0	5.0
		Fatigue strength	0.40	2.0	4.0	4.0	1.0
0.05	Material environmental impact	RoHS (EU) Compliant	0.10	5.0	5.0	5.0	5.0
		CO2 footprint	0.45	3.0	2.0	3.0	5.0
		Recyclable	0.45	5.0	1.0	5.0	5.0
0.1	Technical scale up potential	Scale up potential to 4 meters	0.67	1.7	3.0	1.7	4.0
		Scale up potential to 10 meters	0.33	1.3	1.7	1.3	2.3
0.15	Costs	Total costs		4.0	3.0	3.0	2.0
1		Total score		3.4	2.9	2.6	2.4

Table 31: Materials MCA

Installation Method MCA

The full installation method MCA is given below.

Weight factor	Installation	Weight factor	F&S with	F&S hybrid	Off-bottom	Installation	Reverse	Brewers w	Bottom to	F&S + m	Direction	Hold & Sin
0.15	Installation time	0.45	5	4	3.3	1.3	3.7	3.3	4	3	1.7	4
	Maximum installation weather conditions	0.3	2	2	3.3	2.3	1.7	2.3	3.7	2.3	5	2.3
	Uniqueness and amount of vessels required	0.25	3.7	3.7	3.7	3	3.7	3	3.7	2.7	3.3	3.3
0.2	Sensitivity to seabed irregularities	0.4	2.7	2.7	2	2.7	2.7	4	1	2.7	4.7	3
	To different seabed slope angles	0.3	3.3	3.3	3.3	3	3	4.3	3	3.7	4	3.7
	To a longer length pipe	0.3	3	3	2.3	2.7	2.3	3.7	2	3	2.7	3.3
0.1	Environment interference with seabed	1	2.7	2.7	2.7	2.7	2.7	3	1.3	2.7	4.7	3
0.2	Risks Probability of feasibility	0.4	3.3	3.7	3.3	3	2.3	4	2.7	3.7	1.3	4
	probability of failure before 25 years	0.3	3.7	3.3	2	2.3	3.3	2.7	3	3	3.3	3.7
	Complexity of the installation	0.3	3.3	3.3	2.7	2	2.7	2.7	3	3	1.7	3
0.1	Technical Scale up potential to 4 meters	0.67	2	2	2.7	2.7	1.7	3.7	3	2.3	2.7	3
	Scale up potential to 10 meters	0.33	1.7	1.7	2	2.7	1.3	3	2.3	2	2.7	2
0.1	Safety Amount of workers needed (on vessel(s))	1	3.3	3.3	3.3	2.7	3.7	1.7	3.3	2.7	4.7	2.7
0.15	Costs Installation costs		4	3.3	3.3	2	3	2.3	3.7	3	1	3.5
	Total with costs		3.2	3.1	2.9	2.5	2.8	3	2.8	2.9	3	3.2

Table 32: Installation method MCA

Appendix D: Discretisation of Equation of Motion

D

The general equation of motion for the beam is given in the form of the Euler–Bernoulli beam, shown below.

$$EI \frac{\partial^4 w}{\partial x^4} - T \frac{\partial^2 w}{\partial x^2} + (m_p + m_a) \frac{\partial^2 w}{\partial t^2} + k_d(x)(w - d_{sb}(x)) + c_d(x) \frac{\partial(w - d_{sb}(x))}{\partial t} \quad (C-1)$$

$$= \tau_{Morison}(x, t) - q_{gravity}(x) + f_{vessel}(x)\delta(x - a)$$

Where $m_a = \frac{\pi}{4} \cdot \rho_{sw} C_a D_o^2$, and $m_p = \frac{\pi}{4} \cdot (\rho_{cwp} - \rho_{sw})(D_o^2 - D_i^2) + \frac{\pi}{4} \cdot \rho_{sw} D_i^2$ are both distributed loads in the form of mass per unit length.

The interaction with the seabed is included in this equation, as the seabed is described as a visco – elastic foundation, where $k_d(x)$ is the stiffness of the seabed, and $c_d(x)$ is the damping of the seabed. $d_{sb}(x)$ is the depth of the seabed as seen from the water surface.

Furthermore, with some installation scenarios there are buoys or vessels which apply a force on the CWP. These forces are applied as a point load, by defining $f_{vessel}(x)$ as a distributed load and then using the Dirac-Delta function. This force is included depending on the installation scenario.

The boundary conditions are given as follows:

L.H.S.:

$$x = 0; w = \frac{\partial^2 w}{\partial x^2} = 0 \quad (C-2)$$

R.H.S.:

$$x = L; EI \frac{\partial^3 w}{\partial x^3} - T \frac{\partial w}{\partial x} = -F_{tensvertical} \quad (C-3)$$

$$x = L; \frac{\partial^2 w}{\partial x^2} = 0 \quad (C-4)$$

As the beam is discretized using Finite Difference, the derivatives of the displacement are approximated in the following manner:

$$\frac{\partial w_n}{\partial x} = \frac{w_{n+1} - w_{n-1}}{2l} \quad (C-5)$$

$$\frac{\partial^2 w_n}{\partial x^2} = \frac{w_{n+1} - 2w_n + w_{n-1}}{l^2} \quad (C-6)$$

$$\frac{\partial^3 w_n}{\partial x^3} = \frac{w_{n+2} - 2w_{n+1} + 2w_{n-1} - w_{n-2}}{2l^3} \quad (\text{C-7})$$

$$\frac{\partial^4 w_n}{\partial x^4} = \frac{w_{n+2} - 4w_{n+1} + 6w_n - 4w_{n-1} + w_{n-2}}{l^4} \quad (\text{C-8})$$

By substituting these approximations into the equation of motion, the discretised EOM is found.

This gives the following results:

EOM for node 3 until node N-2:

$$\begin{aligned} \frac{EI}{l^4} (w_{n+2} - 4w_{n+1} + 6w_n - 4w_{n-1} + w_{n-2}) - \frac{T}{l^2} (w_{n+1} - 2w_n + w_{n-1}) + (m_p + m_a) \frac{\partial^2 w}{\partial t^2} + k_d(x) (w - d_{sb}(x)) \\ + c_d(x) \frac{\partial (w - d_{sb}(x))}{\partial t} = \tau_{Morison}(x, t) - q_{gravity}(x) \end{aligned} \quad (\text{C-9})$$

For node 1 and 2, the equations of motion are found by discretizing the boundary conditions, and then substituting into the discretized EOM.

L.H.S.

$$x = 0; w = 0 \quad \text{B.C.1}$$

This gives

$$w = 0 \rightarrow w_{n=0} = 0$$

Which means that the node at the pinned connection is not described with an EOM, as it cannot displace.

For

$$w_1 = w_{n=1}$$

Applying finite differences yields the following equation of motion:

$$\begin{aligned} \frac{EI}{l^4} (w_{-1} - 4w_0 + 6w_1 - 4w_2 + w_3) - \frac{T}{l^2} (w_0 - 2w_1 + w_2) + (m_p + m_a) \frac{\partial^2 w}{\partial t^2} + k_d(x) (w - d_{sb}(x)) \\ + c_d(x) \frac{\partial (w - d_{sb}(x))}{\partial t} = \tau_{Morison}(x, t) - q_{gravity}(x) \end{aligned} \quad (\text{C-10})$$

From the second B.C.:

$$\frac{\partial^2 w_{n=0}}{\partial y^2} = 0 = \frac{w_{n-1} - 2w_n + w_{n+1}}{l^2} = \frac{w_{-1} - 2w_0 + w_1}{l^2} \quad (\text{C-11})$$

And as $w_0 = 0 \rightarrow w_1 + w_{-1} = 0$, it becomes clear that $w_{-1} = -w_1$.

Substituting the obtained results for w_0 and w_1 into the equation of motion for $w_{n=1}$ then gives:

$$w_{n=1} : \frac{EI}{l^4} (5w_1 - 4w_2 + w_3) - \frac{T}{l^2} (-2w_1 + w_2) + (m_p + m_a) \frac{\partial^2 w}{\partial t^2} + k_d(x)(w - d_{sb}(x)) + c_d(x) \frac{\partial(w - d_{sb}(x))}{\partial t} = \tau_{Morison}(x, t) - q_{gravity}(x) \quad (C-12)$$

And for $w_{n=2}$:

$$w_{n=2} : \frac{EI}{l^4} (-4w_1 + 6w_2 - 4w_3 + w_4) - \frac{T}{l^2} (w_1 - 2w_2 + w_3) + (m_p + m_a) \frac{\partial^2 w}{\partial t^2} + k_d(x)(w - d_{sb}(x)) + c_d(x) \frac{\partial(w - d_{sb}(x))}{\partial t} = \tau_{Morison}(x, t) - q_{gravity}(x) \quad (C-13)$$

R.H.S.

For the right hand side, similarly, the equations of motion are found by discretizing the boundary conditions, and then substituting these into the discretized EOM.

$$x = L; \frac{\partial^2 w}{\partial x^2} = 0 \quad \text{B.C. 1}$$

$$x = L; EI \frac{\partial^3 w}{\partial x^3} - T \frac{\partial w}{\partial x} = -F_{tensvertical} \quad \text{B.C. 2}$$

Discretizing BC 1 gives:

$$B.C.1 \rightarrow \frac{\partial^2 w_{n=N}}{\partial y^2} = 0 = \frac{w_{n-1} - 2w_n + w_{n+1}}{l^2} = \frac{w_{N-1} - 2w_N + w_{N+1}}{l^2} \quad (C-14)$$

From this it follows that:

$$w_{N+1} = -w_{N-1} + 2w_N \quad (C-15)$$

Now for BC 2:

$$B.C.2 \rightarrow \frac{EI}{2l^3} (-w_{N-2} + 2w_{N-1} - 2w_{N+1} + w_{N+2}) - \frac{T}{2l} (-w_{N-1} + w_{N+1}) = -F_{tensvertical}$$

By rewriting:

$$w_{N+2} = w_{N-2} - 2w_{N-1} + 2w_{N+1} + \frac{2Tl^3}{EI} \left(\frac{-w_{N-1} + w_{N+1}}{2l} \right) - \frac{2l^3 F_{tensvertical}}{EI} \quad (C-16)$$

By now substituting the expression $w_{N+1} = -w_{N-1} + 2w_N$ into the above equation, the following is obtained:

$$w_{N+2} = w_{N-2} - 4w_{N-1} + 4w_N + \frac{Tl^2}{EI} (-2w_{N-1} + 2w_N) - \frac{2l^3 F_{tensvertical}}{EI} \quad (C-17)$$

By substituting formula C-15 and C-17 into the discretized EOM, equation C-9, the EOM for $w_{n=N}$ can be found.

$$\begin{aligned}
& \frac{EI}{l^4} (w_{N-2} - 4w_{N-1} + 6w_N + 4w_{N-1} - 8w_N) + \frac{EI}{l^4} (w_{N-2} - 4w_{N-1} + 4w_N) \\
& + \frac{EI}{l^4} \left(\frac{Tl^2}{EI} (-2w_{N-1} + 2w_N) \right) + \frac{EI}{l^4} \left(\frac{2l^3 F_{tensvertical}}{EI} \right) \\
& - \frac{T}{l^2} (w_{N-1} - 2w_N - w_{N-1} + 2w_N) + (m_p + m_a) \frac{\partial^2 w}{\partial t^2} + k_d(x) (w - d_{sb}(x)) \\
& + c_d(x) \frac{\partial (w - d_{sb}(x))}{\partial t} = \tau_{Morison}(x, t) - q_{gravity}(x)
\end{aligned} \tag{C-18}$$

Collecting terms gives:

$$\begin{aligned}
w_{n=N} : & \frac{EI}{l^4} (2w_{N-2} - 4w_{N-1} + 2w_N) - \frac{T}{l^2} (2w_{N-1} - 2w_N) + (m_p + m_a) \frac{\partial^2 w}{\partial t^2} + k_d(x) (w - d_{sb}(x)) \\
& + c_d(x) \frac{\partial (w - d_{sb}(x))}{\partial t} = \tau_{Morison}(x, t) - q_{gravity}(x) - \frac{2F_{tensvertical}}{l}
\end{aligned} \tag{C-19}$$

Where the EOM is described as a distributed load. It is important to state that the component of the vertical force due to the tension, $\frac{2F_{tensvertical}}{l}$, occurs only the equation of motion for node N.

Furthermore, the above equations are still written in the form of distributed loads, although this is technically incorrect. As due to the discretisation the system is no longer continuous, the equations of motions are actually discretized forces. As the last node only describes half of an element, the entire equation should be multiplied with $\frac{l}{2}$.

The EOM for node $w_{n=N-1}$ is shorter to derive. The EOM is found by substituting expression C-15 into the general discretized EOM.

This gives the EOM for node $w_{n=N-1}$:

$$\begin{aligned}
w_{n=N-1} : & \frac{EI}{l^4} (w_{N-3} - 4w_{N-2} + 5w_{N-1} - 2w_N) - \frac{T}{l^2} (w_{N-2} - 2w_{N-1} + w_N) + (m_p + m_a) \frac{\partial^2 w}{\partial t^2} + k_d(x) (w - d_{sb}(x)) \\
& + c_d(x) \frac{\partial (w - d_{sb}(x))}{\partial t} = \tau_{Morison}(x, t) - q_{gravity}(x)
\end{aligned} \tag{C-20}$$